III-A1
DECEMBER, 1964

COLD REGIONS SCIENCE AND ENGINEERING

F. J. Sanger, Editor

Part III: Engineering

Sect. A: Snow Engineering

Properties of Snow

U.S. ARMY MATERIEL COMMAND
COLD REGIONS RESEARCH & ENGINEERING LABORATORY
HANOVER, NEW HAMPSHIRE

PREFACE

This monograph summarizes available information on the properties of snow.

This monograph has been reviewed and approved by Headquarters, U. S. Army Materiel Command.

CONTENTS

CONTENTS (Cont'd)

ILLUSTRATIONS

CONTENTS (Cont'd)

ILLUSTRATIONS (Cont'd)

CONTENTS (Cont'd)

ILLUSTRATIONS (Cont'd)

CONTENTS (Cont'd)

TABLES

EDITOR'S FOREWORD

"Cold Regions Science and Engineering" consists of a series of monographs summarizing existing knowledge and providing references for the use of professional engineers responsible for design and construction in Cold Regions, defined as those areas of the earth where frost is an essential consideration in engineering.

Sections of the work are being published as they become ready, not necessarily in numerical order, but fitting into this plan:

I. Environment
   - A. General
     1. Geology and physiography
     2. Perennially frozen ground (permafrost)
     3. Climatology
   - B. Regional
     1. The Antarctic ice sheet
     2. The Greenland ice sheet

II. Physical Science
   - A. Geophysics
     1. Heat exchange at the earth's surface
     2. Exploratory geophysics
   - B. The physics and mechanics of snow as a material
   - C. The physics and mechanics of ice
     1. Snow and ice on the earth's surface
     2. Ice as a material
   - D. The physics and mechanics of frozen ground

III. Engineering
   - A. Snow engineering
     1. Engineering properties
     2. Construction
     3. Technology
     4. Oversnow transport
   - B. Ice engineering
   - C. Frozen ground engineering
   - D. General

IV. Miscellaneous

F. J. SANGER

PROPERTIES OF SNOW

by

Malcolm Mellor

CHAPTER I. FORMATION AND COMPOSITION OF SNOW

Formation, deposition and metamorphism

Snow originates in clouds at temperatures below the freezing point. As moist air rises, expands, and cools, water vapor condenses on minute nuclei to form cloud droplets of the order of 10 μ radius. The condensation nuclei involved in droplet formation may be introduced from oceanic salts, terrestrial dust or combustion gases, or they may be of atmospheric origin. Cloud droplets are more than an order of magnitude smaller than typical raindrops, and they are incapable of falling through unsaturated air without evaporating.

When cooled below 0C, such small droplets do not necessarily freeze, since their large specific surface (high surface/volume ratio) gives a peculiar ability to supercool. In the atmosphere, supercooled droplets commonly exist down to -20C, and occasionally down to -35C. In the laboratory, micron-size drops of very pure water can be cooled to -40C without freezing (Fig. I-1). The ice nuclei which stimulate freezing of supercooled droplets in a cloud seem to be mainly clay minerals from terrestrial dust, and they apparently become increasingly effective as the temperature decreases.

Once a droplet has frozen it grows quickly at the expense of the remaining water droplets, because of the difference in saturation vapor pressures for ice and water. The form of the initial ice crystal (columnar, platelike, dendritic) depends on the temperature at formation, but subsequent growth and structural detail depend also on the degree of supersaturation. Figure I-2 gives Mason's scheme for the influence of temperature and supersaturation on crystal form. The sensitivity of initial crystal form to formation temperature may result from the temperature dependence of molecular surface diffusion to the growth faces, an effect which apparently decreases in significance as the crystal grows. After formation, subsequent growth takes place at the crystal faces as a result of diffusion and condensation, perhaps under changing conditions of temperature and supersaturation since the snow particle begins to fall when it reaches sufficient size. Table I-I gives some observations on the predominant crystal types found in various cloud types, and Table I-II gives some typical dimensions and fall velocities for snow crystals.

During its fall to earth, a snow crystal may undergo considerable change. Variation of temperature and humidity with altitude leads to changes in growth rate and form, and there may even be evaporation or melting of the crystal. Particles may be "recycled" through some layers by turbulence in the air and, during windy conditions at the surface, fragmentation of the more delicate crystal types often occurs.

The character of the surface deposit after a snowfall depends on the form of the crystals and on the weather conditions during deposition. When there is no appreciable wind, dry stellar crystals (which commonly aggregate into large snowflakes) settle as a soft, fluffy mass whose density is generally less than 0.1 g/cm^3. Very small crystals of simple prismatic form, on the other hand, settle to relatively high initial densities (say 0.2 g/cm^3) for obvious geometrical reasons. Snow deposited in wind-free weather has a smooth surface. When a snowfall is accompanied by strong winds, crystals are broken into fragments favorable for close packing, and the surface of the deposited snow is mechanically agitated by wind shear and by the impact of bounding particles. This produces high initial density, commonly greater than 0.3 g/cm^3, and also leads to the formation of snow dunes and sastrugi on the surface.

After deposition, snow may be dissipated by melting and evaporation or it may persist for long periods. If it persists, it will undergo metamorphism, changing its grain texture and structure and eventually turning into hard, impermeable ice if it

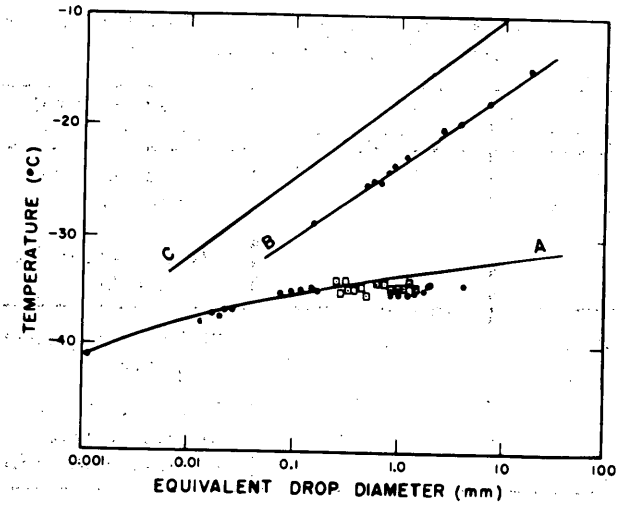

Figure I-1. Relationship between median freezing temperature and droplet size: (A) data for highly pure water, compiled by Mason; (B) and (C) data for droplets containing foreign nuclei, by Bigg (B), and by Dorsch and Hacker, and Levine (C). (References 12-14, 21, 22)*

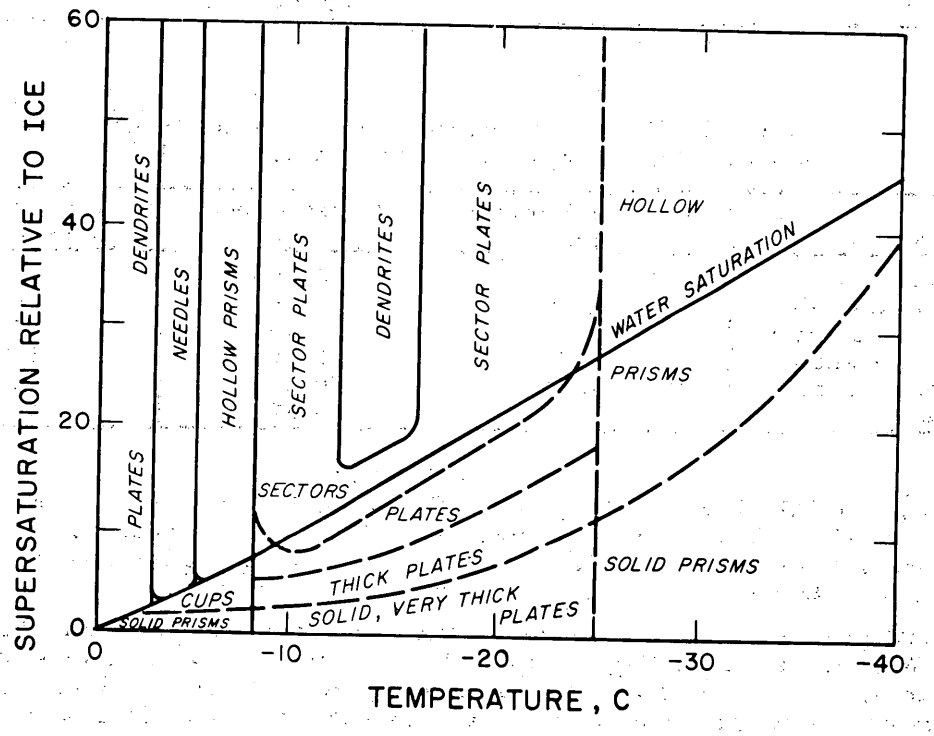

Figure I-2. Mason's scheme for the variation of crystal form with temperature and supersaturation relative to flat ice surface at time of formation.

*References are listed after each chapter.

Table I-I. Crystal types found in various types of clouds. (After Weickmann, ref. 18)

Layer	Cloud type	Temp range	Predominant crystal form	Approx. crystal dimensions
Lower troposphere	Nimbostratus, stratocumulus, stratus	0 to -15C	Thin hexagonal plates	50 μ to 0.5 mm diam, 10 to 20 μ thick
			Stellar dendritic crystals	0.5 to 5 mm diam
Middle troposphere	Altostratus, altocumulus	-15 to -30C	Thick hexagonal plates	200 μ diam
			Prismatic columns, single prisms and twins	200 μ long
Upper troposphere	Isolated cirrus	Lower than -30C	Clusters of prismatic columns, (with cavities)	1 mm diam
			Single hollow prisms	0.5 mm long
	Cirrostratus		Single complete prisms, thick plate crystals	100 μ long

Table I-II. Crystal dimensions and fall velocities for various types of snow. (After Mason, ref. 14)

Snow type	Crystal diameter (mm)	Crystal mass (mg)	Fall velocity (cm/sec)
Needle	1.5	0.004	50
Plane dendrite	3.0	0.04	30
Spatial dendrite	4.0	0.15	60
Powder snow	2.0	0.06	50
Rimed crystals	2.5	0.18	100
Graupel	2.0	0.80	180

is part of a perennial snow deposit. The mechanics and thermodynamics of snow metamorphism, and their dependence on environmental factors, are rather involved; these natural processes are discussed elsewhere[2,3] and it will suffice here to mention the major factors contributing to the transformation of snow to ice.*

The most drastic changes in snow condition are brought about by melting and refreezing. With moderate melting, much of the resulting free water may be retained in place by surface tension, so that subsequent refreezing can provide strong ice bonds between grains. If melting is more intense, free water will percolate down through the snow, refreezing when it reaches colder layers to form ice lenses.

* When snow has been compacted to the stage where it becomes impermeable to air, it is termed ice. In cold, dry snow the transition from permeable snow to impermeable ice occurs at a density of about 0.8 g/cm^3.

In subfreezing temperatures, ice grains change their shape and size, and intergranular bonds develop by sublimation and by molecular diffusion in the ice. Sublimation occurs when differences in vapor pressure exist; the vapor pressure differences arise from changes in temperature and grain surface curvature from place to place in the snow mass. Variations in surface curvature on the constituent ice grains also lead to surface diffusion of molecules, since such variations represent energy gradients. It also appears that bulk diffusion within the ice crystals contributes to the transfer of mass.

In subsurface layers of a snow mass, there is an overburden pressure produced by the weight of more recently deposited material. Compactive deformation takes place and the density of the snow gradually increases. Under the relatively low pressures developed in a snowpack (at least in the uppermost 10 m), the deformation is of a viscous nature, with strain rate proportional to stress, and also dependent on temperature. Since overburden forces are transmitted through the ice grains and their connecting bonds, the crystals are stressed, and it seems likely that this will affect the rate of metamorphism by the molecular transfer processes mentioned above.

Impurities in snow

Chemical impurities and mineral inclusions. Snow acquires small amounts of chemical impurities and mineral inclusions during formation and growth of the crystals. The usual sources are gases and aerosols introduced to the atmosphere from the earth's surface. Further contamination may occur after the snow is deposited on the ground, particularly from windborne particles and gases. Chemical contamination may be severe near industrial areas and seacoasts; snow in the center of the Greenland and Antarctic ice sheets probably has the highest and most consistent purity.

Table I-III establishes typical ranges for concentration of impurities, particularly in polar snow. Figure I-3 illustrates the variation of Na^+ and $SO_4^=$ with depth below the surface of the ice cap at Site 2, NW Greenland.

Snow is generally acidic. Reports from many parts of the world give hydrogen ion concentrations in the range 10^{-4} to 10^{-7} moles per liter. On the ice caps of Greenland and Antarctica, the pH values are commonly about 5.5 for snow which has not been contaminated by human occupancy.

The most abundant quantities of mineral inclusions in deposited snow come from windblown sand and dust. There may, however, be inclusions of rock minerals in falling snow. The role of rock minerals, particularly clay minerals, in the processes of condensation and freezing in clouds was mentioned earlier. This atmospheric source provides only a very small fraction of solids in normal circumstances, but occasionally a snowfall may become heavily contaminated from a major desert dust storm or a volcanic eruption. Heavy contamination by desert dust gives rise to the "yellow", "red", or "brown" snowfalls reported in the literature. This type of contamination may give characteristic layers in deposited snow; the ash layers deposited after major volcanic eruptions may be traced and used as time references by glaciologists.

Fine particles of extra-terrestrial origin have also been detected in snow, and lately there has been considerable interest in the concentration and distribution of cosmic particles preserved in the permanent snows of Greenland and Antarctica. Langway[19] describes extra-terrestrial dust lodged in the Greenland ice sheet; the "black spherule" component of the dust has a size range of 5 to 160 μ, and the deposition concentration is equivalent to 1.17 spherules of mean mass per cubic centimeter per year. The spherules are rich in either Fe or Si.

Organic impurities.* Deposited snow is not a sterile environment; a variety of algae, fungi, bacteria, molds, and insects can live, grow and multiply on snow. These micro-organisms apparently live on or near the surface, where light is plentiful, and thrive when temperatures are close to the melting point. Biological activity is arrested by very low temperatures, but at least some of the organisms can survive deep freezing.

*References too numerous to mention. Probably the most prolific writer on this topic is E. Kol. (See, for example, Bull. Soc. Botan. Genève, Ser. 2, vol. 25, 1934; Smithsonian Inst. pub. no. 3525, 1939; Smithsonian Misc. Collections, vol. 101, no. 16, 1942.)

Table I-III. Concentration of impurities in snow.

Location	Impurity (mg/liter)														
	Na	Ca	Mg	K	P	As	B	I	Cl	SO_4	NH_3	CO_2	H_2SO_4	NO_3	S
Site 2, NW Greenland. Average for uppermost 100 ft of ice cap. (Junge, 1958)	0.029	0.035		0.011					0.037	0.25					
Site 2, NW Greenland. From ice sampled 300 m below the surface. (Langway, 1962)	0.097			0.077					0.156	0.315					
Byrd Station, Antarctica.															
Surface sample	0.16										17.2	2			
Sample from 40 ft depth.	0.03								0.14		0.01	10			
(Allis-Chalmers Co., 1963)															
Antarctica (about 24° E long.)															
Snowfall over the ocean, 68°S	1.54			0.25					2.33						
Coastal snow, 70°S	1.92			0.38					2.06						
Snow on the continent, 70°-72°S	0.56			0.17					0.47						
Snow on the mountains, 72°S	1.07			0.33					0.39						
(Brocas and Delwiche, 1963)															
Syowa Station, Antarctica (coast).															
Sample 1	240	8.9	20		0.081	0.0041		0.01	413	46					
Sample 2	5.3	0.42	0.61		0.48	0.0026		0.0041	8.3	0.8					
(Sugawara, 1961)															
Japan (range of measured values) (Endō and Mashima, 1955; Furukawa, 1957)		0.2-1.9	0.02-1.6	0.04-0.26			0.02-0.11		0.7-70				10		0.2-1.8
Nova Scotia (Herman and Gorham, 1957)											0.13			0.007	0.3
Zugspitze (2690 m), Germany									1.6	1.0				0.8	
St. Moritz (1800 m), Switzerland									-	0.4				0.8	
(Georgii and Weber, 1962)															
Sierra Nevada, Utah, Colorado (Feth, Rogers and Roberson, 1964)	0.46-1.24	0.39-2.23	0.16-0.33	0.31-0.47					0.50-1.60	0.93-2.88					

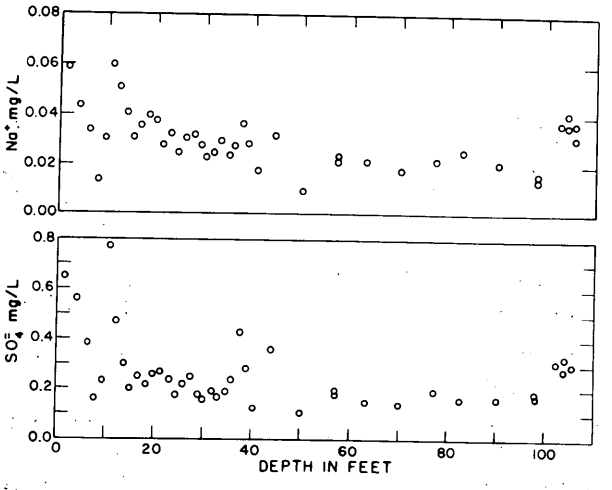

Figure I-3. Variation of Na^+ and $SO_4^=$ with depth below the surface of the ice cap at Site 2, N. W. Greenland. (Junge, 1958)

Many of the "colored snows" seen in various parts of the world (Europe, Asia, N. America, Greenland, the Arctic islands, Antarctica) are organically tinted. Reports of red and green snow are common; yellow snow occurs, though it seems to be more often caused by inorganic matter, and even blue snow has been described.

Red snow is repeatedly found to contain Chlamydomonas nivalis, Sphaerella nivalis, Protococcus nivalis, or Scotiella nivalis. Other species have been described from red snow. Some change color at different stages in the life cycle, e.g. Protococcus changes from colorless to green with maturity and decays to red. Green snow may contain Raphidonema species, Ankistrodesmus tatrae, Stichococcus nivalis, transient stages of the red snow organisms, or other varieties.

Isotopes and trace gases. Snow consists of ice and air; when it undergoes transformation to ice in cold, dry conditions, the interstitial air becomes permanently trapped in closed bubbles. The ice is composed of hydrogen and oxygen, both of which have detectable isotopes, and the air component is a mixture of atmospheric gases, the elements of which also have isotopes.

The heavy isotopes of hydrogen, deuterium and tritium, are present in snow, and there is hope that study of their concentrations will provide, along with fundamental knowledge, methods for dating ice samples. Ice formed from snow which was deposited prior to the first hydrogen bomb explosion has a tritium content which decreases with age; periodic fluctuations superimposed on the general decay of tritium with age may indicate variations of solar activity.[16] Hydrogen bomb testing has confused the picture by introducing additional tritium to the atmosphere and hence to the snows; it has, however, provided a firmly dated tritium horizon in the polar ice caps. Bomb tests have also introduced strontium-90 into snow, providing a further means of dating strata.[20]

The most promising technique for dating snow by isotope techniques so far is based on the content of the heavy oxygen isotope O^{18}. The ratio of O^{18} to O^{16} in precipitation varies with temperature at the time of precipitation, the amount of O^{18} increasing with temperature[6, 8, 15]. Thus there is a seasonal variation of the O^{18}/O^{16} ratio, which shows up when measurements are made through a vertical section of the deposited snow. The ratio of deuterium to ordinary hydrogen varies with temperature in the same way.

CHAPTER I REFERENCES

1. Allis-Chalmers Co. (1963) Private communication.
2. Bader, H. (1962) "Snow as a material" in Cold Regions Science and Engineering (F. J. Sanger, Editor), U. S. Army Cold Regions Research and Engineering Laboratory (USA CRREL) monographs, Part II, Sect. B.
3. _____ (1962) Theory of densification of dry snow on high polar glaciers, USA CRREL, Research Report 108.
4. Brocas, J. and Delwiche, R. (1963) Cl, K, and Na concentrations in Antarctic snow and ice, Journal of Geophysical Research, vol. 68, no. 13.
5. Endo, J. and Mashima, M. (1955) "Koū-chū no ganen ryō" ("The salt content of fallen snow") in Studies in fallen snow (Japan), no. 5 (text in Japanese).
6. Epstein, S. and Sharp, R. P. (1959) Oxygen isotope studies, Transactions, American Geophysical Union, IGY Bulletin no. 21, vol. 40, no. 1, p. 81-84.
7. Furukawa, I. (1957) Hito nigirino yuki no nakani (Analysis of fallen snow), Seppyo, vol. 19, no. 2, p. 50-53 (text in Japanese).
8. Gonfiantini, R., et al. (1963) Snow stratigraphy and oxygen isotope variations in the glaciological pit of King Boudouin Station, Queen Maud Land, Antarctica, Journal of Geophysical Research, vol. 68, no. 13.
9. Herman, F. A. and Gorham, E. (1957) Total mineral material, acidity, sulphur and nitrogen in rain and snow at Kentville, Nova Scotia, Tellus, vol. 9.
10. Junge, C. E. (1958) Snow analyses supplied to SIPRE by Air Force Cambridge Research Center, September, 1958.
11. Langway, C. C. (1962) Some physical and chemical investigations of a 411 m deep Greenland ice core for climatic changes, Symposium of Obergurgl, International Union of Geodesy and Geophysics, Association of Scientific Hydrology.
12. Mason, B. J. (1957) The physics of clouds. Oxford: Clarendon Press.
13. _____ (1961) The physics of clouds, rain and lightning, Imperial College of Science and Technology, London, Inaugural Lecture.
14. _____ (1962) Clouds, rain and rainmaking. Cambridge, England: University Press.
15. Picciotto, E., de Maere, X., and Friedman, I. (1960) Isotopic composition and temperature of formation of Antarctic snows, Nature, vol. 187, p. 857-859.
16. Renaud, A., et al. (1963) Tritium variations in Greenland ice, Journal of Geophysical Research, vol. 68, no. 13.
17. Sugawara, K. (1961) Nankyoku no yuki pōrusui pakkuaisu no kagaku seibun (Chemistry of ice, snow and other water substances in Antarctica), Antarctic Record (Tokyo), no. 11, p. 116-120 (text in Japanese).
18. Weickmann, H. (1948) Die Eisphase in der Atmosphare (The ice phase in the atmosphere), Ministry of Supply, United Kingdom. Translated by Royal Aircraft Establishment (Library translation 272).
19. Langway, C. C. (1963) Sampling for extra-terrestrial dust on the Greenland Ice Sheet, Berkeley Symposium, International Union of Geodesy and Geophysics, Association of Scientific Hydrology.
20. Vickers, W. W. (1963) Geochemical dating techniques applied to Antarctic snow samples, Berkeley Symposium, International Union of Geodesy and Geophysics, Association of Scientific Hydrology.
21. Levine, J. (1950) Statistical explanation of spontaneous freezing of water droplets, NACA, Technical note 2234.
22. Dorsch, R. G. and Hacker, P. T. (1950) Photomicrographic investigation of spontaneous freezing temperatures of supercooled water droplets, NACA, Technical note 2142.

CHAPTER II. MECHANICAL CHARACTERISTICS

Grain sizes for deposited snow

New snow crystals commonly range in size from fractions of a millimeter to one or two millimeters. When dry snow is blown by strong winds, however, some fragmentation occurs and smaller grains are formed. Grain sizes for cold, blown snow are mainly in the range from 0.1 to 1.0 mm equivalent diameter. (Snow actually blowing in the air ranges in size from about 20 μ to 400 μ, with a mean close to 100 μ.) Figure II-1 gives a cumulative mass curve (grading curve) for fresh blown snow, measured by means of microscope observations at an Antarctic station.

After deposition, grain growth occurs, largely as a result of sublimation, and intergranular bonds form by sublimation and diffusion. Grading curves for deposited snow are usually obtained by mechanically disaggregating the snow and sieving it. The grains are parted by rubbing snow on snow, and put through a nest of sieves agitated by a mechanical vibrator. This method tends to exaggerate measured grain size, but it is a self-consistent classification procedure. Figure II-2 gives a grading curve for Greenland drift snow obtained in this manner, while Figure II-3 compares freshly-deposited drift with older snow from the natural snowpack.

In Figure II-4, grading curves for alpine snows (obtained by a different method than the above) are shown, and it can be seen that the older snows are more coarse-grained than the fresh ones.

Fine fractions can be restored artificially to deposited snow by milling with a rotary snowplow. Snow comminuted in this way usually has an average grain size of about 0.5 mm immediately after redeposition. A uniformity coefficient is sometimes used to aid in description of processed snows:

$$\text{Uniformity coefficient, } C_u = \frac{D_{60}}{D_{10}}$$

where D_{60} is the largest diameter of the finest 60% of grains by weight and D_{10} is the largest diameter of the finest 10% of grains by weight. The smaller the coefficient the more uniform is the grain size. Uniformity coefficients for milled snows are about 2.

Figures II-5 and II-6 compare the grading of snow milled by different types of plow. For any given plow a considerable variation in grading will be found with changing distance from the plow ejection chute since, in windy weather, the coarsest fragments fall close to the machine while the finest fraction is carried far downwind.

In Figure II-7, grain sizes in Peter snow of various ages are compared. A curious feature of this graph is the systematic decrease of predominant grain size with time in the first year. Waterhouse* attributes this effect to the disaggregation method used in sieve analysis: in breaking the intergranular bonds by grinding, new fine particles are added to the aggregate while many of the original fine particles still remain.

Density, porosity and void ratio

Density is probably the most useful single indicator of snow properties, since grain packing, bond concentration, and structural characteristics generally show some correlation with density. Deposited snow ranges in density from less than 0.1 g/cm^3 for fresh, fluffy masses of dendritic crystals, to more than 0.7 g/cm^3 for snow which has been soaked with water or compressed by overlying layers. When density exceeds 0.8 g/cm^3, the material is classed as ice, since it is no longer permeable.

Density (or unit weight) is given by the mass (or weight) of the sample divided by the sample volume, i.e., the volume of solid grains plus the volume of voids:

$$\gamma = \frac{m_i}{V_s + V_v}$$

*Personal communication within USA CRREL.

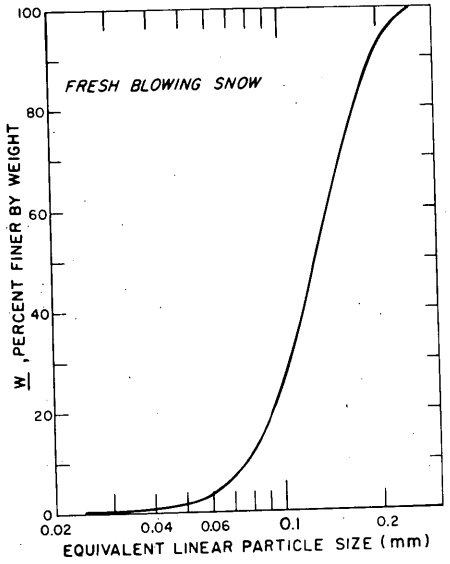

Figure II-1. Cumulative mass curve (grading curve) for fresh blowing snow at an Antarctic station. Samples were collected on glass slides while the snow was actually blowing, and particle sizes were measured using a microscope. (From data by Lister, ref. 12)

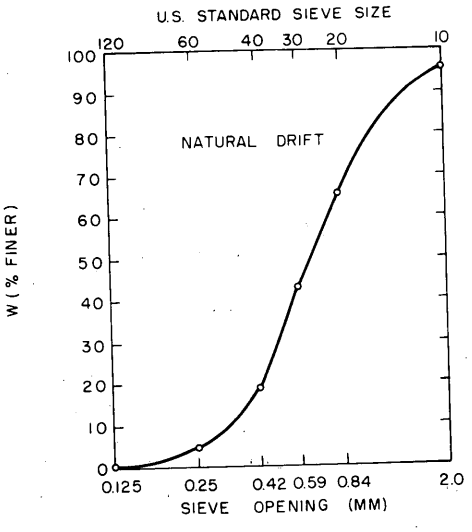

Figure II-2. Grading curve for natural drift snow. The grading was obtained by sieve analysis after disaggregation by rubbing snow on snow, a procedure which may break grains or leave grain separation incomplete. (After Waterhouse, ref. 15)

where

γ = density (usually g/cm^3)

m_i = mass of solid ice grains

V_s = volume of solid ice grains

V_v = volume of voids.

The density of snow expressed in g/cm^3 is numerically equal to the specific gravity, a term which is occasionally used synonymously. In some circumstances it is preferable to use the dimensionless parameters, porosity or void ratio.

Porosity is the ratio of void volume to total volume:

$$n = \frac{V_v}{V_s + V_v} = \frac{\gamma_i - \gamma}{\gamma_i} = 1 - 1.09\gamma$$

where n = porosity and

γ_i = density of solid ice grains (0.917 g/cm^3).

Void ratio $\underline{r}$ is the ratio of void volume to volume of solid ice grains:

$$r = \frac{V_v}{V_s} = \frac{\gamma_i - \gamma}{\gamma} = \frac{n}{1 - n}.$$

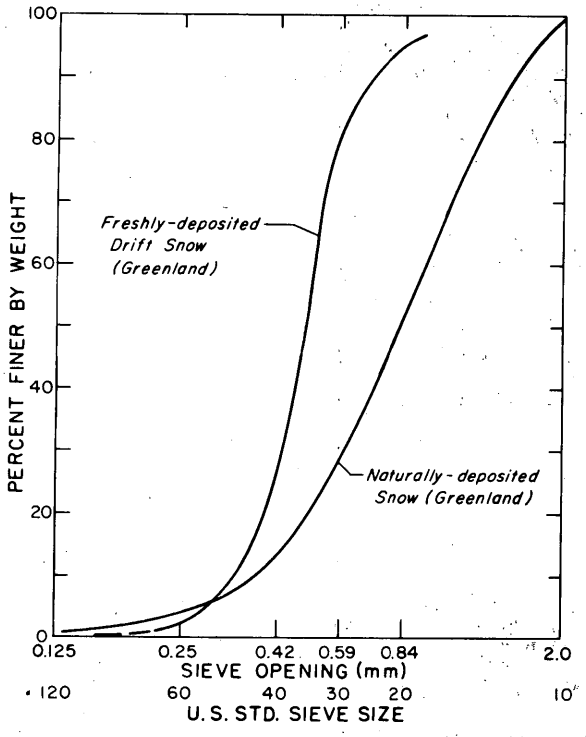

Figure II-3. Grading curves for freshly deposited Greenland drift snow and subsurface snow from the natural snowpack in Greenland. (After Waterhouse, ref. 15)

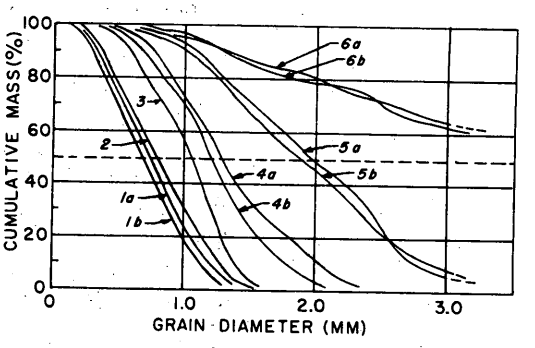

Figure II-4. Grain size distributions for various alpine snows obtained by elutriation. Further data are given by the following key:

Curve	Age (days)	Density (g/cm^3)
1a, 1b	6	0.21
2a, 2b	15	0.29
3	42	0.32
4a, 4b	96	0.28
5a, 5b	118	0.36
6a, 6b	175	0.23

(After DeQuervain, ref. 5)

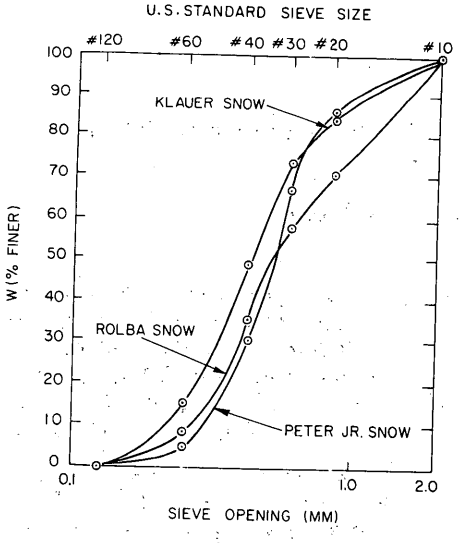

Figure II-5. Grading curves for snows milled by different types of snowplow. (After Wuori, ref. 16)

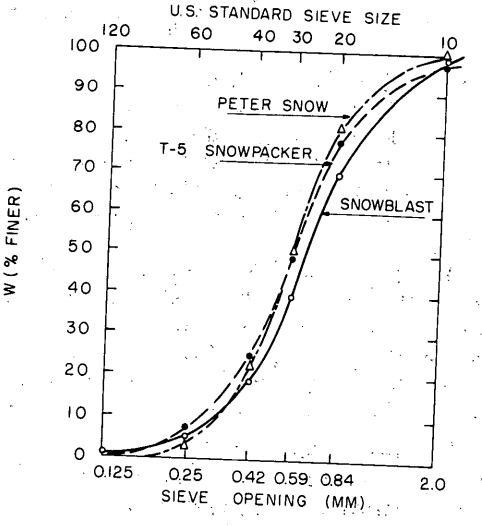

Figure II-6. Grading curves for snows milled by different types of snowplow. (After Wuori, ref. 17)

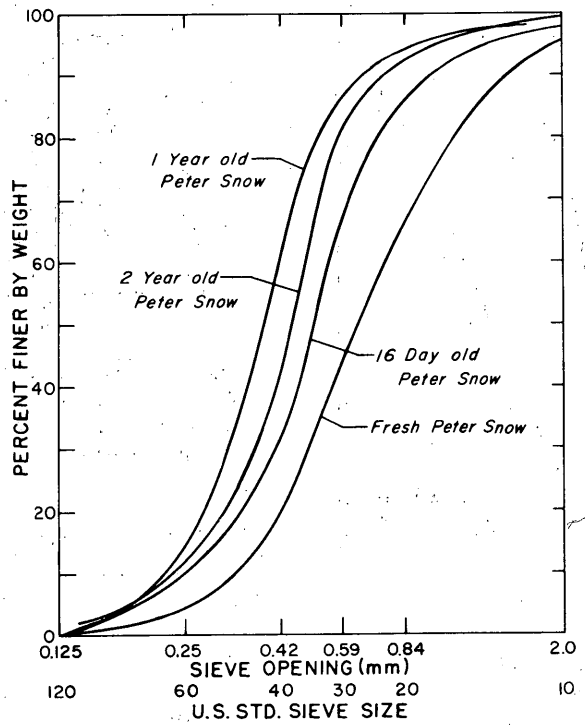

Figure II-7. Grading curves for Peter snow of different ages. See text for explanation of apparent anomalous grain size decrease. (After Waterhouse, ref. 15)

Air permeability

The coefficient of air permeability, K, is defined as

$$K = \frac{Q}{A}\,\frac{L}{\Delta P} = \frac{v}{i} \quad (\mathrm{cm/sec})$$

where Q = rate of air flow by volume ($\mathrm{cm^3/sec}$)
A = cross-sectional area of sample normal to flow direction ($\mathrm{cm^2}$)
L = length of sample in flow direction (cm)
ΔP = air pressure head (cm of water)
v = average flow velocity of air in sample (cm/sec)
i = air pressure gradient ($\Delta P/L$).

Air permeability depends on density (or porosity) and on grain structure (grain size, grading, and bond characteristics). It also varies with temperature as a consequence of the decrease of air viscosity as temperature decreases, but correction of K to a standard temperature can easily be made. If K is to be constant for a given snow, air flow in the pores must be laminar. Experiments give the upper limit of velocity for laminar flow as 5 cm/sec in fine-grained snow and 1 cm/sec in coarse-grained snow.[1]

In Figure II-8 available data on permeability of natural snows are summarized by plotting coefficient of permeability against porosity (and density). In Figure II-9 Bader gives a general impression of the permeabilities of various snow types and corresponding typical grain sizes. Variations of permeability and density with depth below the surface of an ice cap are shown in Figure II-10.

Bader finds empirically that, when snow is compacted artificially, the following relation between permeability K and porosity n holds:

$$K = \frac{anN}{N - n}$$

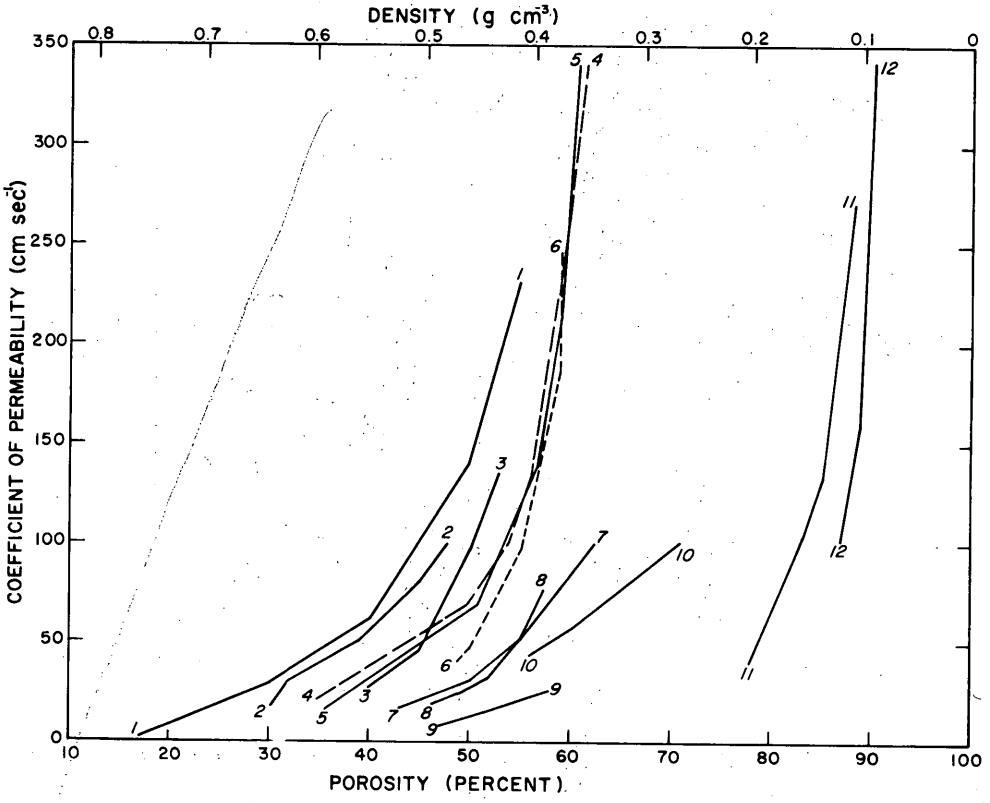

Figure II-8. Coefficient of permeability for snow plotted against density and porosity.

1. Bader, et al. — subsurface snow, Site 2, Greenland.
2. Ramseier — subsurface snow, South Pole.
3. Kotliakov — "last winter's snow", Antarctica.
4. Bender-Waterhouse — subsurface snow, Site 2, Greenland.
5. Bender — coarse-grained snow — grain diam > 1.2 mm.
6. Bader, et al. — snow from top 4 m, Site 2, Greenland.
7. Kotliakov — fresh snow, Antarctica.
8. Bender — old snow.
9. Ishida and Shimizu — granular snow.
10. Ishida and Shimizu — naturally compacted snow.
11. Bender — new snow.
12. Ishida and Shimizu — new snow.

where a and N are constants, determined graphically by plotting $\frac{K}{n}$ against K. The resulting straight line gives a as the intercept on the $\frac{K}{n}$ axis and N as the reciprocal of the slope.

Bender[3] showed that a depends mainly on grain size and suggested the following equation for relating permeability K and grain size d:

$$K = 16.8 \frac{d^{1.63} nN}{N - n}.$$

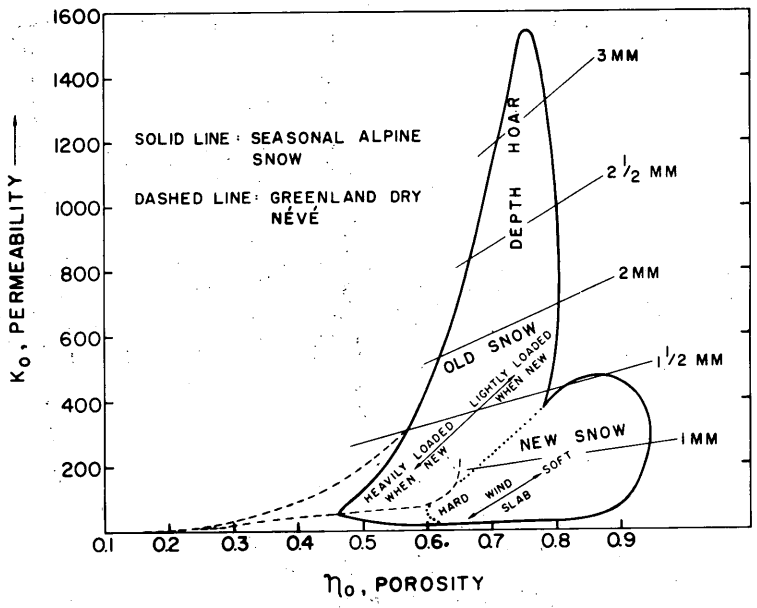

Figure II-9. Range of permeability values for various snow types. (After Bader, ref. 1)

The substitution $a = 16.8\ d^{1.63}$ was derived experimentally, a logarithmic plot of a against d giving a straight line.

Waterhouse [14] has shown that permeability for a snow of given porosity tends to increase with time, indicating that the snow mass becomes more permeable as metamorphism progressively depletes the fine and angular particles. Permeability may therefore give some indication of the degree of bonding in a processed snow.

Bonding and disaggregation of dry snow

A mass of snow grains deposited in cold, dry conditions has little cohesion at first, but soon develops intergranular bonds. In a natural dry snow mass it seems likely that bonds are formed between adjacent grains by two main processes: sublimation and sintering. Both of these processes can take place in isothermal snow masses, and without interstitial convection; under natural conditions, however, they are usually stimulated by temperature gradients and convection in the snow pores.

Sublimation transfer of water molecules results from vapor pressure differences between the grain surfaces. Surfaces with high curvature (small grains and sharp corners) have relatively high surface free energy, i.e., they have a higher vapor pressure than flatter grain surfaces. Hence there is evaporation from areas of high convex curvature and condensation on relatively flat or concave surfaces (larger grains and re-entrants formed by grain contact). Since vapor pressure also increases with temperature, there is also a general mass transfer towards the cold end of a snow mass subject to a temperature gradient.

Sintering is the mechanism by which ice particles adhere and grow bonds, without material transfer in the vapor phase. Kingery[9] explained this phenomenon by surface diffusion of molecules towards the points of contact, though Kuroiwa[11] later concluded that bulk diffusion in the ice grains was more important than surface diffusion. Figure II-11 shows bond growth between ice spheres submerged in cold kerosine, photographed by Kuroiwa.

Overall, the process of bond growth, or age-hardening, represents an expenditure of energy as the grain surfaces in the aggregate become equipotential. Initially, the

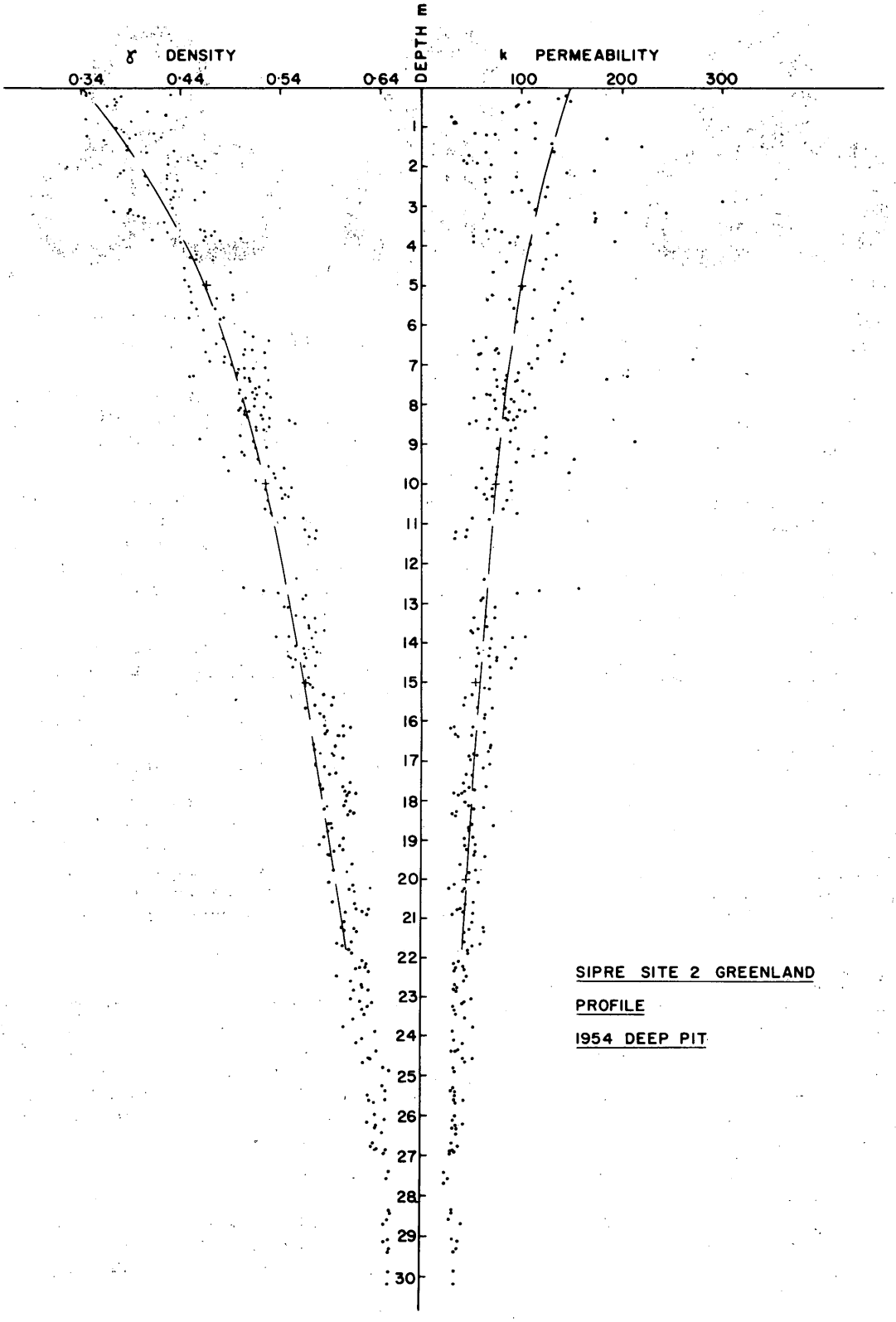

Figure II-10. Changes of air permeability and density with depth below the surface of the Greenland Ice Cap at Site 2. (After Waterhouse, ref. 14)

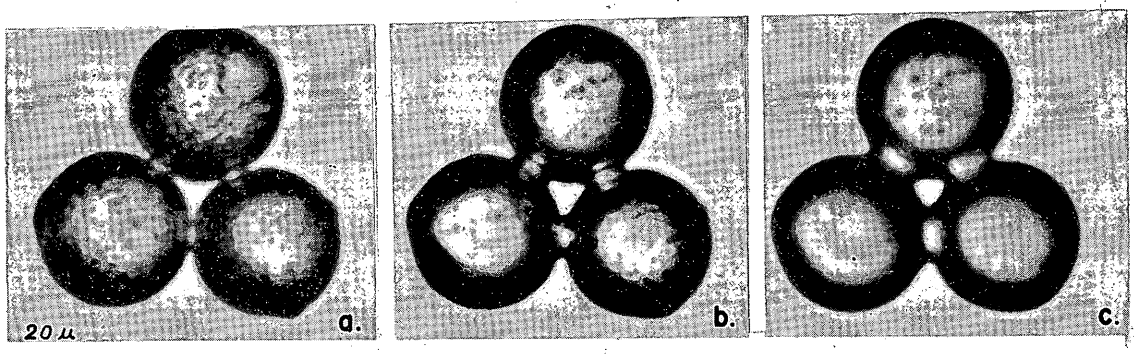

Figure II-11. Growth of ice bonds between three ice spheres immersed in kerosine at -3.5C: (a) after 35 min in contact, (b) after 279 min, (c) after 1369 min. (Photographed by Kuroiwa, ref. 11)

very fine particles, with their large surface to volume ratios, have more surface free energy than the neighboring coarse particles, and an energy gradient exists. In the final age-hardened condition, redistribution of mass has eliminated the energy differences.

Intergranular bond growth and the converse process of mechanical disaggregation are of great practical interest in snow engineering. When snow is moved by disaggregating it, the equivalent of the energy of bond formation has to be expended to destroy the bonds again. As a consequence of disaggregation, however, fine particles are recreated and the snow is "re-energized". This effect explains the use of milled snow (Peter snow) for making load-bearing surfaces and structural elements.

For studies on the energy of disaggregation, a device for measuring the work done when snow is mechanically disaggregated has been developed by Bender.[4] The snow is ground by a spiked wheel, and the driving torque is recorded. As is the case with most mechanical tests, the resulting value is to some extent an arbitrary index, since the work done will vary with the degree of pulverization and will include energy dissipated as heat. Nevertheless, the data should be valuable for a number of purposes.

Figure II-12 shows clearly that the work of disaggregation increases as bonds form during a period of age-hardening. When the snow is fully bonded, the work of disaggregation increases with density (Fig. II-13), as would be expected in view of the correlation between density and bond numbers.[6] Most of the strength tests applied to snow are destructive tests in which bonds are destroyed. It therefore seems reasonable to expect strength to be related to the energy of disaggregation; this is indeed the case, as is shown by the results of Butkovich in Figure II-14.

Mechanical behavior

When high density snow becomes bonded into a cohesive mass by intergranular bond growth it acquires appreciable mechanical strength and is able to resist deformation when load is applied to it. If moderate load is applied for a very short period of time, the snow responds elastically, with strains which are proportional to stress and which are recoverable on removal of the load. If a sustained load is applied, however, the elastic deformation is followed by continuous straining, or creep. Cohesive snow is therefore regarded as a compressible visco-elastic material.

A simplified illustration of the rheological behavior of snow is given by Figure II-15, which shows a strain-time curve for a visco-elastic material to which load is suddenly applied at time zero and suddenly removed again at time t. The various stages of the curve are described in the caption, and are also explained in terms of the spring and dashpot analog shown above the graph (a combination of Maxwell and Voigt rheological models in series).

The Maxwell-Voigt model of Figure II-15 gives a useful representation of the response to a given load for a restricted range of total strain. If snow is severely strained, though, its properties alter and strain rate consequently varies (stage 3 of

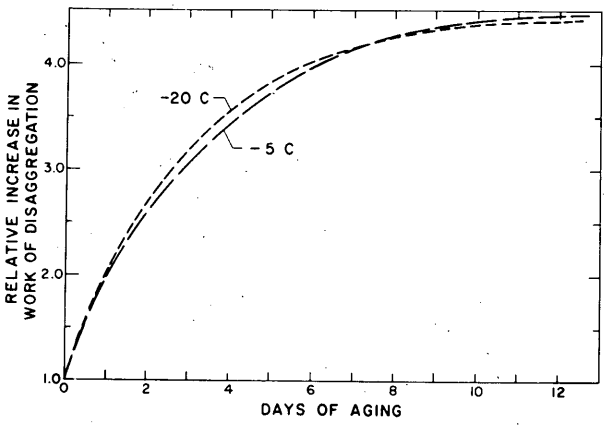

Figure II-12. Increase in the work of disaggregation with time during a period of age hardening. (From Jellinek, ref. 8)

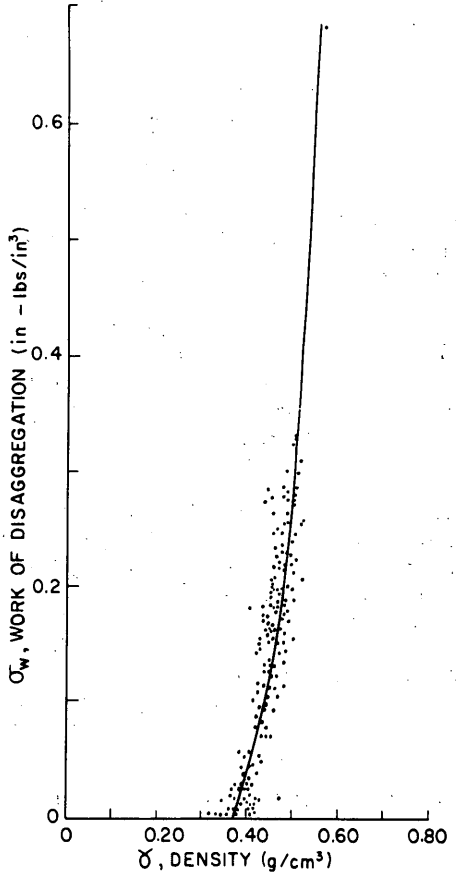

Figure II-13. Work of disaggregation as a function of density for well-bonded snow, from tests by Bender. (After Butkovich, ref. 4)

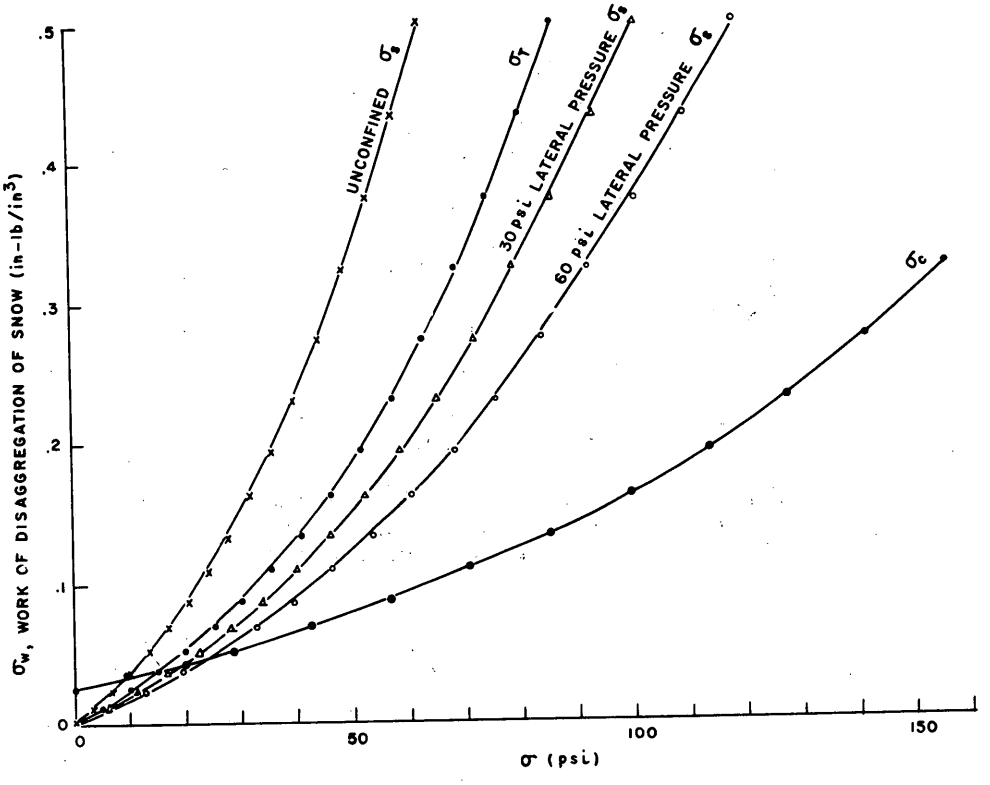

Figure II-14. Work of disaggregation as a function of ultimate strength, as determined by compressive, tensile and shear tests of short duration. (After Butkovich, ref. 4)

Figure II-15 becomes nonlinear). In terms of the analog, the viscosity of dashpot B changes with strain. The model also becomes inapplicable if stress is allowed to vary widely, since snow exhibits Newtonian viscosity only at low stresses (say less than 700 g/cm^2) — at higher stresses, strain rate becomes an increasingly strong function of stress. This would therefore require the viscosity of dashpot B to be dependent on stress.

If the load is sustained indefinitely (instead of unloading after time t), then the rate of straining may start to increase after a certain length of time, assuming that the snow is free to strain continuously (if it is not free, straining may come to a halt). This stage of accelerating creep is usually referred to as tertiary creep, and it marks the onset of failure. Figure II-16 illustrates the transition to tertiary creep schematically. The parameter is stress ($\sigma_1 < \sigma_n < \sigma_5$); it is seen that at low stresses tertiary creep may be delayed indefinitely, but as stress increases tertiary creep, and therefore failure, appears progressively earlier. Creep tests are usually made with a fixed stress on each snow sample which is low enough so that tertiary creep never appears during the test, which may run for as much as 1 year.

In the following two chapters the elastic and visco-plastic properties of snow will be reviewed separately.

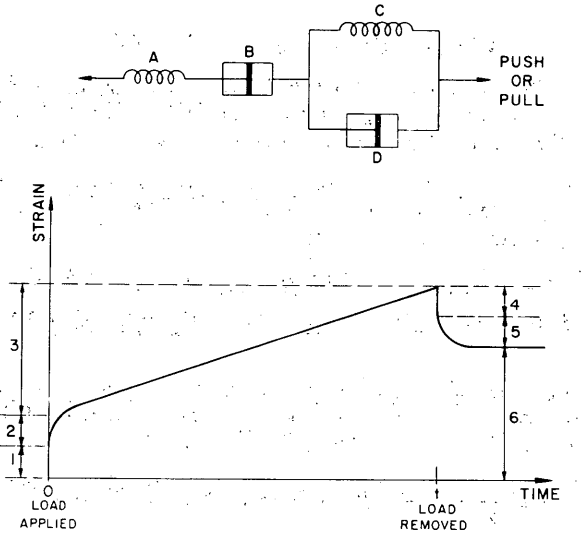

Figure II-15. Strain-time curve for a simple visco-elastic material, with a rheological analog. The stages of the curve are as follows:

Stage 1 — On application of load, instantaneous elastic response occurs (spring A extends or compresses).

Stage 2 — Creep begins, and the "delayed elastic" response occurs (dashpot D slides, but comes to a stop as spring C extends or compresses; dashpot B slides at a steady rate).

Stage 3 — Creep (secondary creep, or quasi-viscous flow) proceeds at a steady rate (dashpot B slides; elements A, C and D are immobile)

Stage 4 — On removal of load, instantaneous elastic recovery takes place (spring A unloads). Strain is equal in magnitude to that of Stage 1.

Stage 5 — Relaxation of the "delayed elastic" component of strain occurs (spring C relaxes, but return is damped by dashpot D). Strain is equal in magnitude to that of Stage 2.

Stage 6 — The permanent strain resulting from creep up to time t. (The amount of travel which occurred in dashpot B.) Strain is equal to that of Stage 3.

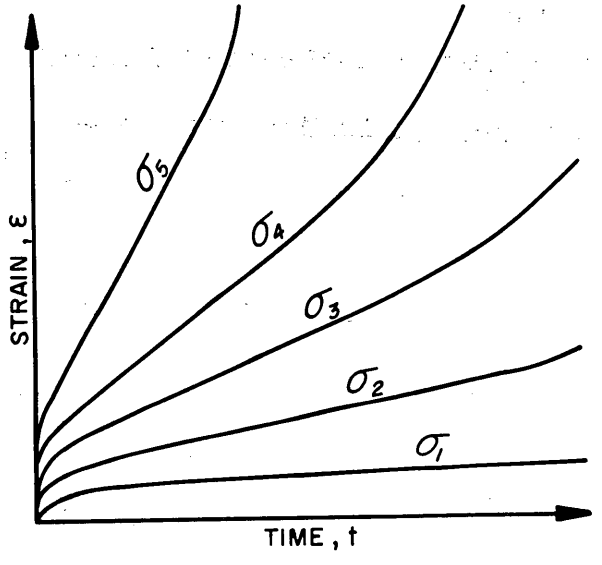

Figure II-16. Schematic creep curves for various stresses, showing onset of tertiary creep.

CHAPTER II REFERENCES

1. Bader, H. (1962) "Snow as a material" in Cold Regions Science and Engineering (F. J. Sanger, Editor), U. S. Army Cold Regions Research and Engineering Laboratory (USA CRREL) monographs, Part II, Sect. B.
2. _____ et al. (1955) Excavations and installations at SIPRE test site, Site 2, Greenland, U. S. Army Snow Ice and Permafrost Research Establishment (USA SIPRE) Technical Report 20.
3. Bender, J. A. (1957) Air permeability of snow, USA SIPRE Research Report 37.
4. Butkovich, T. (1956) Strength studies of high density snow, USA SIPRE Research Report 18.
5. DeQuervain, M. (1948) Korngrössenanalyse von Altschnee durch Sedimentation (Grain size analysis of old snow by sedimentation), Schweizerische Bouzeitung, vol. 66, no. 7, p. 117-118 (text in German).
6. Fuchs, A. (1959) Some structural properties of Greenland snow, USA SIPRE Research Report 42.
7. Ishida, T. and Shimizu, H. (1955) Sekisetsu no tsūki teikō (Daippo) (Resistance of air flow through snow layers (Part I), Teion-Kagaku, Series A, vol. 14, USA SIPRE Translation 60, 1958.
8. Jellinek, H. H. G. (1957) Compressive strength properties of snow, USA SIPRE Research Report 34.
9. Kingery, W. D. (1960) Regelation, surface diffusion and ice sintering, Journal of Applied Physics, vol. 31, p. 833-838.
10. Kotlyakov, V. M. (1961) Snezhnyy pokrov Antarktidy i yego rol'v sovremennom oledenenii materika (Snow cover in the Antarctic and its role in modern glaciation of the continent), Akad. Nauk SSSR, IGY Research Results, Glaciology, no. 7.
11. Kuroiwa, D. (1962) A study of ice sintering, USA CRREL Research Report 86.
12. Lister, H. (1960) Glaciology — solid precipitation and drift snow, Trans-Antarctic Expedition 1955-58, Scientific Reports, no. 5 (London).
13. Ramseier, R. O. (In press) Some physical properties of snow at the South Pole, USA CRREL Research Report 116.
14. Waterhouse, R. W. (1962) Analysis of data from a snow profile, USA CRREL Research Report 90.
15. _____ Personal communication.
16. Wuori, A. F. (1959) Preliminary snow compaction field tests using dry processing methods, USA SIPRE Technical Report 53.
17. _____ (1963) Snow stabilization for roads and runways, USA CRREL Technical Report 83.

CHAPTER III. ELASTIC BEHAVIOR AND ULTIMATE STRENGTH UNDER RAPID LOADING

Snow behaves elastically only under loadings of short duration, with strains small enough to be accommodated without disruption of the grain structure. When rapid strains are so big that the original grain structure is disrupted or destroyed the snow is considered to have "failed", and the maximum stress mobilized in causing failure is taken as the "ultimate strength" of the snow. When a sample is tested to failure in tension, unconfined compression, or unrestrained* shear, the resulting failure is destructive, i.e. there is a complete loss of strength after failure. When a sample is tested in restrained* shear or in confined compression, some strength remains after the initial yield. Snow under strong lateral confinement may become stronger after the initial collapse, since there is an increase of density, and higher stresses must be applied to cause further collapse.

Elastic considerations apply to problems where loads are applied by moving wheels, skis, or feet, by explosive or other impacts, or by blast overpressures. They also apply to small amplitude vibrations, where repeated stress reversal prevents permanent visco-plastic straining.

When testing snow under elastic conditions, and particularly in testing ultimate strength, the sample must be stressed at a speed fast enough to prevent any significant viscous deformation. From the results of laboratory tests Butkovich[12] recommends that load be applied at a rate higher than 0.5 kg/cm^2-sec to cause a sample to fail under elastic conditions (loading rate and strain rate are linearly related under these conditions). The writer finds, however, that rates about twice those used by Butkovich are desirable for tests made at temperatures above -10C.

The ultimate strength of snow is related to the index properties of density, temperature and grain structure. Of these, density (which actually correlates with grain structure) is by far the most significant for cold, dry snow which has age-hardened.†

As density increases, strength increases. Young's modulus and Poisson's ratio also increase with increasing density. Below a density of about 0.4 g/cm^3, snow has very little strength. In this low density range, strength does not appear to be a strong function of density, but seems to depend mainly on grain texture and structure. Low density snow has an open, weakly-bonded grain structure in which grains have considerable freedom of movement, so that the snow is readily compressible. Very high density snow, say of density higher than 0.55 g/cm^3, is relatively strong, and strength is heavily dependent on density. The grains are closely packed, so that the snow can be deformed only by straining the actual grains and the bonds connecting them. A number of workers have noted discontinuities when various density-dependent physical properties for cold snow are plotted against density, and densities of about 0.4 and 0.55 g/cm^3 have been mentioned as significant values for change of behavior. The higher value appears to be the density achieved when the grains are packed as closely as is possible without straining them. This density, corresponding to maximum packing, will vary to some extent with the size, shape and grading of the grains; 0.55 g/cm^3 is probably representative of maximum packing** for a well-graded, milled snow (e.g., Peter snow), while 0.50 g/cm^3 is given by Bader[5] as the density of closest packing for natural dry snow.

Abrupt changes of relationships at certain densities continue to be remarked, and there is probably physical significance in the observations. However, the influence of temperature on these features has not been adequately considered, so that the "magic numbers" for density should be regarded with caution.

The influence of temperature on ultimate strength has not previously been investigated systematically. Bender[6] summarized the scanty data available in 1957 and represented them by an expression which in effect assumes strength s to be proportional to the one-sixth root of degrees of departure from the freezing point:

---

* "Unrestrained shear" is used here to mean shear at zero normal pressure on the shear plane. "Restrained shear" is shear under an applied normal pressure.

† The unqualified term "density" in this section implies that the snow is age-hardened.

** Densities greater than 0.6 g/cm^3 have been attained at times.

$$\log \frac{s_2}{s_1} = 0.16 \log \frac{t_2}{t_1} \quad (1)$$

where t is the number of degrees below freezing.

From measurements made with the Canadian hardness gage, Gold[15] proposed an exponential relation

$$\frac{H_2}{H_1} = e^{-0.063 (T_2 - T_1)} \quad (2)$$

where H is hardness and T is temperature in degrees C.

Data on changes of Young's modulus with change of temperature are given by Nakaya[23, 25] and by Yosida, et al.[35] but they are insufficient to define a general relationship.

Preliminary results from current CRREL tests (by J. H. Smith and the writer) suggest that the change of unconfined compressive strength with temperature might be represented by an expression of the form

$$\sigma - \sigma_0 = a e^{-\frac{b}{t}} \quad (3)$$

where σ is unconfined compressive strength, σ_0 is strength at (or fractionally below) 0C, t is the number of degrees C below 0C, a is a coefficient dependent largely on density (the value of $\sigma - \sigma_0$ for very low temperatures), and b is a constant for a given grain geometry.

The form of the relationship between strength and temperature may change with the type of test used. During failure in restrained shear, for example, intergranular friction is mobilized, in contrast to the failure behavior in tension.

The grain structure of snow influences its strength and elasticity, but the difficulties of measuring and describing grain structure have inhibited formulation of concise relationships. In low density snows the structure may vary considerably, being largely dependent on the size and shape of the constituent grains. This variability is reflected in the strength properties. In high density snow there is less variability of grain shape, and overall structural characteristics depend more on the degree of bonding. In fine-grained dry snow, bond strength usually increases with time at a decelerating rate, temperature being a rate-controlling parameter. Under certain conditions of vapor transfer a snow layer may change into a weakly-bonded mass of coarse grains (depth hoar), which has little strength under unconfined uniaxial loading but which can have appreciable strength in fully confined compression or restrained shear.

Young's modulus for dry snow

Young's modulus is equivalent to the modulus of spring A in the analog of Figure II-15. Since it is not really practical to measure the "static" modulus by observing stress-strain ratios, the sonic or dynamic modulus is measured by applying high frequency elastic vibrations. This can be done by vibrating a small bar of snow and finding its resonant frequency electronically[23], by using the soniscope[22], or by measuring velocities of elastic compression and shear waves in situ by seismic methods.

Young's modulus has been found to be dependent on snow density, temperature, and grain structure (grain size and bond characteristics). Available data are summarized in Figure III-1, where Young's modulus is plotted against density. All the snows tested were age-hardened, but they came from widely separated sites. The agreement is therefore remarkably close. The data from Crary et al. have not been adjusted for temperature, but such an adjustment (from -27 to -10C) would further improve the agreement.

Figure III-2 shows the increase of Young's modulus as temperature falls down to -180C, the two curves being for snows of different density. The total change in E from -5 to -180C is only about 20%. Figure III-3 shows a stronger temperature dependence in the range -2 to -10C.

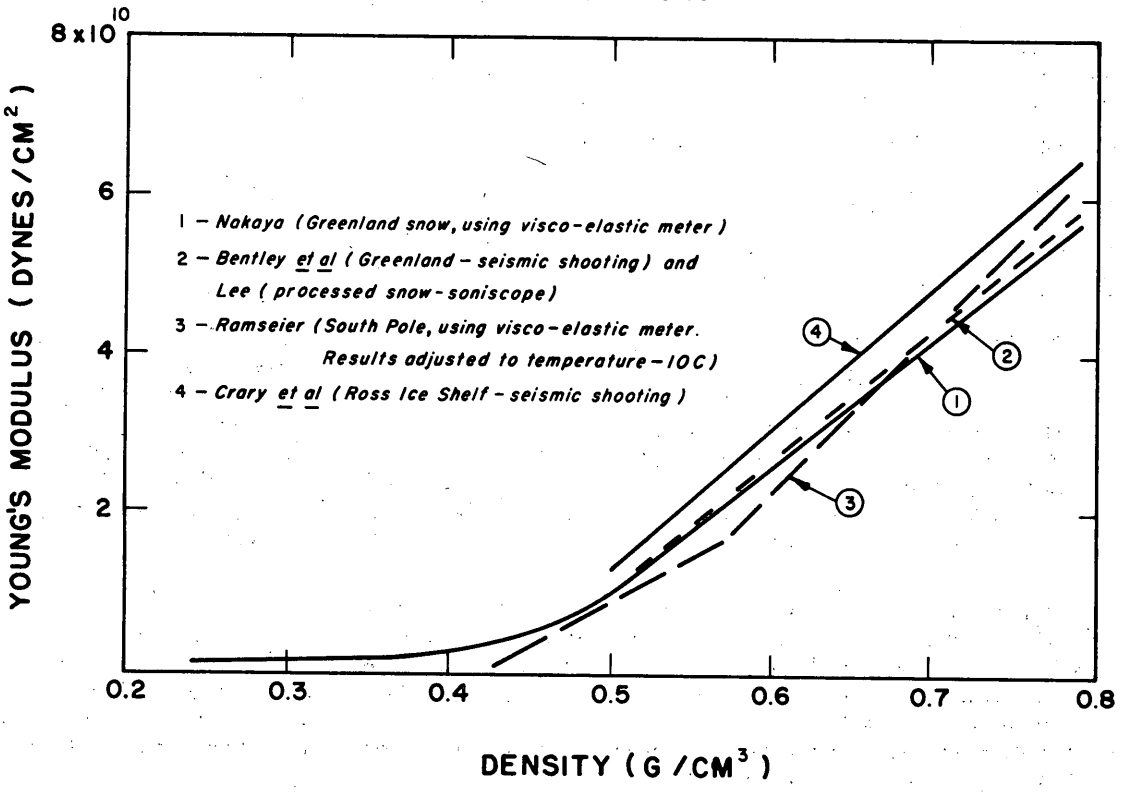

Figure III-1. Dynamic Young's modulus for dry, bonded snow as a function of density.

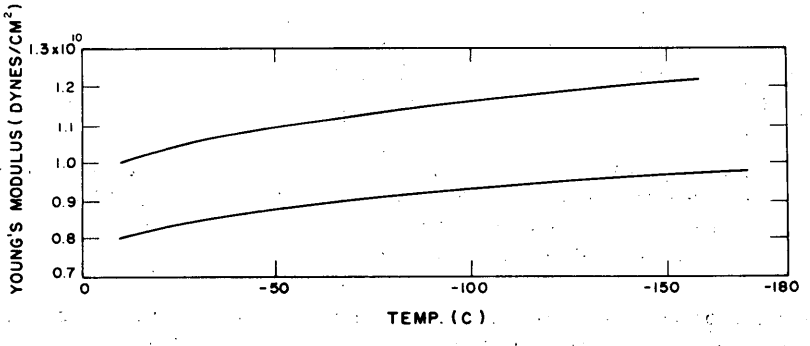

Figure III-2. Dynamic Young's modulus as a function of temperature, for temperatures down to -180C. The two curves are for snows of different densities. (After Nakaya, ref. 25)

It is difficult to show relationships between Young's modulus and grain structure because of present inability to assign numerical values to structural characteristics. However, in Figure III-4 the increase of Young's modulus during age-hardening of Peter snow is shown, thus demonstrating the effects of intergranular bond formation.

Poisson's ratio for dry snow

Poisson's ratio for dry, bonded snow has been calculated mainly from elastic vibration of snow. Most of these values come from seismic measurements in undisturbed snow. Some other measurements have been made by permanent visco-plastic deformation of laboratory specimens, but these data are in rather poor agreement.

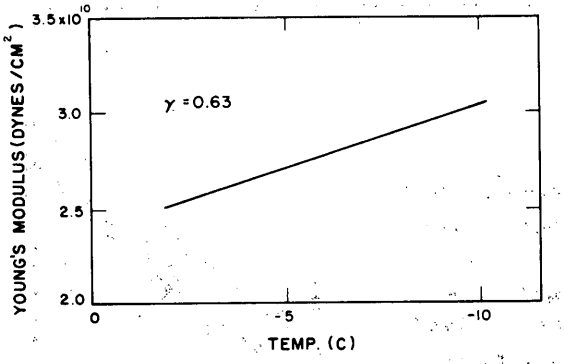

Figure III-3. Dynamic Young's modulus as a function of temperature in the range -2 to -10C. (After Nakaya, ref. 23)

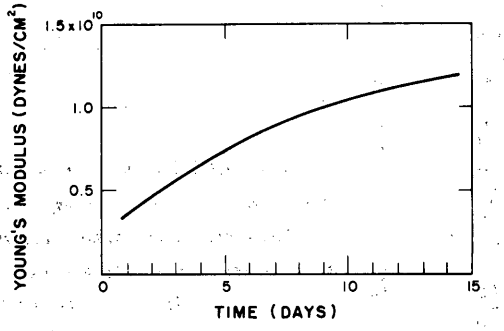

Figure III-4. Dynamic Young's modulus as a function of time during the period of intergranular bond formation (age-hardening). (After Nakaya, ref. 25)

Elastic. Available data for elastic tests are summarized in Figure III-5, where Poisson's ratio is plotted against snow density. For high density snow in the range 0.6 to 0.8 g/cm^3 the findings agree quite well, ν being between 0.26 and 0.29 at density 0.6 g/cm^3 and around 0.3 or 0.31 at density 0.8 g/cm^3. Below 0.6 g/cm^3 there is considerable scatter; some of this is probably real and attributable to structural difference in less dense snow, but some is probably due to shortcomings of the seismic technique when applied to layers near the surface.

For some working purposes it has been convenient to adopt a simple expression for ν in the density range 0.4 - 0.7 g/cm^3, representing the data of Bentley et al.[7] by

$$\nu = 0.15\,\gamma + 0.2 \qquad (4)$$

where γ is density in g/cm^3.

Inelastic. For describing the ratio of lateral to vertical strains in snow samples which have been permanently deformed, European workers have used a "cross-section number";* designated by the letter m. This is the inverse of "Poisson's ratio" for viscous straining.

Since snow is compressible, we expect ν to vary considerably with density; incompressible ice should show a ν value equal to 0.5, while highly compressible, very low-density snow ought to have a ν value approaching zero. This is borne out to some extent by Figure III-6, which summarizes available data.

One rather surprising feature of Figure III-6 is the shape of the curve representing the data of Bader et al.[32] Most density-dependent physical properties approach the limiting ice value asymptotically, but this curve shows the strongest density-dependence in the ice region, i.e., for densities between 0.8 and 0.91 g/cm^3. The data for the curve were obtained by straining samples in unconfined compression under constant load, vertical and lateral strains being measured from time to time. The "Poisson's ratio" values might therefore be regarded as transient values; they should be smaller than "steady state" values. This can be reasoned as follows: If the press were to be stopped, the vertical dimension would remain constant while the lateral dimension increased with time, lateral creep relieving the stress in the sample.

The above remarks, and the data of Figure III-6, refer to snow stressed uniaxially. For snow under triaxial stress (the usual situation in real problems) those values of Poisson's ratio may not apply.

---

*Also called Poisson's number.

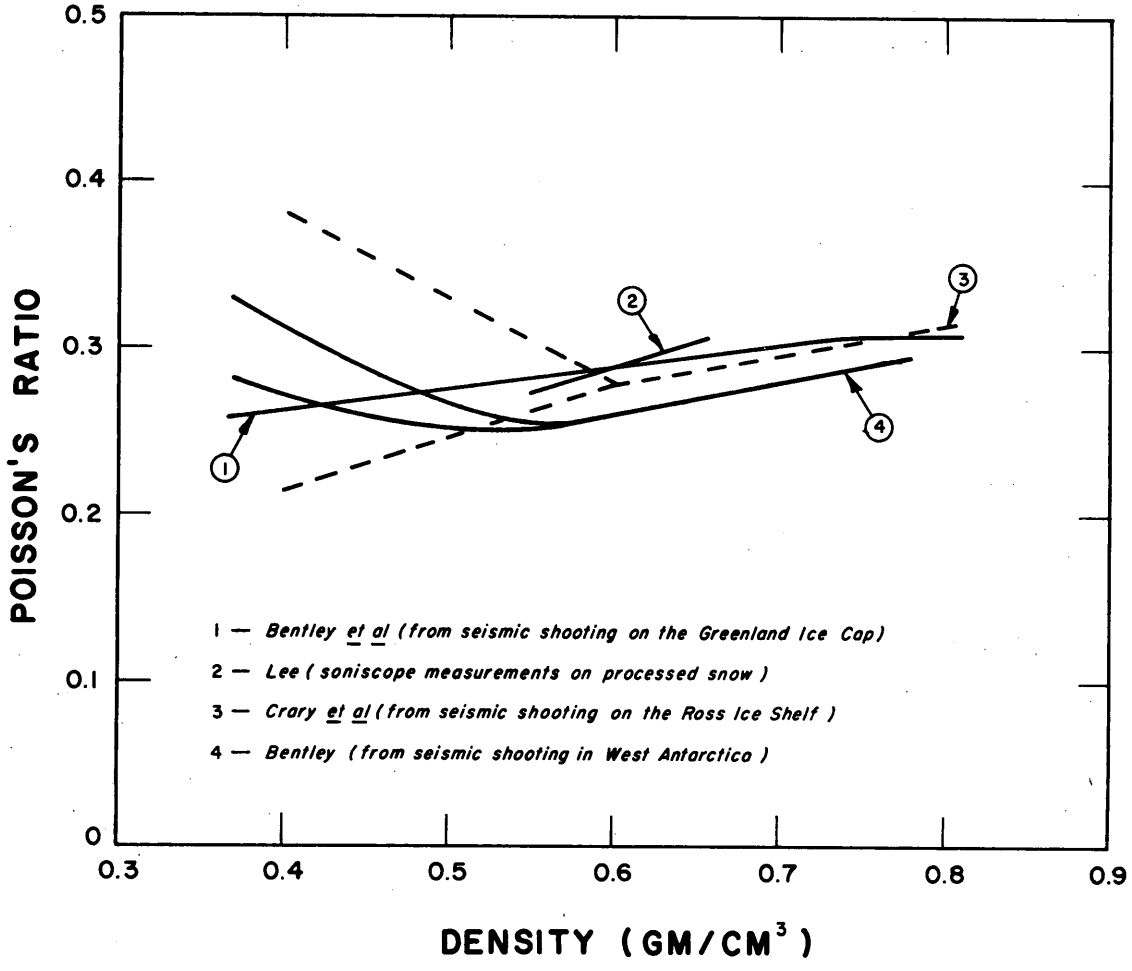

Figure III-5. Poisson's ratio for dry snow as a function of density. The values presented here were obtained by non-destructive elastic tests.

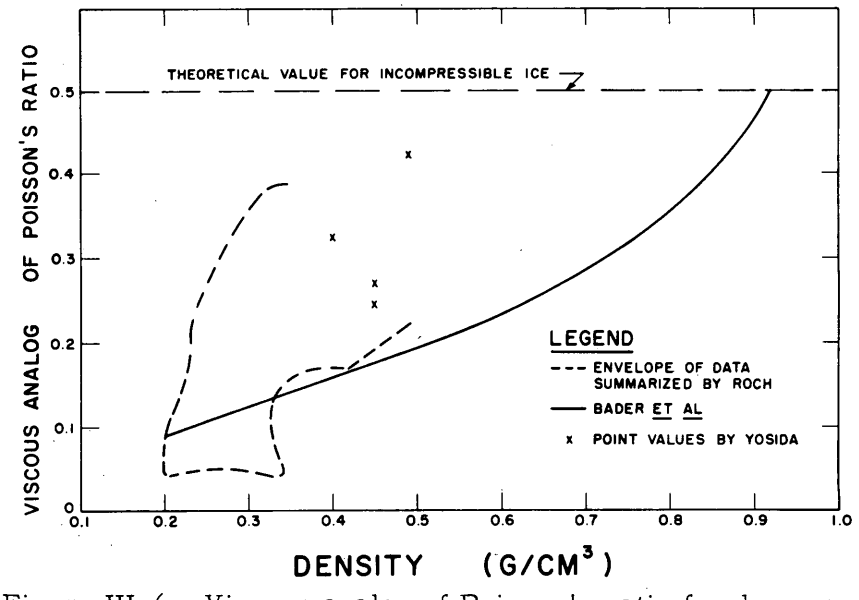

Figure III-6. Viscous analog of Poisson's ratio for dry snow as a function of density. These values were deduced from permanent visco-plastic strains.

To sum up, for problems of snow under sustained loading, any analysis which embodies "Poisson's ratio" should be regarded with suspicion.

Elastic wave propagation (for sonic frequencies)

The velocities of propagation of elastic waves in snow are dependent on density, on Young's modulus (which is itself density-dependent), and on Poisson's ratio*; such wave velocities can therefore be related directly with density, temperature and grain structure.

Figure III-7 gives a number of curves relating the velocity of an elastic dilatational wave (compression wave, or P-wave) and snow density. The results refer mainly to naturally compacted snow in situ, since most of the data are derived from seismic experiments. They have not been adjusted to a common temperature, since indications are that the temperature effect is small.

If Poisson's ratio is not affected by temperature it is reasonable to expect that P-wave velocity will be relatively insensitive to temperature change, since Young's modulus, the only temperature-dependent factor, is only slightly affected by temperature and therefore its square root will show even less variation. Robin's work[28] on ice indicates that a temperature drop of one degree C increases the velocity by 2.3 m/sec (of the order of 0.1% for dense snow).

Figure III-8 illustrates the dependence of wave velocity on grain structure. The curves show how velocity increases as snow age-hardens under cold conditions, and steps in the curves show the effects of structural changes caused by thaw and freeze.

Unconfined compressive strength

Systematic testing of naturally compacted snow in unconfined compression has been carried out in Greenland by Butkovich[12] and in Antarctica by Ramseier[26]. Both investigators crushed cylindrical specimens in a manually controlled press fitted with proving ring and dial gage for load indication. Loading rates exceeded 0.5 kg/cm^2-sec. Tests on snow processed by rotary snow plows have been made by Abele[1], Brunke[9] and Wuori[33, 36]. In these tests a controlled strain rate was used — initially 0.2 in./min, which was perhaps too slow, and later 1.0 in./min. At the time of writing further CRREL tests by Smith and Mellor are in progress; artificially prepared, homogeneous specimens are crushed with density and temperature as variables. Press speeds of 6 in./min are used.

The results of Butkovich are shown in Figure III-9, where unconfined compressive strength is plotted against density for a temperature of -10C. Snows of density less than 0.4 g/cm^3 are seen to have very little strength, while the strength of snows with densities greater than 0.4 g/cm^3 can be approximately represented by the empirical equation

$$\sigma_c = 1418\,(\gamma - 0.39) \qquad (5)$$

where σ_c is the unconfined compressive strength at -10C (psi), and γ is density in g/cm^3.

Ramseier's tests were made at the South Pole at a temperature of -50C (Fig. III-10). All samples with densities less than 0.42 g/cm^3 had low strengths, and snows with densities in excess of 0.42 g/cm^3 showed an approximately linear dependence of strength on density. For snow denser than 0.42 g/cm^3, the results can be represented approximately by the equation

$$\sigma_c = 164.2\,(\gamma - 0.42) \qquad (6)$$

where σ_c is now unconfined compressive strength at -50C (kg/cm^2), and γ is density in g/cm^3.

---

*$V_p = \left[\frac{E}{\gamma}\,\frac{(1-\nu)}{(1-2\nu)(1+\nu)}\right]^{\frac{1}{2}}$ where E = Young's modulus, γ = density, and ν = Poisson's ratio.

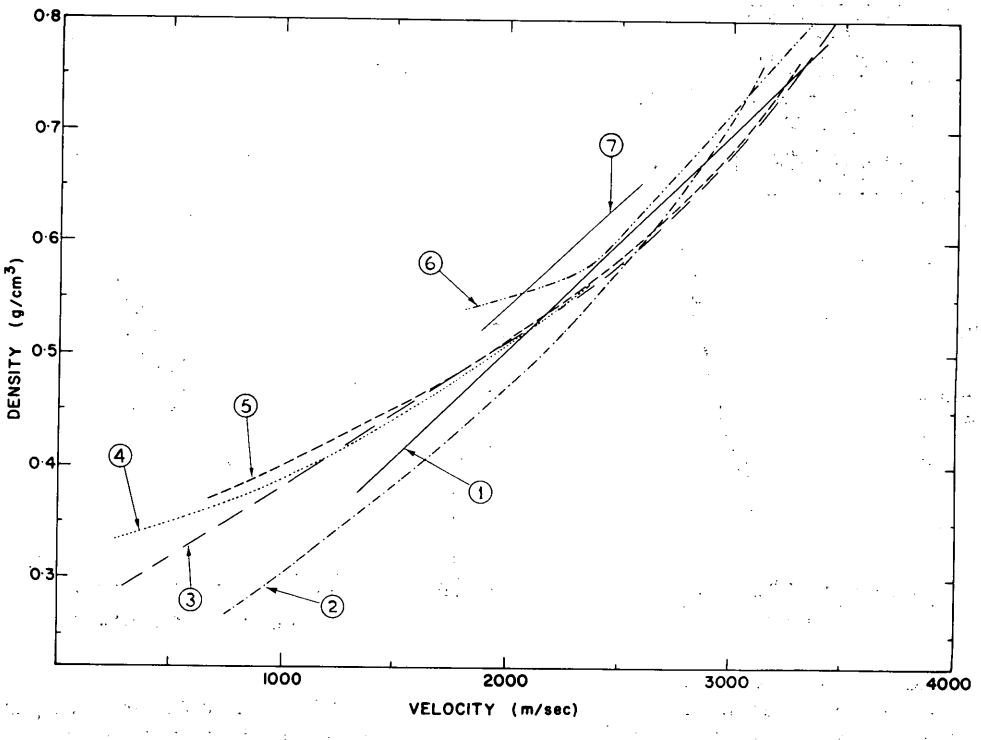

Figure III-7. Velocity of an elastic compression wave in snow as a function of density.

1 — Robin — Jungfraujoch
2 — Robin — laboratory
3 — Crary, et al. — Ross Ice Shelf
4 — Roethlisberger — Greenland
5 — Bentley, et al. — Greenland
6 — Robin — Maudheim
7 — Lee — processed snow

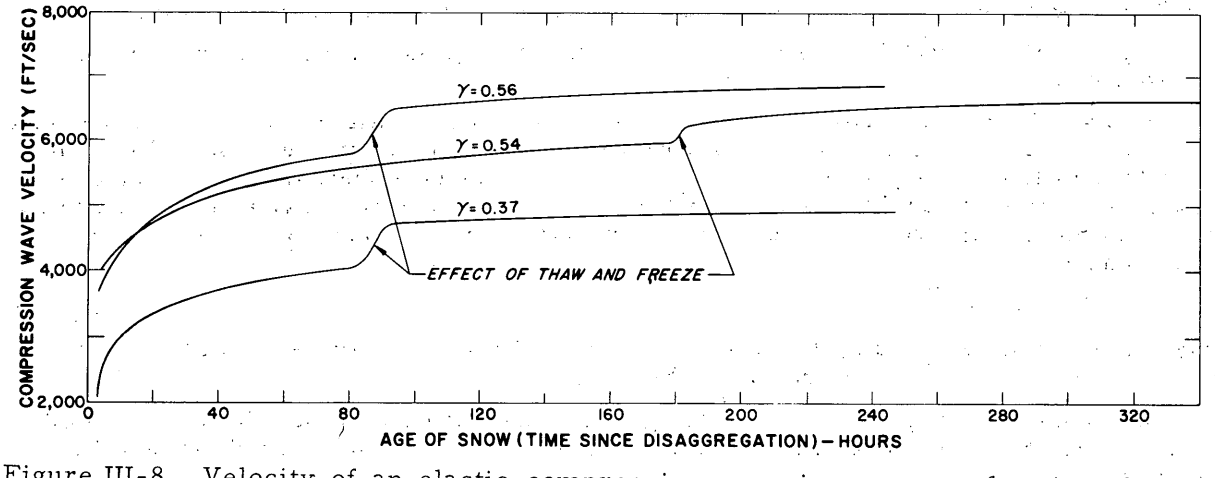

Figure III-8. Velocity of an elastic compression wave in snow as a function of time during the period of intergranular bond formation (age-hardening). (After Lee, ref. 22)

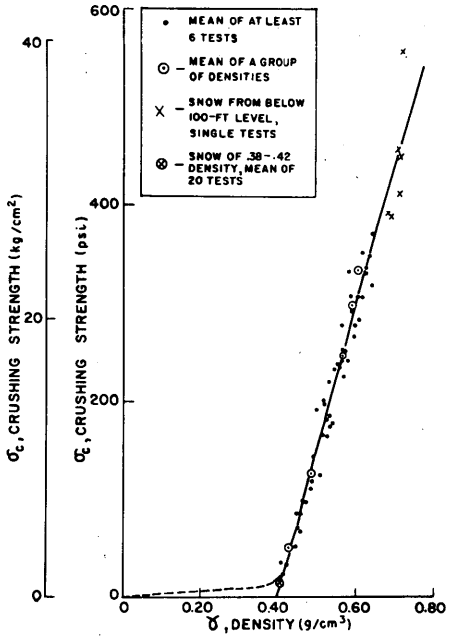

Figure III-9. Unconfined compressive strength as a function of density for snow at Site 2, Greenland. The results are adjusted to a common temperature of -10C.
(After Butkovich, ref. 12)

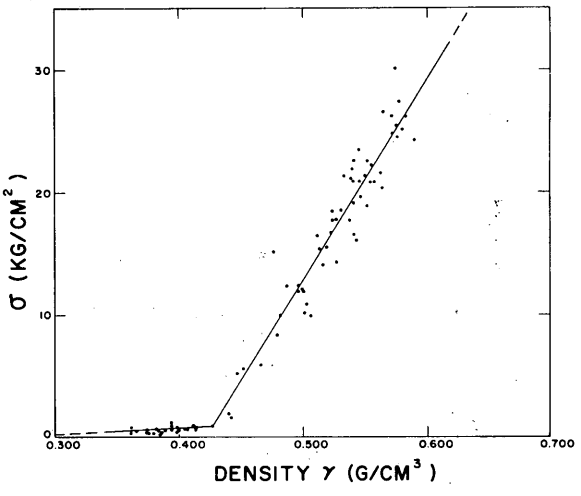

Figure III-10. Unconfined compressive strength as a function of density for snow at the South Pole (temp -50C).
(After Ramseier, ref. 26)

Figures III-11-14 give data on the unconfined compressive strength of snow which has been comminuted by a Peter snow miller (rotary snowplow) and compacted after redeposition. Most of the samples had been age-hardened for 13 days or more before being crushed at a temperature of -13C (±3C). The strength of the Peter snow for any given density is rather less than the strength of naturally-compacted snow of the same density. This can probably be attributed to the shorter time for bond formation (shorter age-hardening period) and the lower sustained contact stresses between grains.

Figures III-15 and III-16 give strength data for snow comminuted by a Snowblast rotary plow.

Straight-line approximations of the strength-density relation are clearly unsatisfactory, as they fail to meet reasonable boundary conditions and misrepresent the transitions to both low density snow and ice. The writer suspects that void ratio may express density in a more tractable form and preliminary results from current tests tend to confirm this notion; unconfined compressive strength σ and void ratio $\underline{r}$ can be related empirically by

$$\sigma = \sigma_i e^{-ar^2} \tag{7}$$

where a is a constant and σ_i denotes the strength of ice. Extrapolation of the linear plots of $\ln\sigma$ against r^2 gives credible values for σ_i.

The scant published evidence relating to temperature effects has been mentioned already; the work mentioned in connection with eq 3, as yet unpublished, yields the relation

$$\frac{\sigma_\theta - \sigma_0}{\sigma_{-10}} = 1.73\, e^{\frac{-4.76}{\theta}} \tag{3a}$$

where σ_θ = strength of a given snow at any temperature, θC below 0C

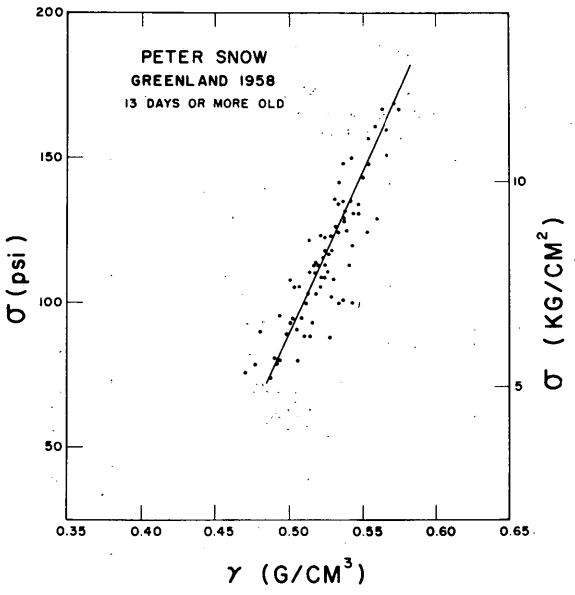

Figure III-11. Unconfined compressive strength as a function of density for Peter snow aged 13 days or more. (Greenland, 1958)(Data by Wuori, ref. 36 and Brunke, ref. 9)

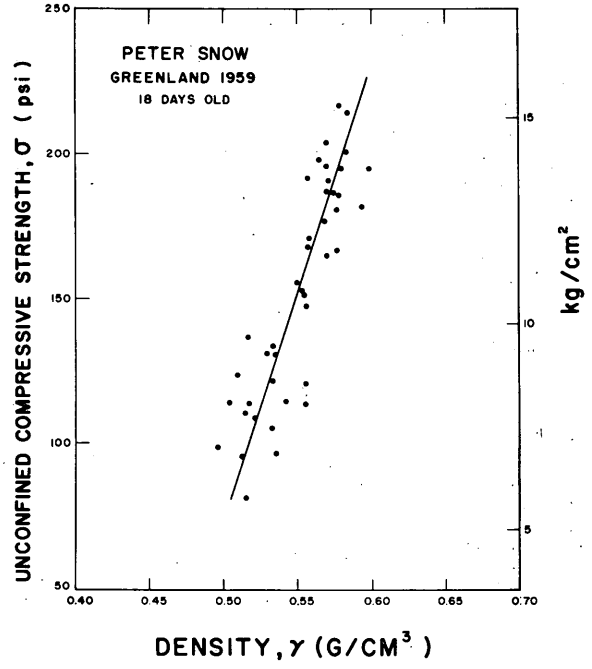

Figure III-12. Unconfined compressive strength as a function of density for Peter snow aged for 18 days. (Greenland, 1959) (Data by Abele, ref. 1)

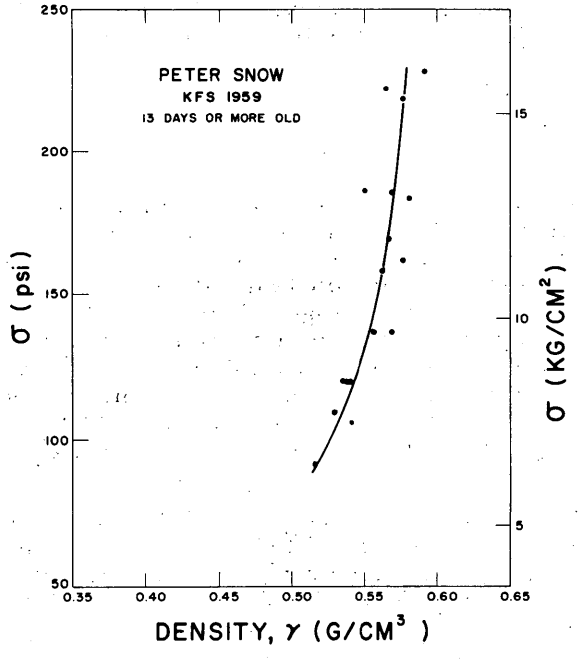

Figure III-13. Unconfined compressive strength as a function of density for Peter snow aged 13 days or more. (Keweenaw Field Station, 1959) (Data by Abele, ref. 1 and Wuori, ref. 33)

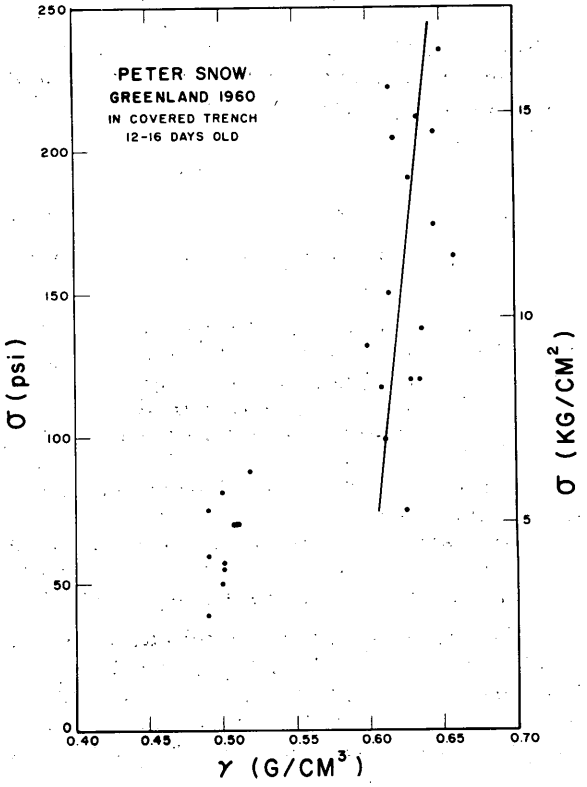

Figure III-14. Unconfined compressive strength as a function of density for Peter snow aged in a covered trench for 12-16 days. (Greenland, 1960) (Data by Abele, ref. 1)

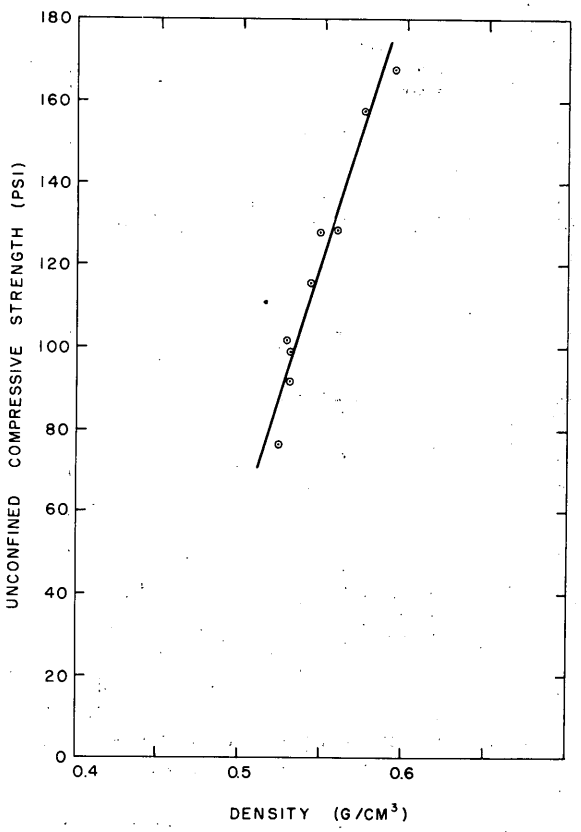

Figure III-15. Unconfined compressive strength of snow milled by a Snowblast rotary plow. (Data by Wuori, ref. 33)

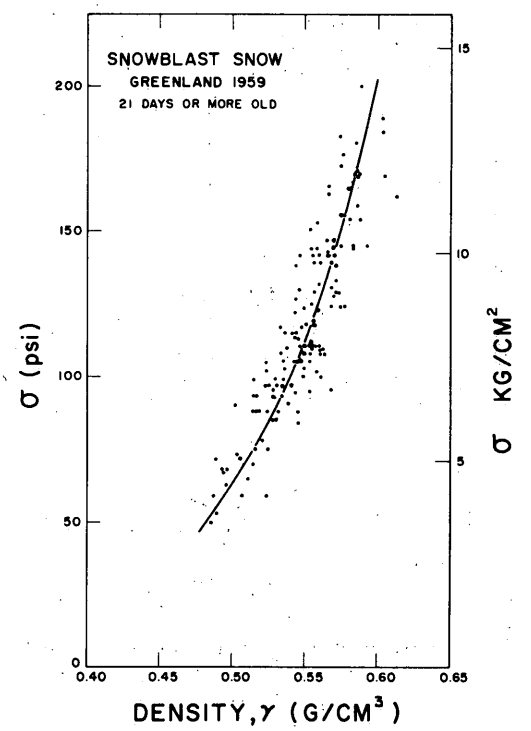

Figure III-16. Unconfined compressive strength of snow milled by a Snowblast rotary plow and aged for 21 days or more. (Greenland, 1959) (Data by Abele, ref. 1)

σ_0 = strength of same snow (dry) at 0C

σ_{-10} = strength of same snow at -10C.

A small amount of experimental work has been done on the relationship between unconfined compressive strength and grain size, but the results are conflicting. Jellinek's data (Fig. III-17) show a trend of strength increase as grain size increases from 0.2 to 0.8 mm, whereas the results of Ramseier and Gow (Fig. III-18) show strength decreasing as grain size increases over the same range. It is possible that the results of Ramseier and Gow were affected by the influence of grain size on age-hardening rate; the fine-grained samples would probably age harden more rapidly than the coarse-grained ones, and the coarse-grained samples may have still been well below "full strength" after the 16 days of hardening at a temperature of about -50C. Ramseier and Gow suggest that the greater angularity of the fine grains contributed to the higher strength of those samples.

Practical experience indicates that the highest strengths are achieved by well-graded snows which initially have ample fine fractions. Coarse-grained snow is usually cohesionless and weak. Theory for tensile strength of granular materials[40] calls for strength to be inversely proportional to the square or cube of grain size, but for a sintered material like snow the situation is probably more complex.

The unconfined compressive strength of newly aggregated snow increases exponentially with time as a result of the metamorphic changes which produce intergranular bonds.

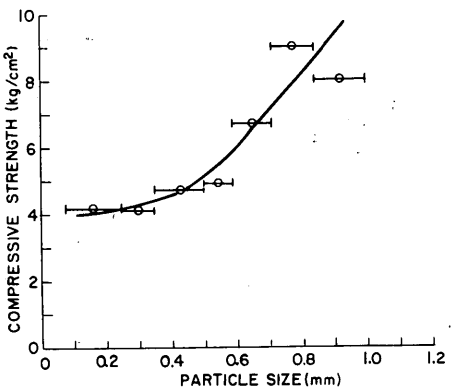

Figure III-17. Unconfined compressive strength as a function of particle size (density 0.55 g/cm³, test temperature -10C, samples aged 168 hr). Each point represents a mean of 10 tests. (After Jellinek, ref. 19)

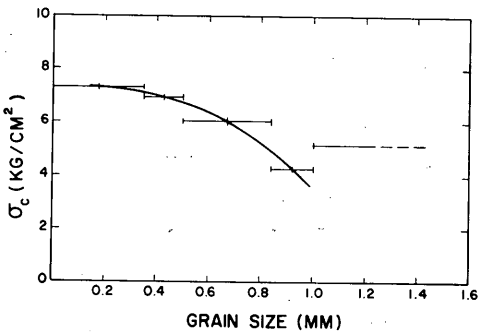

Figure III-18. Unconfined compressive strength as a function of particle size (density 0.55 g/cm³, test temperature -50C, samples aged 384 hr). Each point represents a mean of 5 tests. (After Ramseier and Gow, ref. 27)

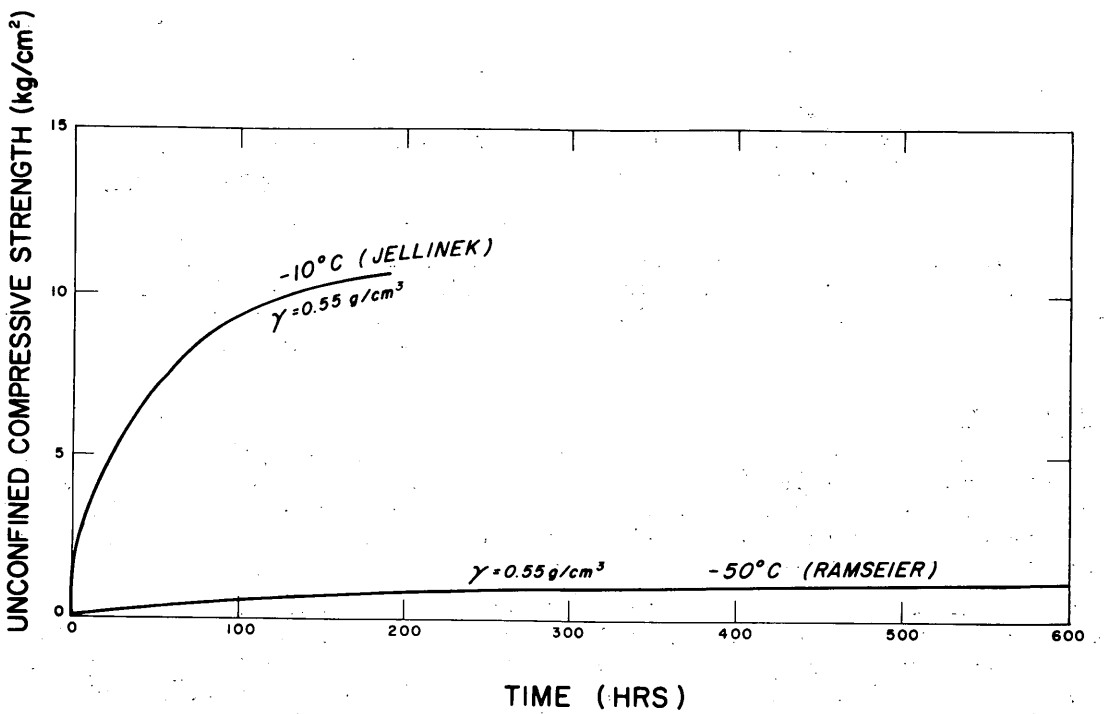

Figure III-19. Unconfined compressive strength as a function of time during the period of intergranular bond formation (age-hardening). (After Jellinek, ref. 19; Ramseier and Gow, ref. 27)

The rate at which this age-hardening proceeds is temperature-dependent, rate increasing with temperature. The rate is also affected by grain size and shape, snows with ample fine and angular particles age-hardening more rapidly than those with larger or more rounded grains. Figure III-19 gives age-hardening curves for artificially disaggregated snows "setting-up" at temperatures of -10 and -50C.

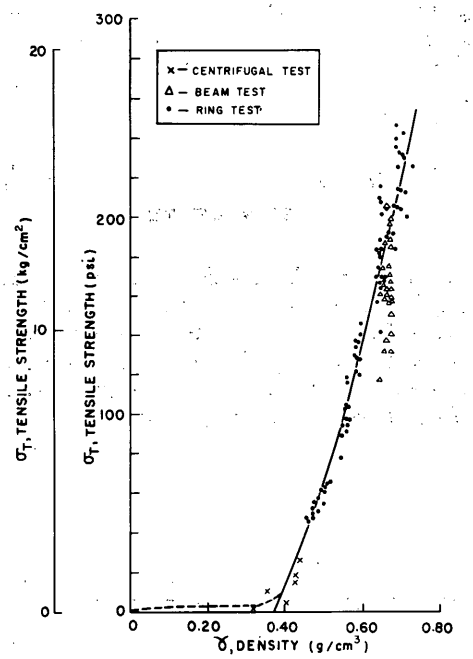

Figure III-20. Tensile strength as a function of density (test temperature -10 C). (After Butkovich, ref. 12)

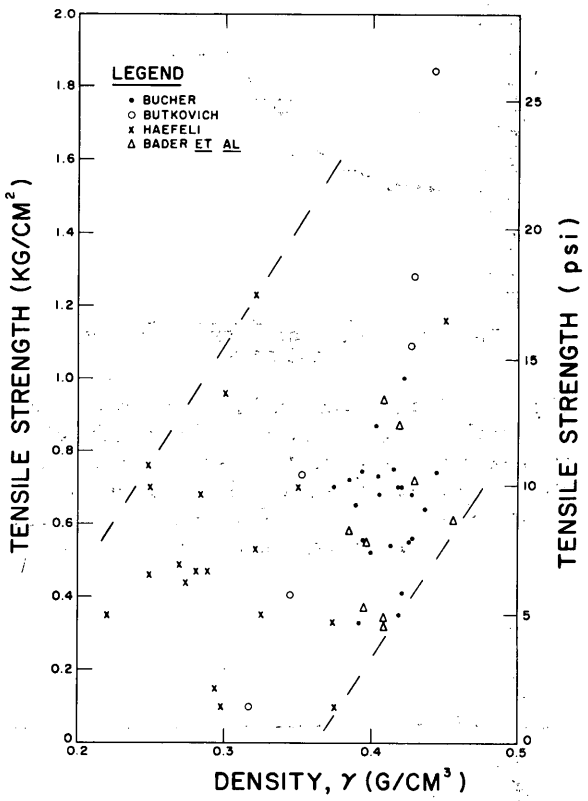

Figure III-21. Tensile strength plotted against density for samples having a density less than 0.45 g/cm³. There is no common grain form or temperature for this presentation.

Tensile strength

Comparatively little work has been done on the tensile strength of snow. Pioneer studies were made by Haefeli[17], who applied direct tensile force to cylindrical samples. A centrifugal technique was later used by Bucher[10], and in recent years CRREL (SIPRE) has tested high-density snow by ring-fracture and beam-breaking methods[12]. All these techniques are described elsewhere in this series.

The results of Butkovich for high-density snow are given in Figure III-20. All available data on the tensile strength of low-density snows are given in Figure III-21. Tensile strength is strongly dependent on density in the high density range. For densities less than 0.42 g/cm³ tensile strength is very low (up to 1.2 kg/cm²), and the widely differing grain textures found in low-density snows lead to considerable strength variations for a given density.

The only relationships between tensile strength and temperature are found in the work of Bucher[10]. Figure III-22 shows Bucher's curves for snows of various densities and grain sizes. The coarse-grained sample of 0.42 g/cm³ density (Fig. III-22a) shows no change of strength with temperature; its low strength for such a high density suggests a very weakly bonded granular snow, so that no marked temperature dependence is to be expected.

Figure III-23 gives Bucher's schematic relationship between tensile strength and grain texture. It is doubtful, however, whether all three grain textures (dendritic,

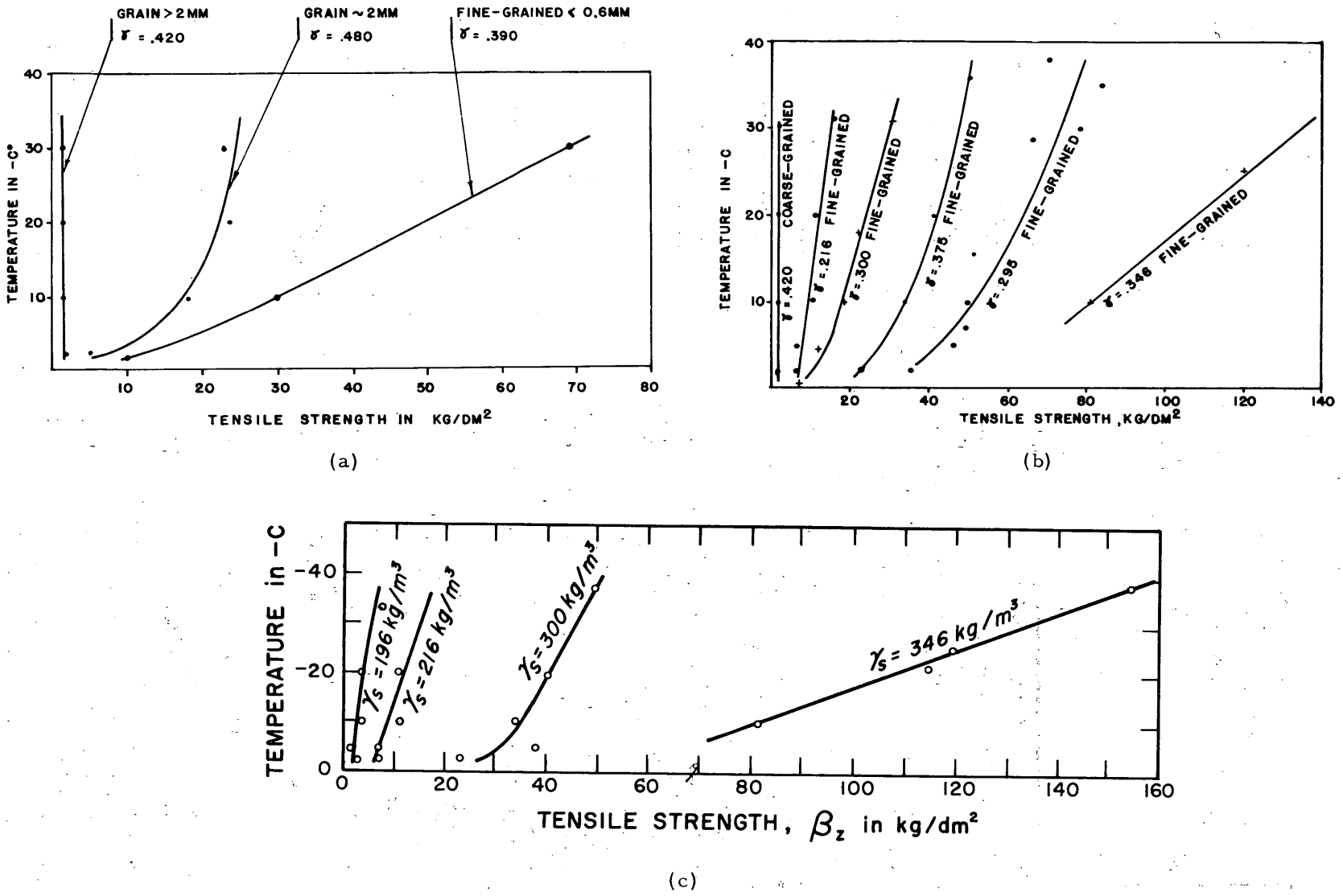

Figure III-22. Tensile strength as a function of temperature.
(After Bucher, ref. 10)

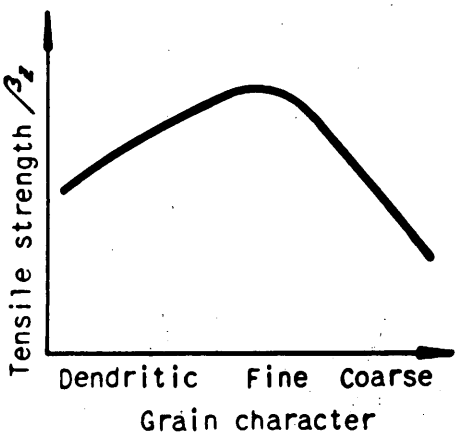

Figure III-23. Schematic relationship between tensile strength and grain form. (After Bucher, ref. 10)

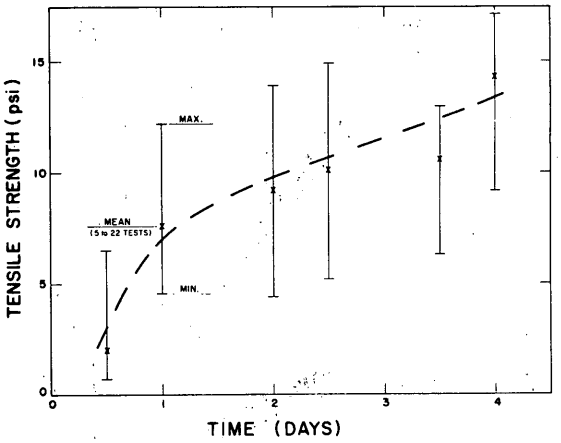

Figure III-24. Tensile strength as a function of time during the period of intergranular bond formation (age-hardening). (Data by Butkovich, ref. 13)

fine, coarse) could be compared for a common density and degree of metamorphism (age-hardening). Dendritic crystals are usually found only in new, low-density snows, while fine and coarse grains commonly settle to a moderately high density.

In medium- to high-density snows, the greatest tensile strengths are likely to be achieved by snow which has an abundance of fine particles, and which has had an adequate period for bonds to form by the age-hardening process. Figure III-24 illustrates the increase of tensile strength with time in an age-hardening snow.

Shear strength

Shear strength of snow has been tested using apparatus for double shear of cylinders, shear boxes, shear vanes, and shear plates.*

Shear strength is related to density, temperature, and grain structure, as other strength properties are, and is also dependent on the pressure normal to the shear direction.

Figures III-25 and III-26 give Butkovich data[12] on the strength of high-density snow in double shear, for the unrestrained condition and for normal pressures of 30 and 60 psi. Unrestrained shear strength is apparently of comparable magnitude to tensile strength for snow of a given density. Bader[5] gives reasons for believing that samples in some unrestrained shear tests actually fail in tension. Butkovich results of torsional tests are presented in Figure III-27.

Attempts have been made to apply the Coulomb equation, a familiar relation in soil mechanics, to snow. The equation relates shear strength to normal pressure in a linear form:

$$s = c + p \tan\phi \qquad (8)$$

where s is shear strength, p normal pressure, c coefficient of cohesion, and ϕ the angle of shearing resistance (angle of friction).

Experiments show, however, that a plot of shear strength against normal pressure for snow is not linear[31] (Fig. III-28). One reason for this is the compressibility of snow: as the normal pressure is increased the snow compresses, so that a test is actually performed on snow of higher density than the measured initial density. The plot of shear strength against normal pressure is thus influenced by a third variable, density.

* Techniques are described elsewhere in this series.

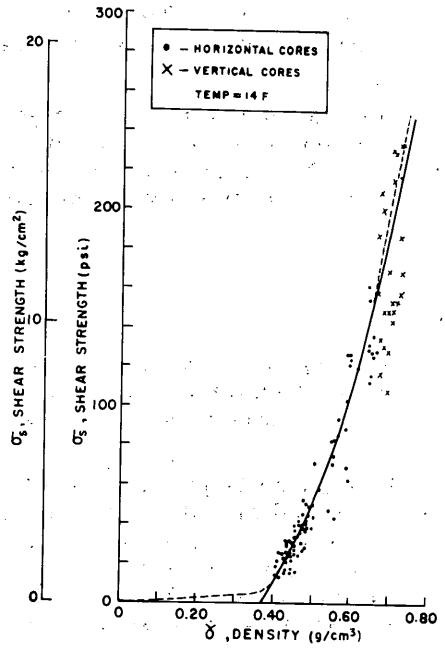

Figure III-25. Strength in unconfined double shear as a function of density (-10C). (After Butkovich, ref. 12)

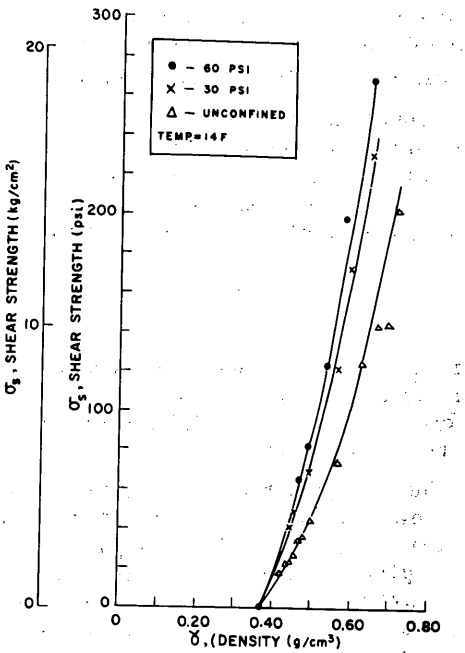

Figure III-26. Shear strength as a function of density for the unconfined condition and for normal pressures of 30 and 60 psi (-10C). (After Butkovich, ref. 12)

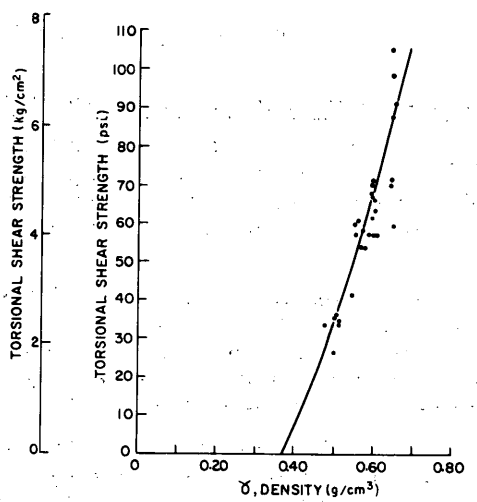

Figure III-27. Torsional shear strength as a function of density (-10C). (After Butkovich, ref. 12)

This is sometimes overlooked. When the sample is compressed the density changes according to

$$\Delta\gamma = \frac{\Delta h}{h - \Delta h}\ \gamma_0 \qquad (9)$$

where γ_0 is initial density, $\Delta\gamma$ the change in density, $\underline{h}$ the initial dimension normal to the shear direction, and Δh the change in $\underline{h}$. From present information, Δh cannot be predicted for given values of $\underline{h}$, $\underline{p}$, and γ_0, but it could be measured by fitting a dial micrometer to the shear apparatus.

Low-density snows can be drastically altered by normal pressure while high-density snows are unaltered by the same normal pressure. This point can be illustrated by drawing on the results of an experiment by Bucher and Roch[11], who relate density with compressive resistance for snow under frictionless lateral confinement. The Bucher and Roch data can be adequately represented by*

$$p_{cr} = e^{(10\gamma - 4.35)} \qquad (10)$$

where p_{cr} is resistance to compressive collapse for density γ. From this expression, the minimum density required to resist further densification under a given pressure can be found. Figure III-29 shows how $\Delta\gamma$ varies with γ_0 for different applied pressures, according to eq 10.

Under certain circumstances, use of the Coulomb equation is justifiable. Very-high-density snow ($\gamma > 0.55$ g/cm^3) is not likely to densify further unless the normal pressures are very high (higher than about 3 kg/cm^2, or 45 psi). If the consideration only applies to a small range of normal pressures, it may be permissible to approximate part of a curve like that of Figure III-28(b) by a straight line. This perhaps justifies the use of the Coulomb equation in trafficability studies, where nominal pressures for tracked vehicles usually lie in the range 1-4 psi.

Shear tests analyzed on the assumption that Coulomb's equation holds have yielded ϕ values from 20° to 55°. The apparent cohesion $\underline{c}$ is a measure of the unrestrained shear strength. It is sometimes regarded as representing the strength of intergranular bonds, an interpretation borne out by the correspondence between unrestrained shear strength and tensile strength.

The shear strength of snow is currently being investigated in detail at CRREL by G. Ballard.

Penetration resistance in semi-infinite snow masses (rapid loading)

Penetration of flat plates. When a flat plate is forced into a mass of snow which has depth and lateral extent large in comparison to the plate width, the snow beneath the plate is compressed under lateral restraint. The compressive resistance of the snow varies with density, temperature, and grain structure, and also with depth of penetration.

The type of deformation caused by penetration of a flat plate changes with the density of the snow. In low-density snows, the plate compresses the material beneath it, shearing it cleanly from the surrounding snow. At higher densities the snow does not compress so easily, and there is more tendency for a "stress bulb" to form. Figure III-30 illustrates this effect. (See also ref. 41.)

The speed of penetration affects the deformation mechanism, particularly in a layered natural snow mass. At low penetration velocity the snow yields by a series of collapses, so that resistance fluctuates for penetration at a constant speed. Figure III-31 illustrates this. The rate of straining also influences the deformation resistance in a more general way, but this effect has not been adequately investigated. It might be expected that resistance would increase as strain rate increased, but the work of Landauer and Royse[20] throws doubt on this expectation.

The effects of plate size and shape on penetration resistance have not been established experimentally. Landauer and Royse[20] suggest that plate geometry is of minor importance, but while this may be the case for large plates it is not likely to be true

* This expression is not intended for general quantitative use. It refers to a particular snow type and a particular test method.

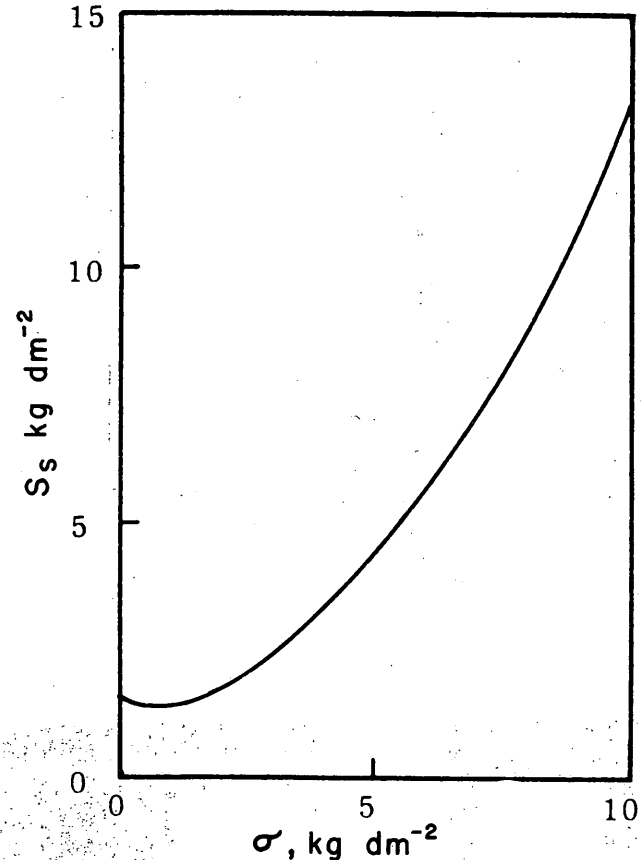

Figure III-28a. Shear strength as a function of normal pressure for new, slightly wind-packed snow. (ref. 31)

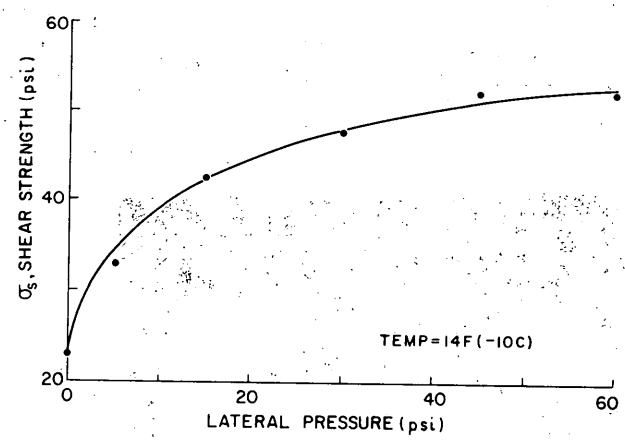

Figure III-28b. Shear strength as a function of normal pressure for ice cap snow of about 0.45 g/cm^3 density. (Butkovich, ref. 12)

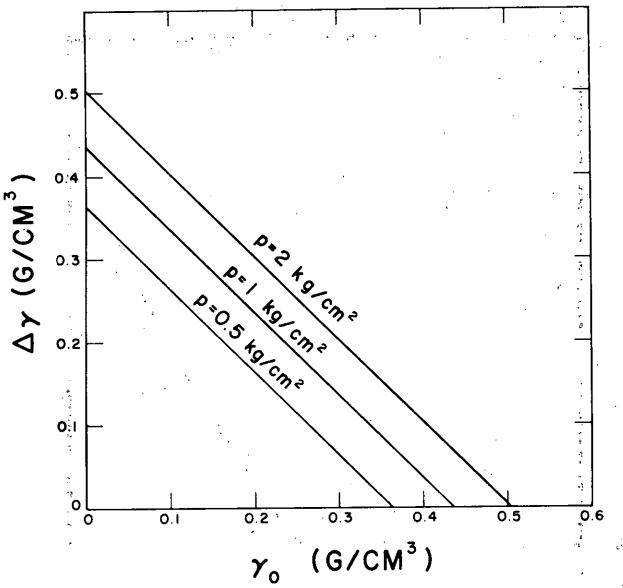

Figure III-29. Increase of density produced by application of pressure to confined samples of snows with various initial densities (assuming eq 8 to apply).

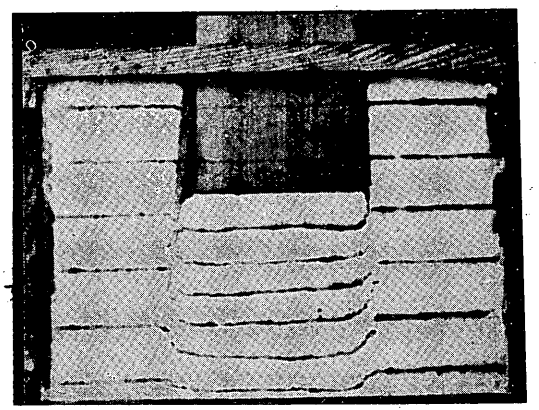

(a) New snow, γ_0 = 0.07 g/cm³, temp = -2.5C

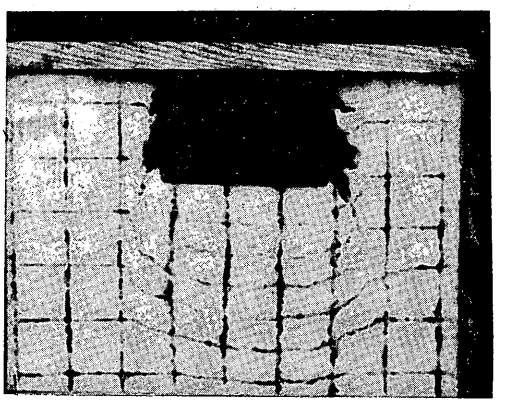

(b) Granular snow, γ_0 = 0.32 g/cm³, temp = -3C

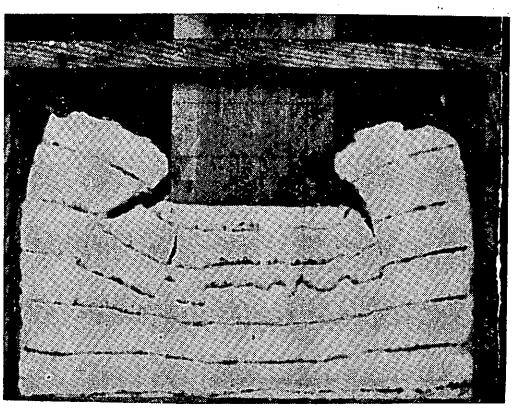

(c) Wet snow

Figure III-30. Modes of compressive collapse for different snow types. (After Yosida, et al., ref. 35)

for small ones, since perimeter shear is a factor and the ratio of perimeter to area decreases as size increases. The probable effect can be deduced theoretically (see Kerr, 1962 and Assur, 1964); as plate size varies the ratio p/z will change by the following factors:

Circular plates $$\left(1 + \frac{2R_0}{R} \cdot \frac{K_1\left(\frac{R}{R_0}\right)}{K_0\left(\frac{R}{R_0}\right)}\right)$$

Long narrow plates $$\left(1 + \frac{B_0}{B}\right)$$

where R is the radius of a circular plate, B is the width of a long plate, and R_0 and B_0 are "characteristic dimensions" determined by compressive and shear moduli for the snow (K and G respectively):

$$2R_0 = B_0 = 2\sqrt{\frac{G}{K}}.$$

K_1 and K_0 denote modified Bessel functions.

Over the past 50 years a number of writers have suggested power relationships between pressure and penetration depth for sinkage of a plate into snow or soil.[8,16] While these are dimensionally undesirable and limited in validity by boundary conditions, the simple power law is convenient for some purposes. Bader et al.[32] show power relationships between pressure and penetration, and the results of CBR* tests by Abele and Wuori[2] can be adequately represented by a power law. Landauer and Royse[20] give power relationships between the energy of snow compaction and penetration depth, which implies a power relation between pressure and penetration, since pressure is the derivative of work with respect to penetration depth z. Investigators studying snow trafficability have used a power law to relate pressure and sinkage for vehicles (see "Oversnow Transport", ref. 37).

Some shortcomings of power relationships are illustrated by Figure III-32, which is a schematic of the general pressure-sinkage relation deduced from various experimental results. With very small pressures the p-z relation is linear, while at moderate pressures (such as those imposed by tracked vehicles) the snow becomes stronger as it is compressed. At high pressures and large relative penetrations (as measured in CBR tests) the snow "weakens" as it is strained, and eventually a yield stress is reached, so that the plate or penetrometer drives continuously into the snow without any further increase of pressure.

Assur[38] has attempted to reconcile the conflict between various early relationships. He gives simple and dimensionally proper expressions which describe some, but not all, of the features shown in Figure III-32. Acceptable approximations can be obtained by choosing the appropriate expression for the range of behavior of most interest. If, however, it is assumed that pressure p and penetration z can be related over a restricted pressure and penetration range by

$$p = k z^n \qquad (11)$$

it is to be expected that the coefficient k and the exponent n will vary with snow type. Although no systematic studies have been made, it appears that n is relatively insensitive to variation of snow type, while k may vary by several orders of magnitude. Whereas n seems to depend only on snow type (defined by density, temperature and grain structure) over a limited stress range, k is probably influenced by size and shape of the plate, and by penetration rate in addition to snow type. Figure III-33 gives the data of Bader et al.[32] on logarithmic scales and in metric units. Figure III-34 shows some of Abele's CBR data, also on logarithmic scales but in English units. In each case the slope of the line gives n, and the value of p where z is unity gives k.

* California Bearing Ratio

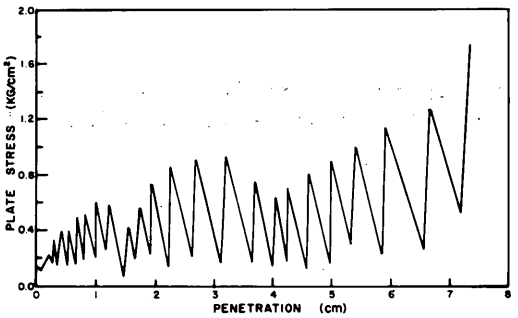

Figure III-31. Fluctuation of penetration resistance as a plate is forced into snow. The snow is apparently deforming by successive collapses. (After Landauer and Royse; ref. 20)

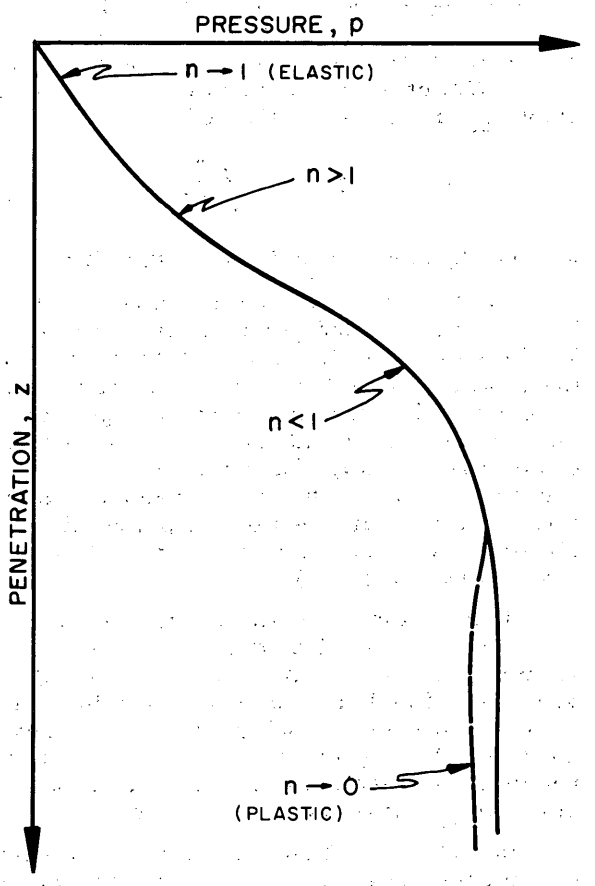

Figure III-32. Suggested schematic relationship illustrating the limitations of power function representations of pressure — sinkage behavior.

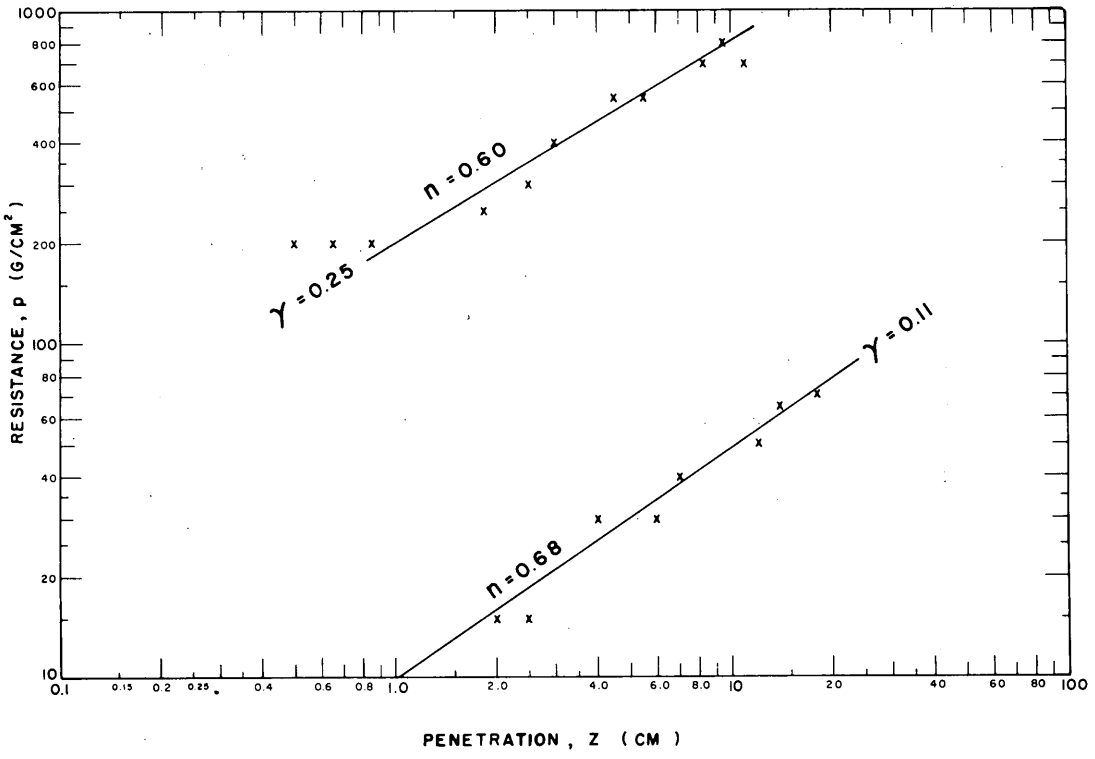

Figure III-33. Relationships between penetration and pressure from disk penetrometer measurements. (Data from ref. 32)

Penetrometers. The Canadian hardness gage and Proctor needle are disk penetrometers used to measure the "hardness" of snow. This "hardness" is a rather ill-defined initial penetration resistance which is taken to be related directly to density, temperature and, occasionally, grain structure. Gold[15] gives a power relationship between hardness and density, and Ager's data relating Proctor (needle) penetration resistance and density[3] (Figure III-35) also suggest a power law. Gold gives exponential relationships between hardness and temperature and between hardness and grain size, but the data on which the expressions are based show broad scatter.

The CBR device and similar instruments (see "Oversnow Transport"[137]) perhaps perform more meaningful tests than the simple penetrometers mentioned above, but so far there has been insufficient theoretical and experimental work to derive full benefit from the data they produce. The CBR equipment, when used according to accepted soils practice, does not seem to be very useful in snow. However, if CBR data could be suitably interpreted for different density ranges (say, 0-0.4, 0.4-0.55, 0.55-0.8 g/cm^3) it might provide a better test of bearing capacity than unconfined compression tests or the empirical penetrometers currently in use. Unfortunately, CBR tests are very time-consuming.

Some drop-weight penetrometers have been used. In some cases these might be preferable to a CBR type of test, although the inertial effects might complicate interpretation.

Conical penetrometers. Of the various cone penetrometers which have been used for testing the strength of snow in situ, the best known and most widely used is the Swiss rammsonde. Other types are the Vicksburg cone and the drop-cone.

There is no acceptable theory for cone penetrometers, and there has been no systematic study of the way a cone stresses and displaces the snow it drives through.

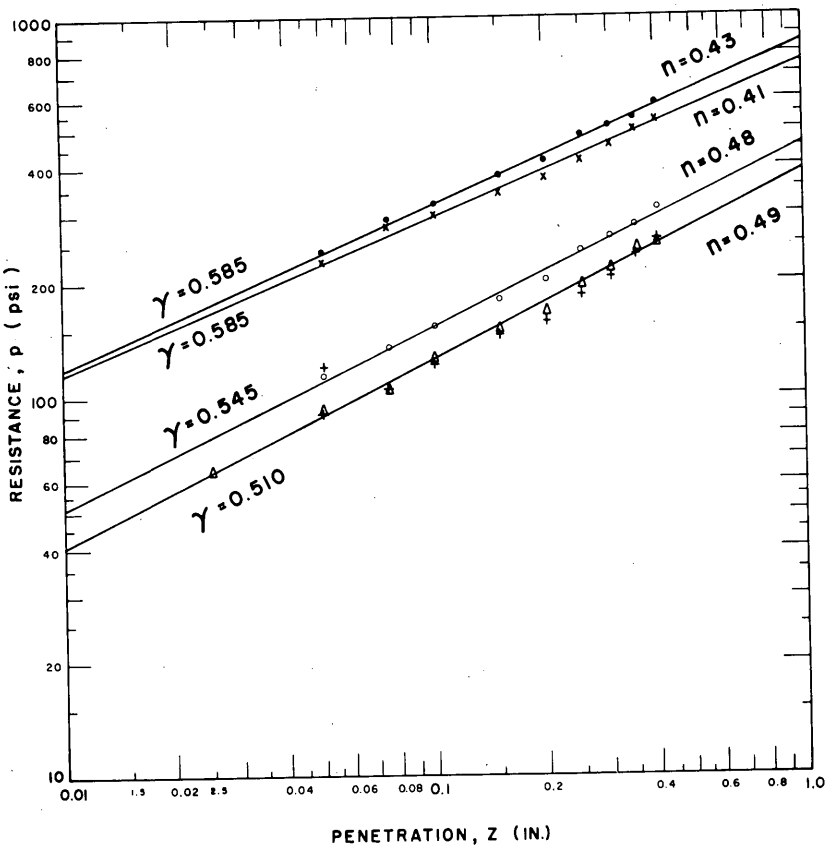

Figure III-34. Relationships between penetration and pressure from CBR tests made at a penetration rate of 0.05 in./min. Tests made on snow processed by a Snowblast plow, compacted to various degrees, and age-hardened for 21 days. (From data supplied by Abele)

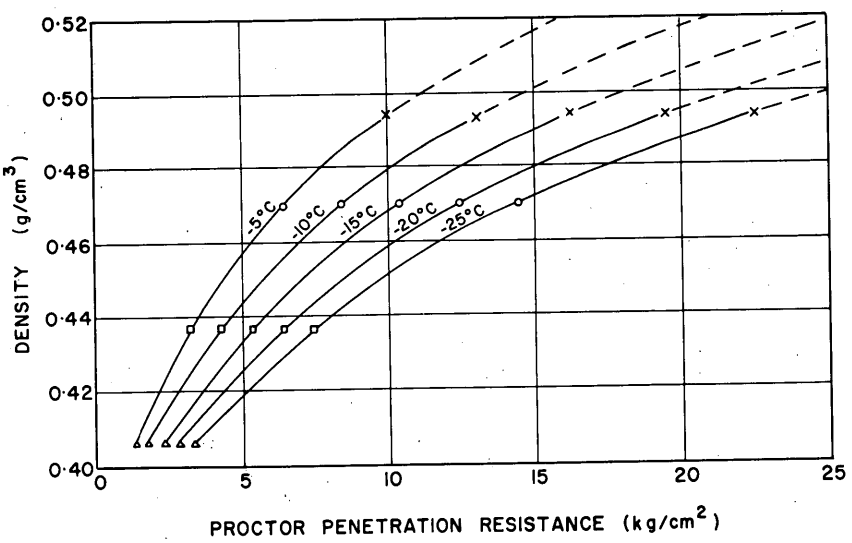

Figure III-35.. Proctor penetration resistance as a function of snow density for various temperatures. The curves suggest a power law relationship. (After Ager, ref. 3)

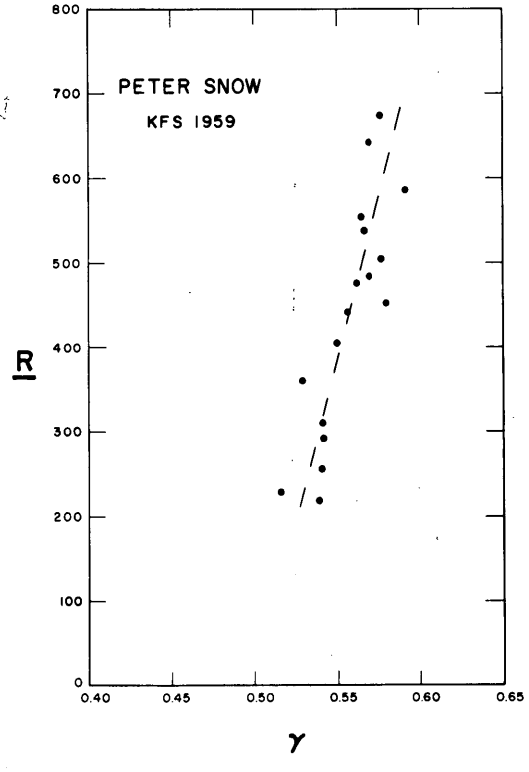

Figure III-36. Ram hardness as a function of density for age-hardened Peter snow (Keweenaw Field Station, 1959). (Data by Abele, ref. 1)

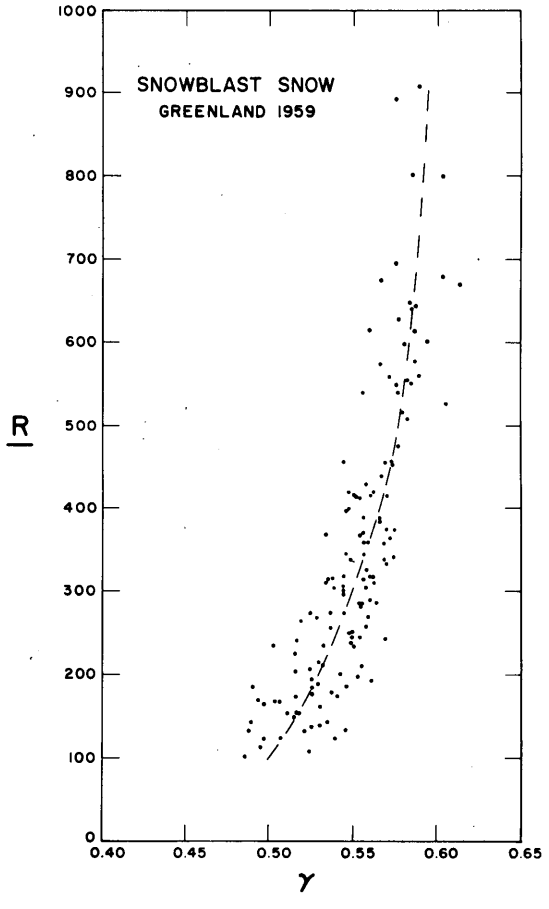

Figure III-37. Ram hardness as a function of density for snow milled by a Snowblast plow and age-hardened (Greenland, 1959). (Data by Abele, ref. 1)

Nevertheless, the rammsonde has proved to be a useful instrument for making rapid measurements of relative snow strength. Ram hardness has been correlated empirically with the supporting capacity of snow for wheels and vehicle tracks, with shear strength, and with unconfined compressive strength. In avalanche work it is used to determine the strength variations with depth in the snow pack.

Figures III-36 to III-39 give plots of ram hardness against density for milled and compacted snow in the range 0.5-0.6 g/cm^3. Figure III-40 gives an example of ram hardness changes during age-hardening. Correlations of ram hardness with unconfined compressive strength and with shear strength are given later.

Some penetrometers (e.g., the Vicksburg cone) may give a measure of the yield stress illustrated in Figure III-32.

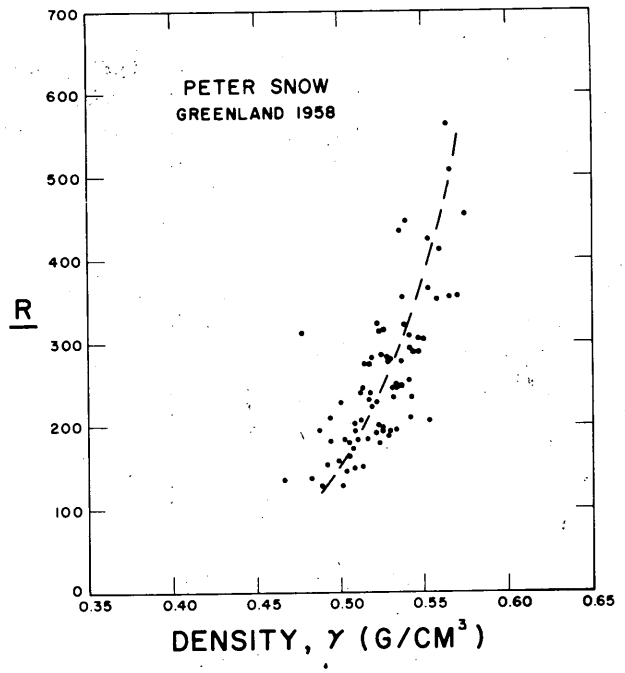

Figure III-38. Ram hardness as a function of density for age-hardened Peter snow (Greenland, 1958). (Data by Abele, ref. 1)

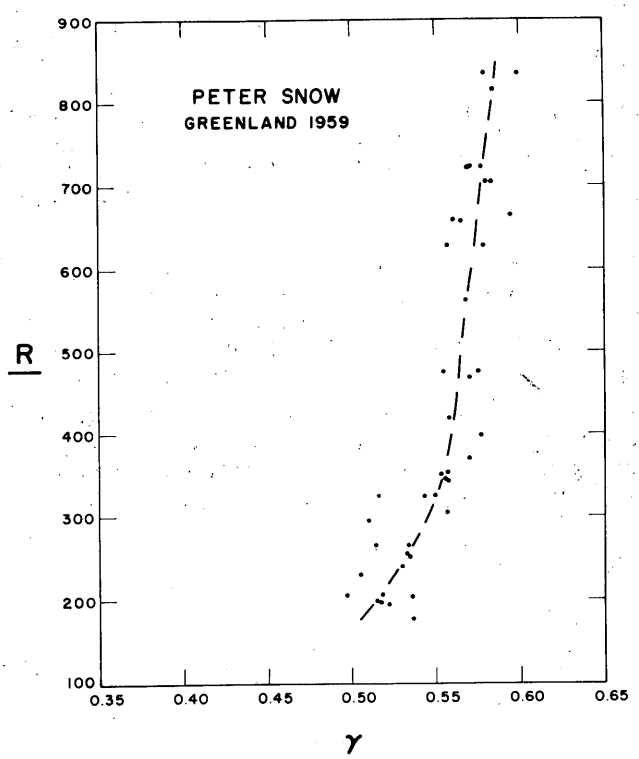

Figure III-39. Ram hardness as a function of density for age-hardened Peter snow (Greenland, 1959). (Data by Abele, ref. 1)

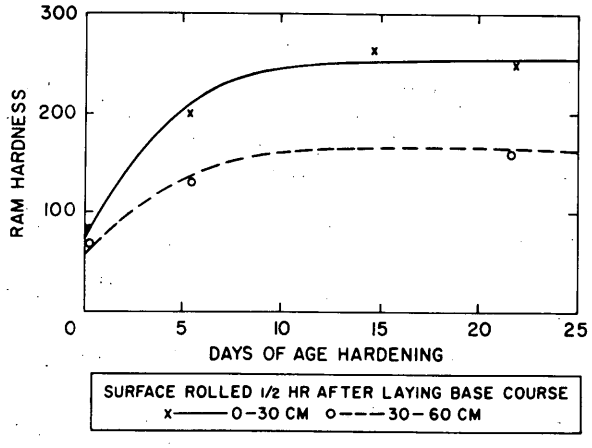

Figure III-40. Ram hardness as a function of time during the age-hardening period. This snow was rolled after disaggregation by a Klauer plow, and age-hardened at temperatures fluctuating from 0-30F. (After Wuori, ref. 33)

CHAPTER III REFERENCES

1. Abele, G. (1963) A correlation of unconfined compressive strength and ram hardness of processed snow, U. S. Army Cold Regions Research and Engineering Laboratory (USA CRREL) Technical Report 85.

2. _____ and Wuori, A. F. (1963) Results of CBR tests of processed snow pavements, USA CRREL Technical Note (internal).

3. Ager, B. H. (1956) Packad snö som transportunderlag (Compacted snow as a transport substratum), Norrlands Skogsvardsförbunds Tidskrift, no. 3, p. 293-384. National Research Council of Canada, Technical Translation 865, 1960.

4. Anderson, D. L. and Benson, C. S. (1963) "The densification of snow" in Ice and snow-processes, properties and applications (C. W. D. Kingery, Editor). Cambridge, Massachusetts: M.I.T. Press.

5. Bader, H. (1962) "Snow as a material" in Cold Regions Science and Engineering (F. J. Sanger, Editor), USA CRREL monographs, Part II, Sect. B.

6. Bender, J. A. (1957) Testing of a compacted snow runway, American Society of Civil Engineers, Journal of the Air Transport Division, Paper 1324.

7. Bentley, C. R., Pomeroy, P. W., and Dorman, H. J. (1957) Seismic measurements on the Greenland Ice Cap, Annales de Géophysique, tome 13, no. 4.

8. Bernstein, R. (1913) Problems of the experimental mechanics of motor ploughs, Der Motorwagen, vol. 16.

9. Brunke, H. (1959) A correlation of crushing strength and hardness values of processed snow, Michigan College of Mining and Technology, M.S. Thesis.

10. Bucher, E. (1948) Beiträge zu den theoretischen Grundlagen des Lawinenverbaus (Contribution to the theoretical foundations of avalanche defense construction), Beiträge zur Geologie der Schweiz, Geotechnische Serie, Hydrologie, Lieferung 6. U. S. Army Snow, Ice and Permafrost Research Establishment (USA SIPRE) Translation 18, 1956.

CHAPTER III REFERENCES

11. Bucher, E. and Roch, A. (1946) Reibungs-und Packungswiderstände bei raschen Schneebewegungen (Friction and resistance to compaction of snow under rapid motion), Mitteilungen des Eidgenoss, Davos-Weissfluhjoch, Instituts für Schnee und Lawinenforschung (text in German).

12. Butkovich, T. R. (1956) Strength studies of high-density snow, USA SIPRE Research Report 18.

13. _____ (1962) Studies of the age-hardening of processed snow, USA CRREL Research Report 99.

14. Crary, A. P., et al. Glaciological studies of the Ross Ice Shelf, Antarctica, 1957-60, American Geographical Society, IGY Glaciological Report, no. 6.

15. Gold, L. W. (1956) The strength of snow in compression, Journal of Glaciology, vol. 2, no. 20.

16. Goriatchkin, B. P. (1936) "Theory and development of agricultural machinery," reported in Theory of land locomotion (by M. G. Bekker), University of Michigan Press, 1956.

17. Haefeli, R. (1939) "Snow mechanics with references to soil mechanics" in Der Schnee und seine Metamorphose (Snow and its metamorphism) (by Bader, et al.), Beitrage zur Geologie der Schweiz, Geotechnische Serie, Hydrologie, Lieferung 3. USA SIPRE Translation 14, 1954.

18. Inaho, Y. (1941) Sekisetsu no kōdo ni tsuite (On the hardness of snow), Seppyō, vol. 3, p. 343-349 (text in Japanese). USA SIPRE Translation 33, 1955 (out of print).

19. Jellinek, H. H. G. (1957) Compressive strength properties of snow, USA SIPRE Research Report 34.

20. Landauer, J. K. and Royse, F. (1956) Energy of snow compaction and its relation to trafficability, USA SIPRE Research Report 14.

21. Lee, T. M. (1961) Note on Young's modulus and Poisson's ratio of naturally compacted snow and processed snow, USA CRREL Technical Note (internal).

22. _____ (1961) Note on pulse propagation technique in measuring age effects of processed snow, USA CRREL Technical Note (internal).

23. Nakaya, U. (1959) Visco-elastic properties of snow and ice from the Greenland Ice Cap, USA SIPRE Research Report 46.

24. _____ (1961) Elastic properties of processed snow with reference to its internal structure, USA SIPRE Research Report 82.

25. _____ (1959) Visco-elastic properties of processed snow, USA SIPRE Research Report 58.

26. Ramseier, R. O. (1963) Some physical and mechanical properties of polar snow, Journal of Glaciology, vol. 4, no. 36.

27. _____ and Gow, A. J. (1963) Age-hardening of snow at the South Pole, Journal of Glaciology, vol. 4, no. 35.

28. Robin, G. de Q. (1958) "Seismic shooting and related investigations" in Glaciology III, Scientific Results of the Norwegian-British-Swedish Antarctic Expedition, 1949-52, vol. V, Oslo.

29. Roch, A. (1948) Discussion sur la valeur du nombre de Poisson m pour la neige, (Discussion of the value of Poisson's number m for snow), Davos- Weissfluhjoch, Mitteilungen aus dem eidg. Institut fur Schnee-und Lawinenforschung, Interner Bericht no. 89 (text in French).

30. Roethlisberger, H. Private communication.

CHAPTER III REFERENCES

31. University of Minnesota (1951a) Review of the properties of snow and ice, USA SIPRE Technical Report 4.

32. _____ (1951b) Preliminary investigations of some physical properties of snow, USA SIPRE Technical Report 7.

33. Wuori, A. F. (1963) Snow stabilization for roads and runways, USA CRREL Technical Report 83.

34. Yosida, Z. (1962) "Physical properties of snow" in Ice and snow-processes, properties and applications, (W. D. Kingery, Editor). Cambridge, Massachusetts: M.I.T. Press.

35. _____, et al. (1955) Physical studies on deposited snow, Institute of Low Temperature Science, Hokkaido University, Sapporo, Japan.

36. Wuori, A. F. (1960) Snow stabilization using dry processing methods, USA SIPRE Technical Report 68.

37. Mellor, M. (1963) "Oversnow transport" in Cold Regions Science and Engineering (F. J. Sanger, Editor), USA CRREL monographs, Part III, Sect. A4.

38. Assur, A. (1964) Locomotion over soft soil and snow, Congress of the Society of Automotive Engineers, Detroit, Paper no. 782 F.

39. Kerr, A. (1962) Settlement and tilting of footings on a viscous foundation, USA SIPRE Research Report 81.

40. Smalley, V. and Smalley, I. J. (1964) Tensile strength of granular materials, Nature, vol. 202, no. 4928, p. 168-169.

41. Wuori, A. F. (1962) Supporting capacity of processed snow runways, USA CRREL Technical Report 82.

42. Arctic Construction and Frost Effects Laboratory, Corps of Engineers (1947) Report of Corps of Engineers observers on Project Snowman of Atlantic Division, ATC (1947-48), Technical Report 15.

43. _____ (1949) Investigation of snow compaction methods and equipment conducted for Engineer Research and Development Laboratories (FY 1949), Technical Report 22.

44. _____ (1954) Project Mint Julep, investigation of a smooth ice area of the Greenland Ice Cap, Part IV — Report of Arctic Construction and Frost Effects Laboratory, Technical Report 50.

CHAPTER IV. CREEP UNDER SUSTAINED LOADING

The general form of the relationship between strain and time for snow under a constant sustained load has been outlined in Chapter II. Following the initial elastic strain and the stage of decelerating transient creep, a constant stress tends to produce a constant strain rate. With low stresses the steady strain rate is maintained over long periods, but with high stresses the snow may soon be modified by strain, with consequent effect on the strain rate. For example, if the snow densifies under load the strain rate will decrease with time, but if it is in direct shear a high stress may induce accelerated straining, leading to complete failure. For practical and academic problems, however, creep under relatively low stresses is usually of greatest interest. In these cases it is customary to consider the "steady-state" creep (secondary creep). The strain rate thus determined can then be related to stress, density, temperature and grain structure.

Strain as a function of time

The shape of the creep curve for metals has been described by numerous expressions relating strain and time, and interpretations in accordance with creep models have been made.[14,15] For creep curves developed from compressive tests on snow, Ramseier and Pavlak[11] find that the strain-time relation can be adequately represented by a power function of the form

$$\epsilon = \epsilon_0 + bt^n$$

where ϵ is strain, ϵ_0 is instantaneous (elastic) strain, t is time, and b and n are constants for given stress and snow type. Frequently, however, strain rates and viscosity coefficients for secondary creep are determined by discarding data from the "delayed elastic" portion of the curve and regarding strain thereafter as a linear function of time.

Strain rate as a function of stress

Experiments show non-linear relationship between strain rate and stress for snow.[7] At low stresses it exhibits linear (Newtonian) viscosity, while at high stresses it tends towards plastic behavior. Strain rate and stress can be conveniently related by a hyperbolic function,[2,7] following theoretical proposals for creep of metals:[14,15]

$$\dot{\epsilon} = \frac{\sigma_0}{\eta} \sinh\left(\frac{\sigma}{\sigma_0}\right)$$

where $\dot{\epsilon}$ = strain rate (often compressive in snow problems)
σ = stress (often compressive)
σ_0 = an empirical constant with the dimensions of stress, which normalizes the variable. It may be expected to vary to some small extent with snow type and temperature.
η = a constant for given temperature and snow type which is regarded as a viscosity coefficient.

For small values of σ/σ_0 (say less than 0.8), the hyperbolic sine function is close to linear, since the first term of the series for $\sigma_0 \sinh \sigma/\sigma_0$ is dominant. Thus snow behaves as a Newtonian viscous solid (strain rate directly proportional to stress) for low stresses ($\sigma \leq 0.8\ \sigma_0$). Landauer[7] found a value for σ_0 of 700 g/cm^2 (10 psi) from creep experiments on snow of density 0.38-0.42 g/cm^3 in the temperature range -3 to -14C. Bader[3] found values of σ_0 from 660 to 770 g/cm^2 by analysis of depth-density curves from sites in Greenland and Antarctica. The assumption of linear viscosity for compressive creep of polar snow is therefore likely to be valid for stresses up to 550 g/cm^2 (about 8 psi, or 1100 psf). This is convenient for the study of certain practical problems; for example, spread footings can often be designed within, or not much in excess of, these stress limits. Another convenient approximation contains linear and cubic terms in stress, i.e. essentially the first two terms of the sinh series.

Figure IV-1 shows hyperbolic sine curves fitted to experimental data by Landauer. They illustrate why snow under sustained loading is sometimes referred to as a visco-

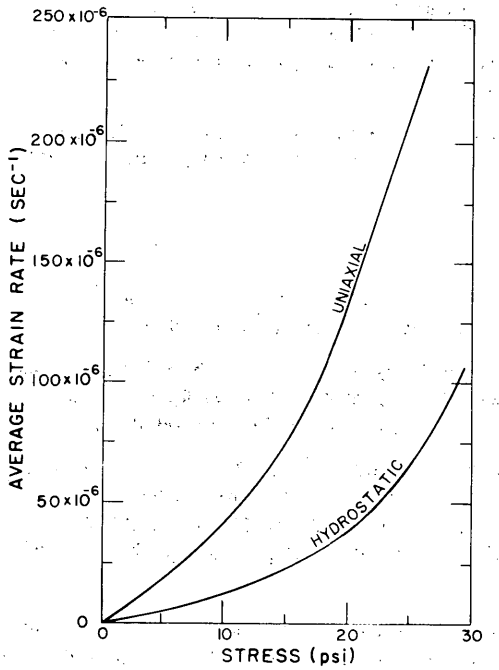

Figure IV-1. Hyperbolic sine curves fitted to experimental creep data by Landauer. Initial snow density 0.38 g/cm³; test temperature -8.4C. (After Landauer, ref. 7)

plastic material. At the lower limit of the stress range there is a linear relation between strain rate and stress ($\frac{d\dot{\epsilon}}{d\sigma}$ = const.), i.e., the snow is viscous. At the highest stresses, strain rate tends to become exceedingly rapid ($\frac{d\dot{\epsilon}}{d\sigma} \rightarrow \infty$) and the material is therefore plastic rather than viscous. Actually, under triaxial compression snow might densify to incompressible ice before it could yield plastically.

Strain rate as a function of density

Strain rate for a given stress and temperature is dependent on the grain structure of the snow, i.e., it depends on size, shape, and gradation of grains, on grain packing, and on the structural connections between grains. As has been mentioned before, the only practical and currently available index of grain structure is density, which seems to give a fair indication in dry snow which has been adequately age-hardened. However, there is reason to believe that density might be expressed advantageously in terms of void ratio.

The effect of density on deformation resistance has been studied by a number of investigators, all of whom present their findings in terms of a "coefficient of compressive viscosity". It should be kept in mind that this coefficient η_c is to be interpreted in accordance with eq 1 above.

Kojima[5] and Yosida[12] represent the results of their observations on the natural settlement of seasonal snows ($0.1 < \gamma < 0.5$ g/cm³) by a simple exponential equation:

$$\eta_c = Ae^{a\gamma} \qquad (2)$$

where A = a "constant" (which probably varies with snow type and temperature, but is apparently of the order 10^5 g cm^{-2} sec for the types observed between -1 and -10C)

a = an exponent constant (which is apparently about 21 cm³/g.

Equation 2 does not satisfy the probable boundary conditions for extremes of density. Since natural settlement of snow is, in effect, compression under complete lateral restraint (the snow layers are infinitely wide), it seems reasonable to expect that compressive viscosity should tend to zero as density goes to zero, and that compressive viscosity should tend to infinity as density tends towards the value for incompressible ice.

Bader[3] in his analysis of the densification of ice cap snows, also uses an exponential relationship, but contrives to fit the boundary conditions mentioned above by introducing the reciprocal of void ratio as a factor:

$$\eta_c = B\left(\frac{\gamma}{\gamma_{ice} - \gamma}\right) e^{b\gamma} \qquad (3)$$

where B is regarded as constant for a given ice cap site, and takes values ranging between 0.41 and 3.6 g cm^{-2} yr for sites in Greenland and Antarctica, b is an exponent constant for a given site, but which varies somewhat from place to place (15.8-21.7 cm^3/g for sites in Greenland and Antarctica).

Landauer[8] chooses to relate compressive viscosity and void ratio exponentially, obtaining a good fit to data for $0.35 < \gamma < 0.50$ g/cm^3. This is actually equivalent to a density relationship of the form

$$\eta_c = Ce^{-\frac{c}{\gamma}} \tag{4}$$

where C is a site constant (with the dimensions of viscosity) and c is a constant (with the dimensions of density). Assur[1] introduces a viscous analogue for Poisson's ratio.

It will be seen from Figure IV-3 that this actually gives a relationship very similar to Bader's up to a density of 0.55 g/cm^3, although Landauer's viscosity values in this range are about three times smaller than Bader's for the same Greenland site.

Bucher[4] made compressive creep tests on unconfined cylinders of snow in the laboratory. His limited data in the range of $0.2 < \gamma < 0.4$ can be represented by a simple exponential such as eq 2, but with a much smaller exponent constant than those corresponding to the data of Kojima and Bader (7.3 cm^3/g, compared with 21 cm^3/g or more) (Fig. IV-2).

Mellor and Hendrickson[9] made compressive creep tests on snow samples confined within steel cylinders. To facilitate regression analysis of data while fitting the boundary conditions, they adopt a power relationship between η_c and the inverse of void ratio:

$$\eta_c = N\left(\frac{\gamma}{\gamma_{ice} - \gamma}\right)^n \tag{5}$$

where N = a constant for given snow type and temperature (of the order 10^{11} - 10^{12} g cm^{-2} sec for Antarctic sites),

n = an exponent regarded as constant for snow of a given type (a site constant), which is found to be 1.5 for the South Pole and 3.0 for Byrd Station.

The same data can be represented by an expression of the form of eq 2 for $0.35 < \gamma < 0.60$ g/cm^3, giving exponent constants of 7.1 for the South Pole and 13.4 for Byrd Station (Fig. IV-4).

Ramseier and Pavlak[11] made unconfined compressive creep tests at Camp Century, Greenland, and at South Pole and Byrd Stations, Antarctica, obtaining the results shown in Figure IV-4. For their lowest density samples ($\gamma < 0.47$ g/cm^3) viscosity is strongly dependent on density, the relations being similar to those found from natural densification studies. In the range $0.48 < \gamma < 0.62$ g/cm^3, however, viscosity seems to be almost independent of density. For the highest densities ($\gamma > 0.62$ g/cm^3) they suggest that density again begins to affect viscosity strongly.

A similar trend to that suggested by Ramseier and Pavlak can be seen in results obtained from Antarctic snow pit studies by Kojima[13]; a linear relation between log η_c and γ was obtained for medium density snow, but deviations occurred at the high and low extremes of the density range. In Kojima's case, however, η_c still showed a marked density dependence in the medium density range (η_c increased by about one order of magnitude as γ increased from 0.4 to 0.5 g/cm^3).

Summing up, it seems that studies of natural snow densification show a very strong dependence of viscosity on density, while laboratory creep tests indicate that viscosity is a relatively weak function of density, at least in the mid-range of densities. For both densification studies and creep testing there are independent investigations leading to similar results, so that the effect must be regarded as real. A possible explanation of the discrepancy is that the natural densification process and the artificial creep test are rheologically dissimilar, perhaps because of test sample geometry, non-uniform distributions of stress and strain, and the duration of a given load.

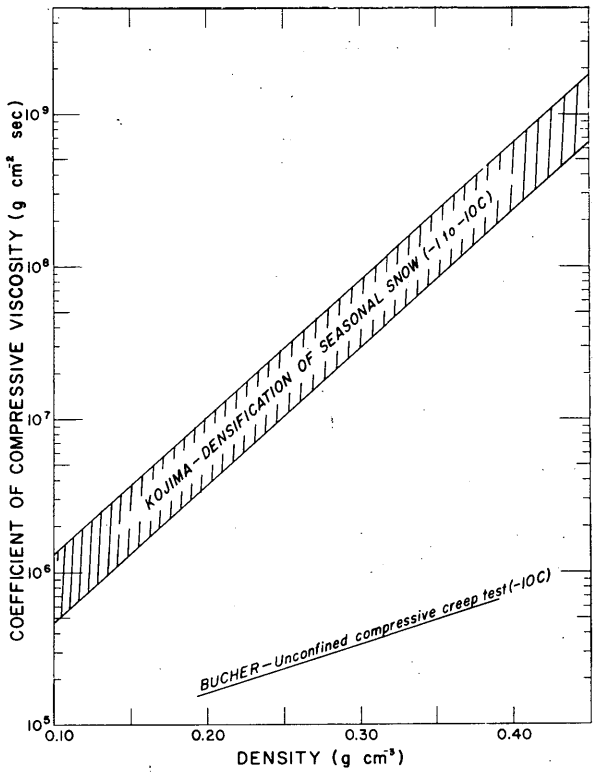

Figure IV-2. Compressive viscosity as a function of density. (After Kojima, ref. 5; Bucher, ref. 4)

Another possibility is that ice cap samples used in creep tests have already acquired preferred crystal orientation by previous straining, whereas crystal reorientation lags the strain under natural conditions. That ice cap snow is anisotropic in creep seems to be confirmed by Ramseier's data showing viscosity greater for snow loaded parallel to the original stratification than for the same snow loaded perpendicular to that stratification.

One other approach to the problem should be mentioned. Nakaya[10] has calculated dynamic viscosity coefficients for snow from measurements on the viscous damping of flexural vibrations (sonic frequencies) in tiny snow beams. Values are calculated on the assumption that relevant snow properties are represented by the Maxwell rheological model. Nakaya finds an exponential relationship between the dynamic viscosity coefficient and density for snow in the range $0.25 < \gamma < 0.50$ g/cm^3, and a different exponential relationship for snow and ice of density greater than 0.60. If Nakaya's data for Site 2, Greenland (Fig. IV-5), corresponding to a test temperature of -9C, are interpreted in accordance with eq 2, then the approximate values of the coefficient A and the exponent constant a for the low-density range are as follows:

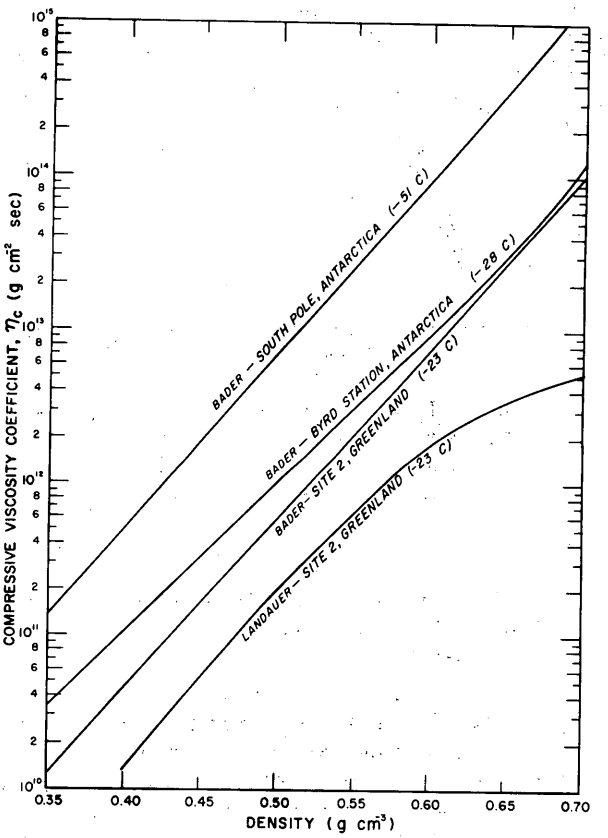

Figure IV-3. Compressive viscosity as a function of density. (After Bader, ref. 3; Landauer, ref. 8)

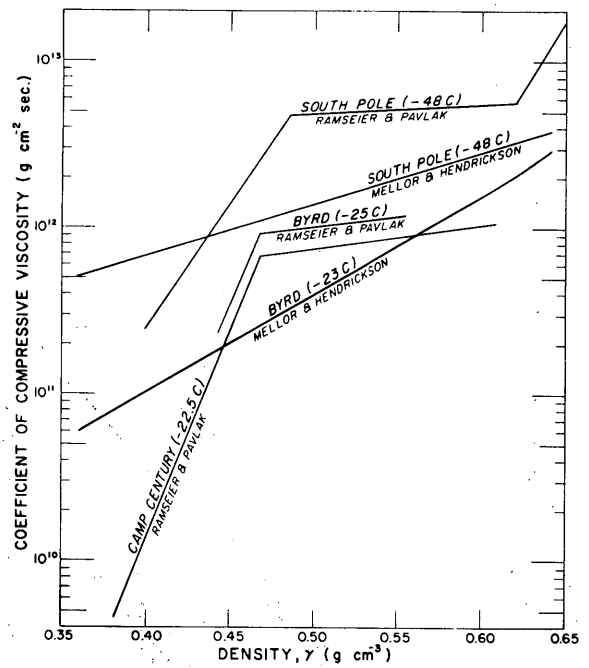

Figure IV-4. Compressive viscosity related to snow density. (After Ramseier and Pavlak, ref. 11; Mellor and Hendrickson, ref. 9).

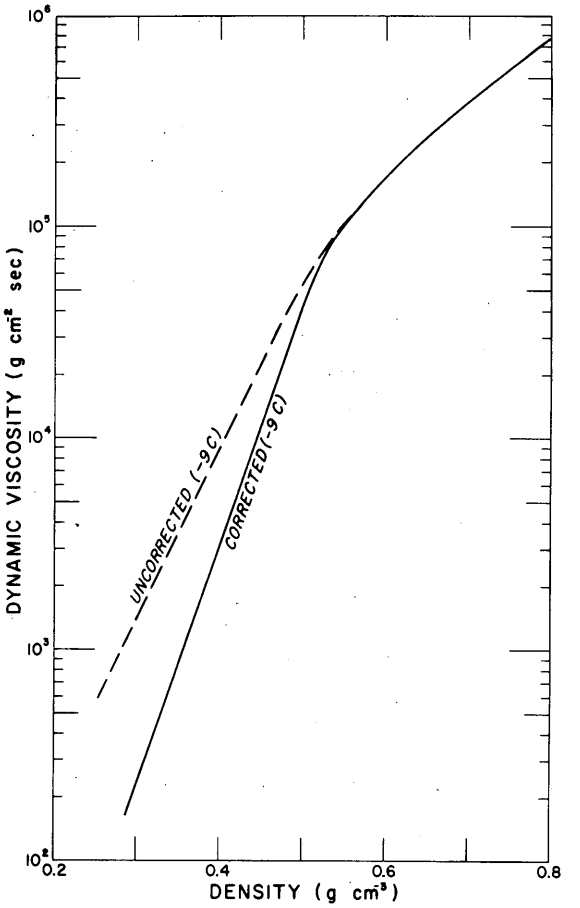

Figure IV-5. Dynamic viscosity coefficient as a function of density. The dynamic coefficient is calculated from data on the damping of flexural vibrations for small snow beams. (After Nakaya, ref. 10)

A: 6 g cm^{-2} sec for the uncorrected data; 0.1 g cm^{-2} sec for data subjected to a frequency correction. a: 18 for uncorrected data; 26 for data subjected to a frequency correction.

It will be noted that the high values of a correspond with those found from the snow densification studies. Bader's value for Site 2 lies halfway between Nakaya's corrected and uncorrected values. The actual values of the dynamic viscosity coefficient at any given density, however, are many orders of magnitude smaller than the compactive coefficients of Bader and Landauer.

Strain rate as a function of temperature

For a given stress and snow type, strain rate increases with temperature, i.e., viscosity is inversely related to temperature. The relationship is found experimentally to be exponential,[4] and in considering sub-freezing snow it is customary to adopt the following expression, for which there is some physical justification based on thermodynamics and chemical rate theory:[14, 15]

$$\eta = k e^{\frac{Q}{RT}} \qquad (6)$$

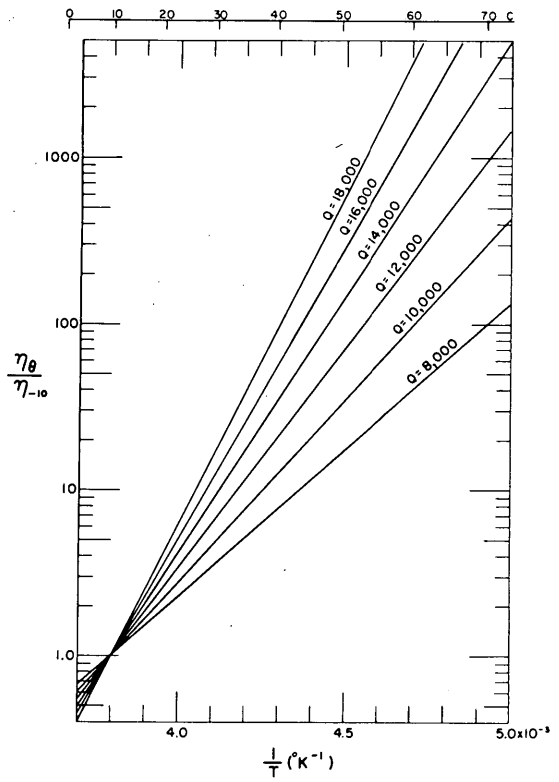

Figure IV-6. The ratio of viscosity at temperature θC to the viscosity at -10C plotted against the reciprocal of absolute temperature (a non-linear Centrigrade temperature scale is also given). The lines are based on eq 6 with activation energy as parameter.

where k = constant for given stress and snow type (a reference viscosity)
Q = the activation energy of the snow
R = the gas constant
T = absolute temperature.

Eq 6 does not represent temperature variations close to the melting point very well, but appears to be an adequate form for representing changes at low (say less than -5C) temperatures. Unfortunately, experiments show that Q is not a true constant; for snow and ice, mechanical studies give values between about 7000 and 25,000 cal/mole. While 14,000 cal/mole is sometimes adopted as a representative value for polar snow, all that can be truly said as a generalization is that Q is of the order of 10^4 cal/mole. Variations in Q may arise from impurities in the ice matrix, or from changes of structural characteristics which affect the ratio of surface to volume of ice grains and the degree of bonding between adjacent grains.

Eq 6 may be normalized to compare viscosities at various temperatures with the viscosity at some reference temperature. In Figure IV-6 the ratio of viscosity at a given temperature to the viscosity at temperature -10C is plotted against the reciprocal of absolute temperature and the temperature in degrees C for a range of activation energy values. Controlled experiments to test the validity of eq 6 are needed.

Grain size effects

The effect of grain size on strain rate has not been studied systematically, but there is evidence that viscosity increases as mean grain size increases in the range 0.2 to 2.0 mm diam. Drawing on limited data from depth-density profiles and from the experiments of Bucher,[4] Bader[2] suggests that strain rate may be inversely proportional to the third power of grain size, or

$$\eta \propto D^3$$

where D is grain diameter.

The relatively high creep resistance of very coarse-grained snow, such as depth hoar, may be responsible for the sudden yielding which appears to release avalanches or trigger firn quakes in some circumstances.

CHAPTER IV REFERENCES

1. Assur, A. (1961) Compactive deformation of snow, U. S. Army Cold Regions Research and Engineering Laboratory (USA CRREL) Technical Note (internal).
2. Bader, H. (1962) "Snow as a material" in Cold Regions Science and Engineering (F. J. Sanger, Editor), USA CRREL monographs, Part II, Sect. B.
3. _____ (1962) Theory of densification of dry snow on high polar glaciers, part II, USA CRREL Research Report 108.
4. Bucher, E. (1948) Beiträge zu den theoretischen Grundlagen des Lawinenverbaus (Contribution to the theoretical foundations of avalanche defense construction), Beiträge zur Geologie der Schweiz, Geotechnische Serie, Hydrologie, Lieferung 6. U. S. Army Snow, Ice and Permafrost Research Establishment (USA SIPRE) Translation 18, 1956.
5. Kojima, K. (1958) Sekisetsusō no nensei asshuku, IV (Viscous compression of natural snow layers, IV), Low Temperature Science, Series A, vol. 17, p. 53-64 (text in Japanese).
6. Landauer, J. K. (1955) Stress-strain relations in snow under uniaxial compression, USA SIPRE Research Paper 12.
7. _____ (1957) Creep of snow under combined stress, USA SIPRE Research Report 41.
8. _____ (1957) On the deformation of excavations in the Greenland névé, USA SIPRE Research Report 30.
9. Mellor, M. and Hendrickson, G. (1963) Confined creep tests on polar snow, USA CRREL Research Report 138.
10. Nakaya, U. (1959) Visco-elastic properties of snow and ice from the Greenland Ice Cap, USA SIPRE Research Report 46.
11. Ramseier, R. O. and Pavlak, T. (in preparation) Unconfined creep tests on polar snow, USA CRREL Research Report.
12. Yosida, Z. (1963) "Physical properties of snow" in Ice and snow, processes, properties and applications (W. D. Kingery, Editor). Cambridge, Massachusetts: M.I.T. Press.
13. Kojima, K. (1964) "Densification of snow in Antarctica" in Antarctic snow and ice studies (M. Mellor, Editor). Washington, D. C.: American Geophysical Union.
14. Kennedy, A. J. (1962) Processes of creep and fatigue in metals. Edinburgh: Oliver and Boyd, 480 p.
15. Stanford, E. G. (1949) The creep of metals and alloys. London: Temple Press, 162 p.

CHAPTER V. SURFACE FRICTION AND ADHESION

Sliding friction

In practical problems involving the sliding of a solid body over natural snow, the resistance to motion usually includes both surface friction and sinkage resistance. Sinkage resistance arises partly from the expenditure of energy in compacting the snow beneath the slider, and partly from shearing snow at the front and the edges of the slider. If the snow is sufficiently firm to bear the weight of the slider without sinkage, however, the resistance is purely frictional. The following remarks apply to pure friction, particularly for skis and sledge runners.

The classical laws of dry friction state that frictional resistance is directly proportional to the normal force between the sliding surfaces, but independent of the area of contact; the coefficient of friction expresses the ratio of the sliding resistance to the normal force, and it is a constant for any given pair of materials. Friction between snow and a solid slider frequently conforms approximately to these laws at a given temperature, but there may be significant deviations. The coefficient of friction may vary with size, shape and bearing pressure of the contact area, with sliding speed, and with temperature. To explain the effects of temperature and slide speed, some of the size and pressure effects, and the remarkably low friction of snow, it seems necessary to invoke the existence of a liquid water film (or, at least, a "liquid-like" film), so that the contact is lubricated rather than dry.*

The presence of a water film beneath sliding skis has been demonstrated by electrical conductivity measurements, which indicated formation of a continuous film at temperatures near the melting point but showed only localized areas of water film forming at lower temperatures.[1,3] The experiments suggested that, while pressure melting may be significant at temperatures near 0C, frictional heating is the dominant effect at low temperatures and at high sliding velocities.† Other experiments were made with skis having widely different thermal conductivities to test whether pressure melting or frictional heat contributed most to water formation, and it was confirmed that frictional heating provides the water film when ambient temperatures are well below the melting point and when the ski has an appreciable speed.[1,3]

Effect of temperature. There is ample evidence, ranging from the accounts of sledge travelers to experimental data (Fig. V-1 to 3), that the coefficient of friction for most runner materials shows a marked dependence on temperature. Friction is low on dry snow at temperatures near the melting point, but at very low ambient temperatures, say -25C, snow loses its exceptional attribute of low friction and becomes comparable to dry sand or other powdered solids.

Minimum friction occurs at 0C with the snow in a "dry" condition, i.e. with no appreciable amount of unbound water. If the snow becomes wet and slushy, the coefficient of friction will increase abruptly for some materials. The materials most adversely affected by wet snow are those which are water absorbent, or which become "wetted" (contact angle decreases) after prolonged exposure to water.

As temperature decreases, the friction of metals and polymers on snow increases almost linearly.[1,2,5] The effect is similar to the variation of adhesive bond strength with temperature for the same materials frozen onto ice. Some ski waxes, however, show (Fig. V-4) an abrupt increase of friction as temperature drops to -10C or so. (There is a suggestive similarity here to the abrupt increase of adhesion which occurs near the eutectic temperature for contaminated ice frozen to stainless steel[2].)

The increase of kinetic friction with decreasing temperature, attributed to diminution of the water film, may be expected to depend to some extent on the thermal properties of

* An alternative theory of lubrication by a film of water vapor was proposed by McConica.[10,11]

† An electrical explanation of the liquid-like film has also been put forward.[15]

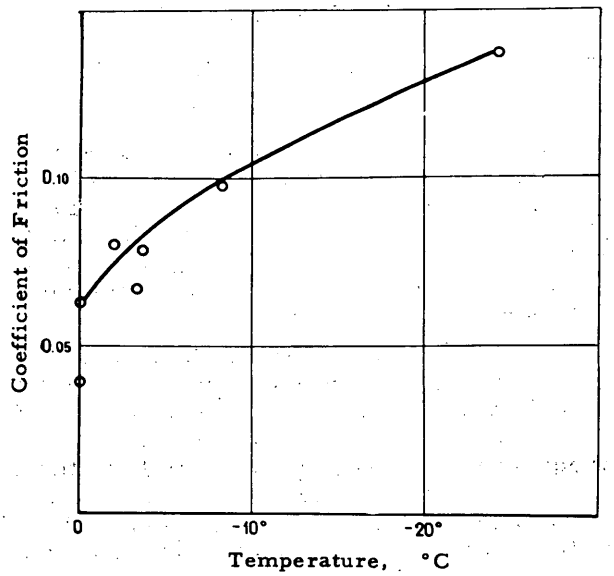

Figure V-1. Coefficient of friction as a function of temperature for steel runners sliding on new snow at 2.5 m/sec. Nominal bearing pressure 0.33 kg/cm^2. (After Ericksson, ref. 5)

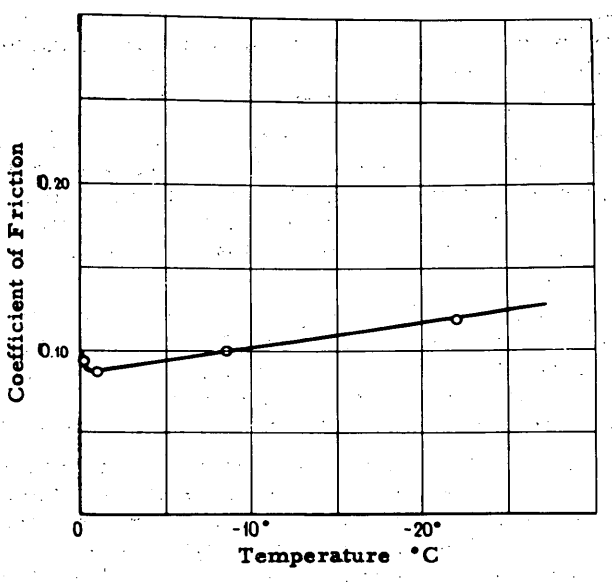

Figure V-2. Coefficient of friction as a function of temperature for wooden runners (coated with paraffin-wax) sliding at 2.5 m/sec. Nominal bearing pressure 0.033 kg/cm^2. (After Ericksson, ref. 5)

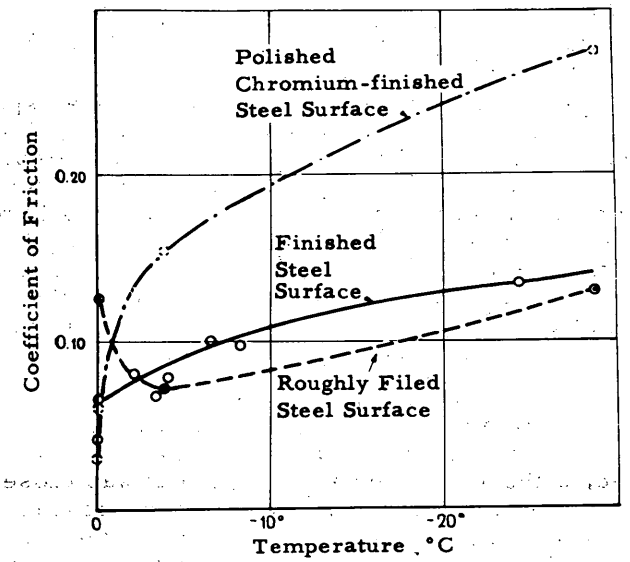

Figure V-3. Coefficient of sliding friction for steel runners plotted against temperature, with surface finish as parameter. Nominal pressure 0.33 kg/cm^2, sliding speed 2.5 m/sec. (After Ericksson, ref. 5)

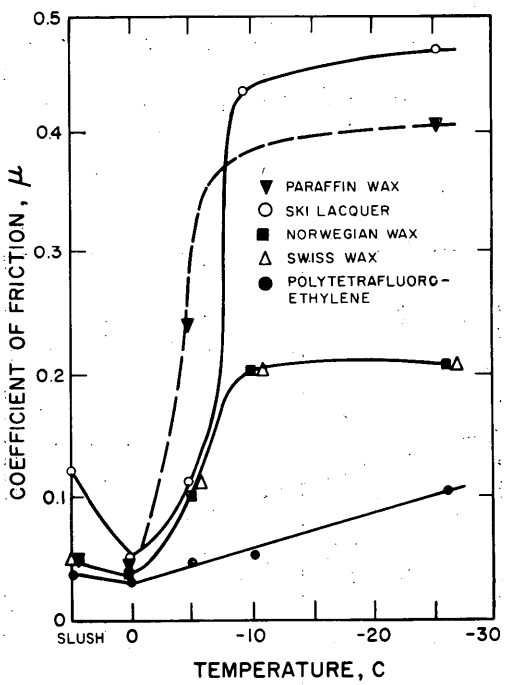

Figure V-4. Coefficient of static (low speed) friction plotted against temperature for various ski-facing materials. (After Bowden, ref. 1)

the runner. A material of high thermal conductivity will remove frictional heat from the slide surface relatively rapidly, so that water lubricant is not formed as readily and friction is comparatively high.

Effect of sliding velocity. In general, friction decreases as speed of sliding increases. Bowden[1, 2] ran miniature skis of waxed wood, lacquered wood, Perspex (Plexiglas) and aluminum on snow at -10C. He found that the coefficient of friction at 0.03 m/sec was close to the static coefficient, but at a speed of 5 m/sec the friction was an order of magnitude smaller. In experiments with Bakelite sliding on ice at -15C, McConica[11] found that the coefficient of friction continued to decrease with increasing slide velocity for velocities up to 8 m/sec. This effect can be explained by frictional melting and lubrication[2]. Bowden[2] also found that on reducing the speed of a ski after a high-speed run, snow adheres to most surfaces, apparently because the melt water refreezes. An exception was the strongly hydrophobic P. T. F. E. (Teflon)*.

Shimbo[13] performed experiments with a Teflon slider at speeds up to 7.2 m/sec and found no significant variation of friction with speed above 0.05 m/sec (there was a decrease of friction with increasing speed up to 0.05 m/sec). The experimental temperature was unspecified, although it seems likely that it was close to the melting point. On snow at 0C slide speed may be unimportant, since a lubricating film is already present and pressure melting may increase the amount of water irrespective of speed. A further point relevant to the Shimbo experiment is that Teflon exhibits low friction at all speeds[2], as its peculiar characteristics render it less dependent on water lubricant.

Effect of bearing pressure and runner size. If pressure melting makes a significant contribution to the lubrication of a sliding interface, then a variation of coefficient of friction with contact pressure might be expected.

Bowden[2] found that, to a first approximation, friction was proportional to normal load and independent of apparent contact area. Shimbo[13] also failed to detect a variation of friction with bearing pressure over the range 20 - 70 g/cm^2, but since he worked with Teflon over a small pressure range this is perhaps inconclusive. Ericksson, however, slid steel runners at 2.5 m/sec on new snow at 0C and found that the coefficient of friction decreased from about 0.065 to 0.04 as the apparent normal pressure increased from 10 to 800 g/cm^2 (Fig. V-5). From experiments with Bakelite sliding on smooth ice

* Polytetrafluoroethylene

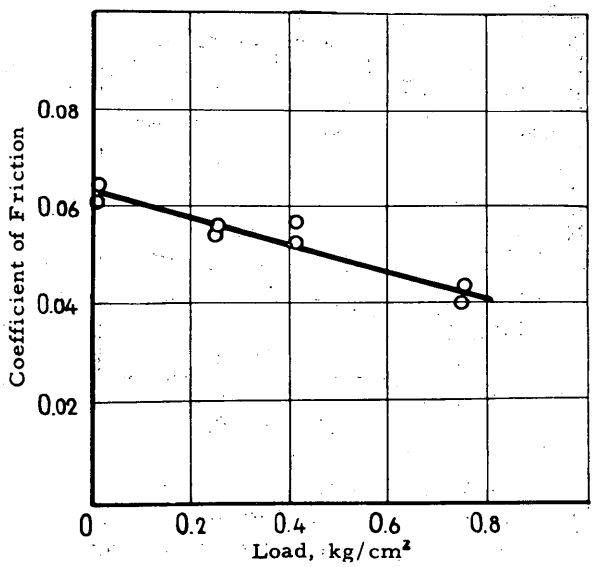

Figure V-5. Coefficient of friction as a function of nominal bearing pressure for steel runners sliding on new snow at 2.5 m/sec. Snow temperature 0C. (After Ericksson, ref. 5)

at -15C, McConica[11] found that the coefficient of friction increased with nominal pressure at pressures less than 50 g/cm^2, reached a maximum between 50 and 80 g/cm^2, and decreased again exponentially as pressure increased further. In another experiment on ice, Ericksson[5] slid steel runners at 2.5 m/sec and increased the area of the sliding surface from 20 to 160 cm^2 while maintaining a constant load of 40 kg. This procedure confuses the effects of pressure and bearing area but, as bearing area increased through the range (and pressure thus decreased), the results showed an increase of the coefficient from 0.02 to more than 0.03 at -10C and from less than 0.04 to about 0.05 at -20C.

The available data are not in complete harmony, but it seems likely that increase of bearing pressure produces some decrease in friction in the pressure range which is of practical interest (e.g. man on skis about 20 g/cm^2, heavy cargo sled about 500 g/cm^2). Whether the effect is of much practical significance is another matter, as the penalties of increased sinkage resistance at higher pressures would probably outweigh any frictional advantage.

It might be expected that friction would decrease to some extent as size of the slider increased, since the frictional heating theory of lubrication suggests a favorable modification of snow by passage of the slider. Furthermore, deleterious edge effects increase in proportion to a linear dimension of the slider, while areal effects vary with the square of a linear dimension; hence there is proportionately less "edge effect" on a large slider. Bowden[2] did not find any significant size effects in his experiments, but Ericksson[5] found that the coefficient of friction for steel runners sliding on ice at -4C decreased markedly as the length of the runner increased from 0.1 to 1.7 m, the length to breadth ratio remaining constant at 20:1.

Simple theoretical considerations suggest that a surface which is elongated in the direction of travel should slide more easily than a broad but short surface of the same area. Although no reports of controlled experiments have been found, practical experience with skis seems to provide adequate confirmation of this supposition (there are, of course, additional reasons for using long narrow skis).

Effect of grain size. Average grain sizes of surface snow range through more than an order of magnitude, from about 100 μ to more than 1 mm diam. Surface properties of the grains consequently vary appreciably, and some effects on adhesion and melting might be expected. There is the further possibility that real contact area may be sensitive to grain size, particularly if asperities on the slider surface have dimensions comparable to those of snow grains.

Ericksson[5] found that the coefficient of friction increased as grain size decreased (Fig. V-6) in experiments made at -2C and -25C. It is also known to skiers that friction is relatively low on old, coarse-grained snow. This effect is explainable by the water film theory, but the low friction of coarse, cohesionless snow has also been attributed (less convincingly) to a "ball-bearing" action by surface grains.[14]

Properties of slider materials. It is evident from the foregoing that there is no single value for coefficient of friction of a given material sliding on snow; however, Tables V-I through V-IV give an idea of absolute magnitudes for some common runner materials.

At temperatures close to 0C most runner materials have a low coefficient of friction. High sliding speed is unnecessary, since pressure melting can occur. At low temperatures and low sliding velocities there is little lubrication, and friction on snow is not much different from friction on sand or other powdered solids.[2] Under these conditions the frictional properties of different materials become marked; substances which develop weak molecular forces at the interface (as indicated by high contact angle) have the lowest friction. A number of plastics, with Teflon as the outstanding example, exhibit superior frictional qualities at all temperatures and slide speeds; they appear to be largely independent of water lubrication, since they slide with low friction on non-melting solids.

Metals sliding at low temperatures lose their frictional heat quite rapidly as a consequence of high thermal conductivity, and thereby suffer. They are also prone to adhesion of snow when melt water refreezes after they slow down from a high-speed slide.

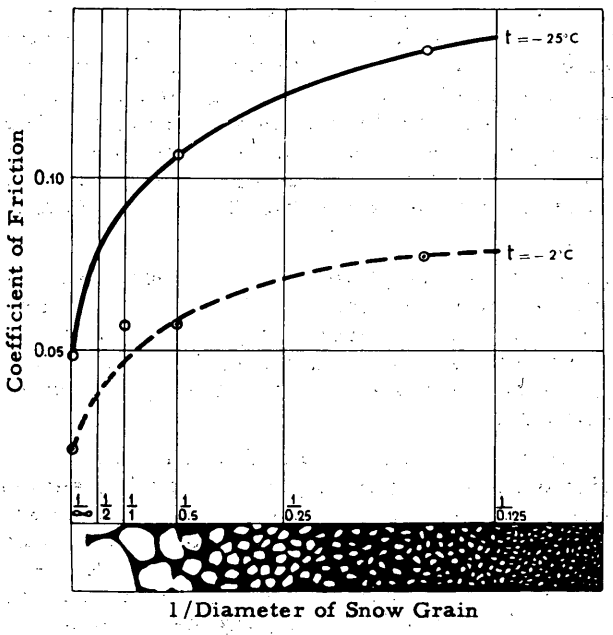

Figure V-6. Relation between coefficient of friction and snow grain size for steel runners sliding at 2.5 m/sec. Nominal bearing pressure 0.33 kg/cm^2. (After Ericksson, ref. 5)

In wet snow, hydrophobic materials retain their low friction, but those substances which can be wetted show an abrupt increase of friction in wet snow. Some materials, including certain ski waxes, apparently become increasingly hydrophilic as they are rubbed[2], so that their friction increases with length of use in wet snow.

A curious effect of surface roughness was found by Ericksson[5], who slid steel runners with various surface finishes on snow at a variety of temperatures. At temperatures below about -5C, there was an inverse relation between friction and surface roughness, highest coefficients being given by polished chromium plate, lower coefficients by a machined surface, and the lowest coefficients by a roughly filed surface. At 0C this ranking order was reversed (Fig. V-3).

Static friction and adhesion

The resistance which must be overcome to put a slider into motion is customarily regarded as the static friction. On snow, however, a runner which has been left standing for some time at temperatures below the melting point will actually become bonded to the snow mass. It therefore seems desirable to make a distinction between static friction and adhesion.

Static friction is the resistance which must be overcome to restart the motion immediately after a "cold" slider has been brought to rest, i.e. after zero contact time. Bowden and Tabor[2] find that static friction defined in this way is very close to the kinetic friction for very low slide velocities, so that for practical purposes static friction may be regarded as the limiting zero-velocity value of sliding friction (so long as there is no residual frictional heat from higher speed sliding). Adhesion, on the other hand, is the shear strength of the bond developed between snow and a runner by metamorphism at the interface.

True static friction should always be somewhat greater than sliding friction.* From frictional melting theory the coefficient of static friction at 0C would not be expected to

* There are a few reports of static friction being lower than sliding friction, perhaps because the snow surface was favorably modified by prolonged contact, or because the slider face was unfavorably modified by rubbing (some polymers may become more hydrophilic[2]).

be much higher than the sliding coefficient, but at low temperatures the static coefficient should be considerably higher than the kinetic coefficient, since there is no lubrication until sliding begins. At temperatures which are too low for significant pressure melting beneath a stationary runner, the static coefficient would not be expected to show much dependence on temperature.

The variations of true static friction should closely parallel the effects observed for kinetic friction where frictional heating is not a major factor. Adhesion, which constitutes the principal starting resistance in most practical situations where temperatures are sub-freezing, involves different considerations, since the several factors controlling snow metamorphism and bond formation must be taken into account.

Formation of adhesive bond. When a slider comes to rest on snow, much of the water film beneath it will freeze if temperatures are below the normal melting point, thus forming an ice bond. The rate of refreezing will depend on the conductivity of the runner. If the runner continues to lie in the same place for considerable time, further bonding between its face and the snow surface may develop as a result of sublimation or molecular diffusion in the snow. The rate of bond formation by "dry" metamorphism of this kind will depend on temperature, snow type, and the direction and magnitude of temperature gradients immediately below the snow surface. Heat conduction in the runner, and absorption of solar radiation on its upper face, will also be factors. One further consideration is viscoelastic compaction of the snow during prolonged contact. Snow under the runner will deform with time, gradually increasing the real area of contact.

In general the strength of an adhesive bond will increase with time.

Shear strength of adhesive bond. The adhesion of ice to metals and polymeric materials has been studied by Jellinek[6,7] and Raraty and Tabor[2,16]. It is found that the shear strength of the adhesive bond increases almost linearly as temperature falls from 0C. In the case of metals a limiting strength of adhesion was reached in both sets of experiments, the limit apparently being set by the shear strength of the ice itself (the actual temperature at which the limit is reached seems to depend on the test method and the strain rate). The shear strength of the bond developed between ice and polymers continued increasing to lower temperatures, and shear always occurred at the interface and not in the ice, as was the case for metals. Thus it appears that interfacial forces, determined by molecular characteristics of the substrate material, are much lower for the plastics tested than for metals. Contamination of a metal surface seems to reduce the real area of contact between metal and ice, so that adhesion decreases. When ice contaminated with certain salts was frozen to stainless steel[2], there was an abrupt increase of adhesion as temperature fell below the eutectic temperature.

Corresponding effects probably occur when snow adheres to solid surfaces, although the low shear strength of snow (relative to ice) may set the limiting adhesive resistance for a wider range of conditions. For a runner frozen down to the snow the adhesive resistance can never exceed the shear strength of the snow for a normal pressure equivalent to the bearing pressure of the runner.

Ericksson[5] gives a relation between the apparent coefficient of static friction (adhesion) and the average grain size of snow on which the steel runner has been lying for 5 sec at -3C (Fig. V-7). There is an increase of starting resistance with decreasing grain size, and Ericksson suggests that finer grains give a greater real contact area. It also seems possible that more vigorous molecular diffusion at the surface of small grains produces more rapid bonding. A further possibility is that any viscous effects produced by a liquid-like layer would probably be more pronounced at the surface of small grains.

While the physics of adhesion is still not fully understood on the atomic scale, it seems to be generally agreed that the contact angle between water and a given solid provides a useful indicator of the adhesion between ice and that solid. Bowden[2] and Jellinek[6,7] give values for the contact angle between water and a number of materials which are of interest for runners and ice-inhibiting coatings.

Table V-I. Coefficients of sliding friction for plastics. (From Shimbo, ref. 13)

Plastics	Air temp.	μk (-20C)	μk (-1C)	μk (+2C)
Polytetrafluoroethylene		0.04	0.03	0.02
Polyethylene		0.05	0.04	0.03
Polypropylene		0.05	0.04	0.03
Polycarbonate		0.04	0.03	0.03
Polyurethane		0.04	0.03	0.06*
Polyamid (Nylon)		0.04	0.04	0.07*
Polyvinyl chloride		0.06	0.03	0.08*
Epoxy resin		0.05	0.03	0.07*
Celluloid		0.05	0.05	0.08*
Urea resin		0.06	0.04	0.11*
Amyno-alkyd resin		0.06	0.05	0.10*
Melamine resin		0.06	0.05	0.05*
Phenolic resin		0.04	0.03	0.07*
Styrol butadiene copolymer		0.04	0.03	0.08*
Styrol acrylonitrile butadiene copolymer		0.04	0.03	0.08*

*Abnormal increase of μk was observed.
Speed: 2.4 m/sec, pressure 21 g/cm^2.

Table V-II. Coefficients of friction for skis on snow. (After Klein, ref. 8)

Ski surface material	Coefficient of sliding friction Min	Max	Coefficient of adhesion or static friction Min	Max
Smooth beeswax	.029	.288	.092	.808
16 g brass	.122	.428	.226	.977
16 g Monel metal	.103	.167	.197	.847
22 g stainless steel	.128	.322	.056	.992
Bakelite varnish	.072	.211	.336	.631
White ash treated with linseed oil	.069	.215	.420	.811
Bakelite, fabric base	.064	.223	.227	.620
Bakelite, graphite incorporated	.068	.162	.145	.605

Table V-III. Coefficients of friction of various materials on wet snow. (After Bucher and Roch, ref. 4)

Material	Air temperature (°C)	Velocity v in m/sec v = 0.18	v = 0.40	v = 0.70	v = 1.25
Glass	0	-	-	-	-
		0.015	0.012		
	+8.5	0.015	0.012	-	-
Aluminum	0	0.046	0.041	0.040	0.040
		0.043	0.041	0.039	0.043
	+8.5	0.039	0.041	0.038	0.046
Iron	0	0.189	0.124	0.088	0.075
		0.148	0.121	0.050	0.043
	+8.5	0.107	0.118	0.012	0.012
Wood lacquered	0	0.140	0.119	0.111	0.071
		0.163	0.138	0.116	0.099
	+8.5	0.186	0.157	0.121	0.127
Wood unlacquered	0	-	0.069	0.071	0.071
		0.183	0.165	0.124	0.128
	+8.5	0.183	0.164	0.158	0.185

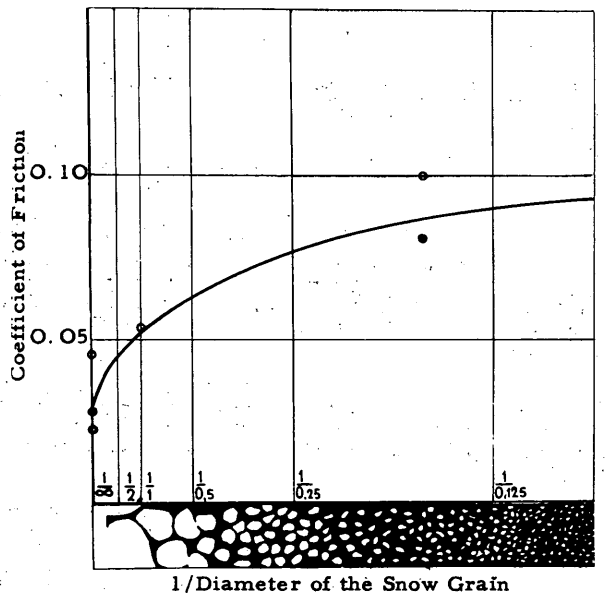

Figure V-7. Relation between coefficient of static friction (contact time 5 sec) and snow grain size for steel runners. Nominal pressure 0.3 kg/cm^2, temperature -3C. (After Ericksson, ref. 5)

Table V-IV. Coefficients of friction of sled runners on compacted virgin snow (Greenland).(After Rula, ref. 12)

Payload (tons)	Steel runners			Kel-F runners			Teflon runners		
	Dry	Moist	Wet	Dry	Moist	Wet	Dry	Moist	Wet
	Coefficients of kinetic friction								
5	0.12	0.09	0.08	0.11	0.06	0.06	0.06	0.05	0.05
	0.15	0.18	0.14	0.11	0.08	0.10	0.06	0.06	0.10
10	0.12	0.12	0.08	0.12	0.08	0.05	0.07	0.06	0.05
	0.15	0.17	0.16	0.12	0.10	0.12	0.06	0.08	0.10
15	0.12	0.07	0.08	0.10	-	0.07	0.07	0.05	0.05
	0.15	0.13	0.18	0.10	-	0.12	0.09	0.07	0.11
	Coefficients of static friction								
5	0.30	0.34	0.42	0.27	0.19	0.21	0.17	0.20	0.17
	0.37	0.48	0.51	0.11	0.08	0.10	0.06	0.06	0.10
10	0.40	0.37	0.40	0.28	0.19	0.17	0.20	0.19	0.19
	0.44	0.49	0.57	0.21	0.20	0.26	0.16	0.17	0.24
15	0.35	0.37	0.39	0.25	-	0.17	0.14	0.13	0.17
	0.31	0.48	0.50	0.22	-	0.26	0.16	0.16	0.27

CHAPTER V REFERENCES

1. Bowden, F. P. (1955) Friction on snow and ice and the development of some fast-running skis, Nature, vol. 176, no. 4490, p. 946.
2. _____ and Tabor, D. (1950) The friction and lubrication of solids. Oxford University Press. Also Part II (1964).
3. _____ (1956) Friction and lubrication. London: Methuen.
4. Bucher, E. and Roch, A. (1946) Reibungs-und Packungswiderstände bei raschen Schneebewegungen (Friction and resistance to compaction of snow under rapid motion), Mitteilungen des Eidgenoss, Davos-Weissfluhjoch, Institut fur Schnee und Lawinenforschung.
5. Ericksson, R. (1949) Medens friktion mot snö och is (Friction of runners on snow and ice), Foren. Skogsarbet., Kgl. Domänstyrelsens Arbetsstud., Med. 34-35. U. S. Army Snow Ice and Permafrost Research Establishment (USA SIPRE) Translation 44, 1955.
6. Jellinek, H. H. G. (1957a) Contact angles between water and some polymeric materials, USA SIPRE Research Report 36.
7. _____ (1957b) Adhesive properties of ice, USA SIPRE Research Report 38. Also Part II (1960), USA SIPRE Research Report 62.
8. Klein, G. J. (1947) The snow characteristics of aircraft skis, National Research Council of Canada, Division of Mechanical Engineering, Aeronautical Report AR-2.
9. Kuroda, M. (1942) Sori no teikō ni kansuru kenkyū (Resistance of snow to a sledge), Seppyo, vol. 4. USA SIPRE Translation 36, 1955.
10. McConica, T. H. (1948) Friction on snow, Office of the Quartermaster General, U. S. Army, Unpublished report to Research and Development Division.
11. McConica, T. H. (1950) Sliding on ice and snow, Office of the Quartermaster General, U. S. Army, Unpublished report to Research and Development Division.
12. Rula, A. A. (1960) Trafficability of snow, USA Waterways Experiment Station, Vicksburg, Technical Memorandum no. 3-414.
13. Shimbo, M. (1961) "The mechanism of sliding on snow" in Snow and ice commission, General Assembly of Helsinki, International Union of Geodesy and Geophysics. International Association of Scientific Hydrology, Pub. no. 54.
14. University of Minnesota (1951) Review of the properties of snow and ice, USA SIPRE Report 4.
15. _____ (1955) Friction on snow and ice, USA SIPRE Report 17.
16. Raraty, L. E. and Tabor, D. (1958) The adhesion and strength properties of ice, Proceedings of the Royal Society, vol. 245A, p. 184-201.

APPENDIX V-A.

Friction of tires on snow

Considering the practical importance of friction between tires and snow, there is surprisingly little information available. Where tire traction is concerned, it is not always clear whether the limiting factor is friction between rubber and snow, or internal friction of the snow itself (shear strength), particularly in the case of tires with aggressive treads. If skid-braking on compact snow is considered, however, it seems that friction between rubber and snow may provide the major motion resistance.

Wehner* measured the friction of automotive tires on compact snow using an instrumented trailer. He obtained values for the apparent coefficient of friction in the range 0.20-0.35. Abele† conducted skid tests with a 5-ton truck fitted alternately with three types of heavy-duty tires. The snow had a surface density in excess of 0.6 g/cm^3 and its temperature was -10C. He calculated apparent coefficients of friction from energy and momentum consideration, finding values in the range 0.13-0.34. A curious feature of the Wehner and Abele results (Fig. V-A1) is the apparent increase of friction with speed; a contrary trend might have been expected in view of the findings for pure sliders.

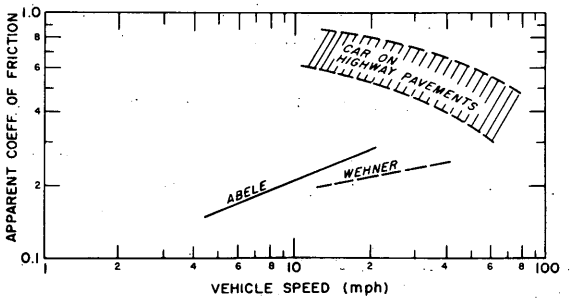

Figure V-A1. Apparent coefficients of friction for automotive tires on compact snow compared with values for dry pavements. (After Abele†)

*Wehner, B. (1959) Special observations on the resistance to sliding on snow covered or icy road surfaces, Rev. gén. caoutchouc, vol. 36.
(1960) Griffigkeitsmessungen auf winterglatten Fahrbahnen (Measurements of traction on slippery winter roads), Strasse u. Verkehr, vol. 46. (text in German)

†Abele, G. (1963) Skid tests performed with a wheeled vehicle on a processed snow trench floor, U. S. Army Cold Regions Research and Engineering Laboratory (USA CRREL) Technical Note (internal).

CHAPTER VI. THERMAL PROPERTIES AND RADIATION CHARACTERISTICS

Heat transfer through snow

Heat may travel through snow in any or all of the following ways:

Conduction. Conduction through the ice grains is usually the dominant factor when heat passes through a considerable thickness of dense, non-aspirated snow. The coefficient of thermal conductivity is dependent on the degree of continuity of the ice matrix in the direction of heat flow; it may therefore be expected to increase with density and also to vary with the degree of ice bonding between adjacent grains. Conduction through air in the pores of the snow also takes place, but is only significant in low-density snow.

Convection and vapor diffusion in the pores. A temperature gradient may cause air to move through the pores, carrying sensible and latent heat. An exception is the one-dimensional case where temperature decreases with depth, and air stratification is stable. Convection may be additionally stimulated by surface wind, by barometric pressure changes, or by artificial means. A temperature gradient necessarily produces a gradient of vapor pressure, so that latent heat transfer by vapor diffusion is always present.

Radiation through the snow. Thermal radiation is absorbed and scattered strongly in snow, so that significant transmission is limited to small distances (a meter or so at the most). The radiation flux, and hence the energy available for absorption, is a function of the distance from the source, so that the temperature distribution in the snow can be significantly affected by radiation. Radiation from grain to grain in the snow mass is probably negligible.

Even though heat transfer is controlled by this variety of processes in snow, for practical purposes the assumption of conduction alone is often adequate, so long as a suitable "effective conductivity" is used and the boundary conditions of the problem are appropriately stipulated. To illustrate this, the general approach to some common problems of heat flow and temperature distribution in snow is outlined below.

Seasonal temperature variations in deep polar snow

Subsurface temperatures in the dry snow of polar ice caps fluctuate periodically in response to the cyclic variation of surface temperature. It is customary to regard these temperature changes as a simple problem of solid conduction without phase changes, an assumption which seems justifiable, since temperatures are low and icy crusts in relatively high-density snow inhibit air movement through the pores.

Assuming that temperature in a horizontal plane at any given time and depth does not vary appreciably, and neglecting radiation absorption, which is effective only near the surface, the problem reduces to one of linear conduction in a semi-infinite solid according to the equation

$$\frac{\partial^2 \theta}{\partial z^2} - \frac{1}{a} \frac{\partial \theta}{\partial t} = 0 \qquad (1)$$

where the diffusivity a is given by $a = \frac{k}{\gamma c}$, (k = conductivity, γ = snow density, c = specific heat).

A solution is required for the boundary conditions

$z = 0 \qquad \theta = f(t)$

$z \to \infty \qquad \theta \to \theta_m$.

θ_m is the mean annual surface temperature for the site, and $f(t)$ is a harmonic function, which could be a Fourier representation of the annual temperature cycle, but which can be assumed to be a simple sine wave for most purposes, since high frequency components are rapidly "filtered-out":

$$\theta_{0,t} = \theta_m + A_0 \sin(2\pi nt) \quad (2)$$

where $\theta_{0,t}$ = surface temperature at time t (see footnote)*

θ_m = mean annual surface temperature

A_0 = amplitude of the surface temperature wave

n = wave frequency (1 cycle per year).

The solution of eq 1 thus becomes

$$\theta_{z,t} = \theta_m + A_0 e^{-z\sqrt{\frac{\pi n}{a}}} \sin\left(2\pi nt - z\sqrt{\frac{\pi n}{a}}\right). \quad (3)$$

The temperature at any depth in the snow therefore fluctuates sinusoidally around the annual mean, the amplitude being reduced below that of the surface wave by a factor $e^{-z\sqrt{\frac{\pi n}{a}}}$, and the subsurface wave lagging the surface wave by an angle of $z\sqrt{\frac{\pi n}{a}}$ radians (Fig. VI-1 and 2). At any depth z, the wave amplitude and time lag are given by

$$A_z = A_0 e^{-z\sqrt{\frac{\pi n}{a}}}$$

$$t = \frac{z}{2\sqrt{\pi n a}}$$

and the temperature wave travels into the snow (Fig. VI-3) with an apparent velocity

$$V = 2\sqrt{\pi n a}.$$

Such an analysis permits the effective thermal conductivity to be calculated from suitable field data or, alternatively, surface temperature data can be used to predict the effects at depth if a value for the thermal conductivity is assumed. The mean annual surface temperature for ice cap locations θ_m can be obtained from measurement of the snow temperature at 10-15 m depth†, where wave amplitude is sufficiently close to zero for most practical purposes ($A_z < 0.5C$). If the surface amplitude can be estimated from data for comparable sites, a good estimate of θ_m can be made from snow temperature measurement at shallow depths.

Temperature changes under the surface of snow exposed to solar radiation

Absorption of solar radiation in snow affects the temperature distribution in layers just below the surface; a maximum temperature may be developed under the surface, and subsurface melting can occur. Absorbed radiation has the effect of a distributed heat source, and the differential equation describing changes of temperature with depth and time has the form

$$\frac{\partial^2\theta}{\partial z^2} - \frac{1}{a}\frac{\partial\theta}{\partial t} + \frac{S_z}{k} = 0. \quad (4)$$

*Here time is measured from the moment in spring when surface temperature rises above the annual mean temperature, i.e., $t = 0$ when $\theta_{z=0} = \theta_m$.

† Mean surface temperature changes from year to year, and Lachenbruch[20] has pointed out that the temperature at this depth is slightly modified by "memory" of the mean for the last-year-but-one.

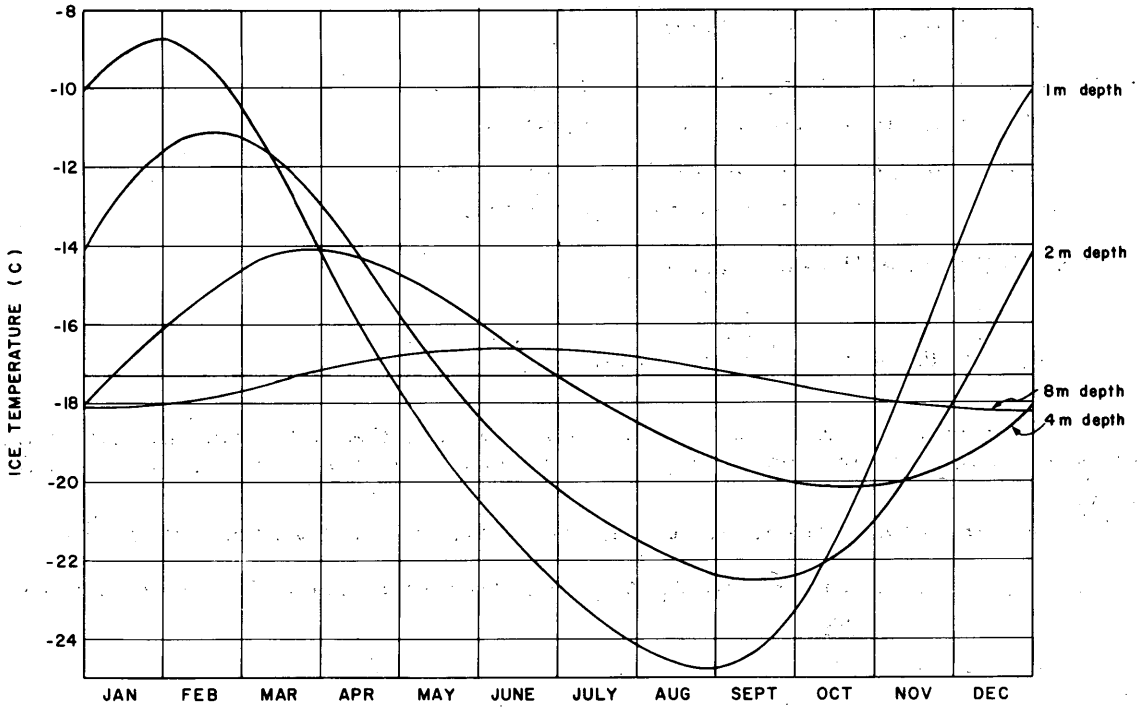

Figure VI-1. Annual temperature waves (smoothed) at various depths in the upper layers of an Antarctic ice shelf. (After Schytt, ref. 27)

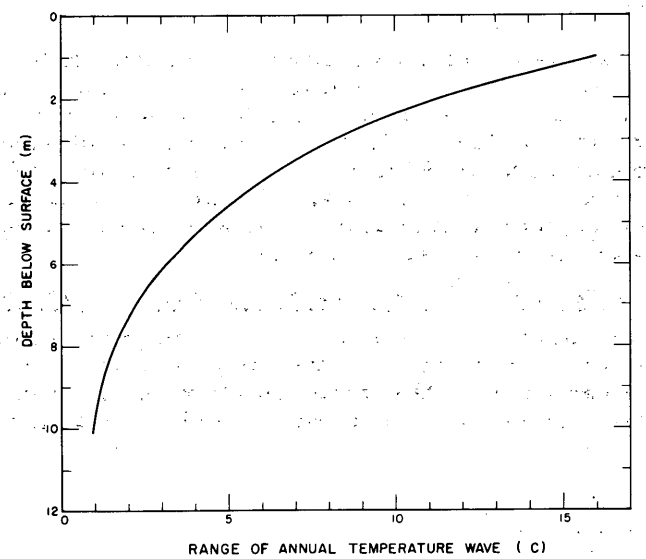

Figure VI-2. Amplitude of annual temperature waves plotted against depth. This exponential curve shows the attenuation of the waves drawn in Figure VI-1. At 10-m depth the annual fluctuation of temperature is about 1C. (From data by Schytt, ref. 27)

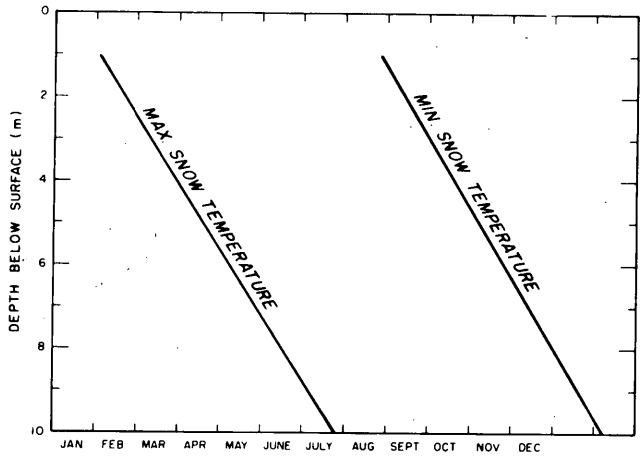

Figure VI-3. Times of occurrence of maximum and minimum temperatures at various depths in the snow, from the data of Figure VI-1. The slopes of the lines give the rate at which a temperature wave travels into the snow, and from this speed of penetration the effective thermal diffusivity of the snow can easily be calculated. These lines show a rate of penetration of about 1.6 m per month. (From data by Schytt, ref. 27)

The heat generation rate at any depth z, S_z, is the rate of radiation absorption, which can be expressed for homogeneous snow as

$$S_z = I_0 \nu e^{-\nu z} \tag{5}$$

where I_0 is the flux density of radiation penetrating the surface (i.e., the incident radiation minus the reflected radiation), and ν is the extinction coefficient for the particular snow type.

Seasonal temperature variations in snow subject to summer melt

Seasonal temperature variations in snow which melts in summer are less amenable to analysis, since phase changes are involved and heat is transferred by melt water percolation. Figure VI-4 gives an example of annual temperature changes at various depths in snow which melts at the surface in summer. The problem is somewhat similar to that concerning freezing and thawing in the active layer of permafrost, which has received some attention.[19]

Temperatures in snow exposed to nuclear radiation

Temperature distribution in snow exposed to nuclear radiation can be calculated by regarding the radiation as a distributed heat source within the mass. Taking suitable boundary conditions for the particular problem and making the heat generation term some function of distance from the source, temperature distribution is obtained from the solution of the general equation.

$$\nabla^2 \theta - \frac{1}{a} \frac{\partial \theta}{\partial t} + \frac{S_{(x, y, z)}}{k} = 0 \tag{6}$$

where $S_{(x, y, z)}$ = heat generation rate at (x, y, z) due to radiation,

k = thermal conductivity (assumed constant).

The steady-state form of eq 6 has been solved analytically for simple boundary conditions by Tien[29] who treated the problem of a continuous source in an infinite medium. More complex cases can be treated numerically.

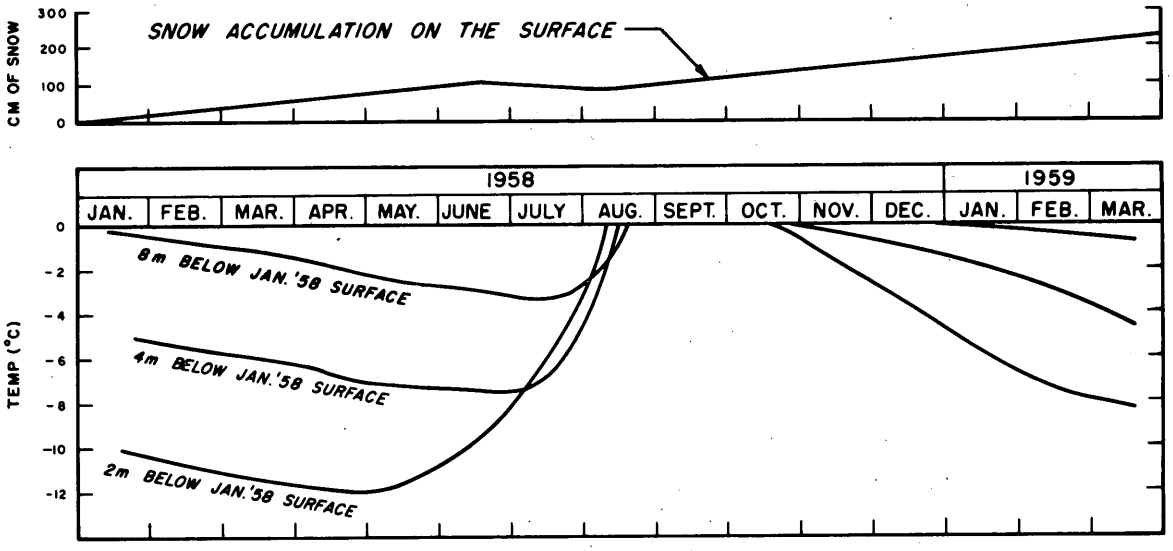

Figure VI-4. Annual temperature changes in snow subject to summer melting at the surface and infiltration of melt water. (From data by Chizhov, ref. 8)

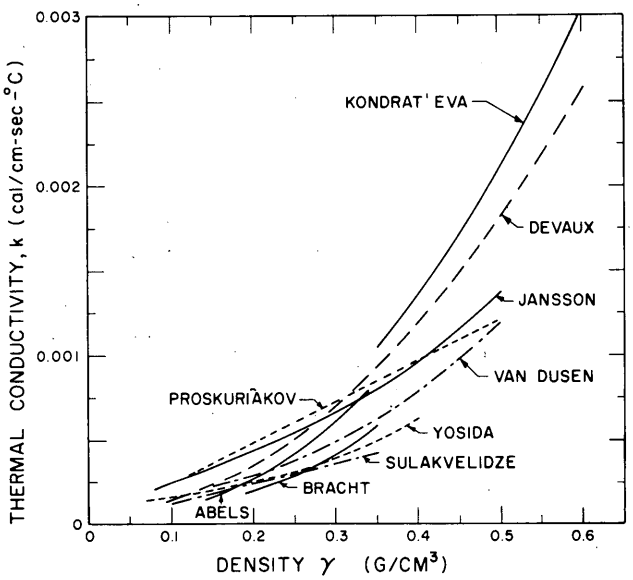

Figure VI-5. Thermal conductivity of dry snow as a function of density.

Thermal conductivity

A number of determinations of thermal conductivity have been made, usually with only density measurement describing the snow type. The investigators have given empirical relationships between conductivity and density to represent data over limited density ranges. These data are summarized in Figure VI-5 and Table VI-I.

It seems likely that some of the determinations listed in Table VI-I include the effects of heat transfer by vapor diffusion. The coefficients are therefore "effective conductivities," which may perhaps vary with the magnitude of the temperature gradient.

Table VI-I. Thermal conductivity of snow.

Investigator	Date	Expression (k = cal/cm-sec-C; γ = g/cm^3)	Density range (g/cm^3)
Abels[9]	1894	$k = 0.0068\gamma^2$	$0.14 < \gamma < 0.34$
Jansson[9]	1901	$k = 0.00005 + 0.0019\gamma + 0.006\gamma^4$	$0.08 < \gamma < 0.5$
Van Dusen[9]	1929	$k = 0.00005 + 0.0010\gamma + 0.0052\gamma^3$	
Devaux[9]	1933	$k = 0.00007 + 0.007\gamma^2$	$0.1 < \gamma < 0.6$
Kondrat'eva[16]	1945	$k = 0.0085\gamma^2$	$0.35 < \gamma$
Yosida[34]	1955	$k = e4.606\,(\gamma^{-2})$	$0.07 < \gamma < 0.4$
Bracht[6]	1949	$k = 0.0049\gamma^2$	$0.19 < \gamma < 0.35$
Sulakvelidze[3]	1958	$k = 0.00122\gamma$	$\gamma < 0.35$
Proskuriakov[3]		$k = 0.000005 + 0.00242\gamma$	

An interesting feature of Figure VI-5 is the apparent dispersion of the results as density increases; in summaries of other density-dependent physical properties, it is often found that agreement improves as density increases, presumably because there is less variation of grain structure in high density snows.

Conductivity may be expected to depend on grain structure; it should increase as intergranular bond growth increases the concentration of continuous ice paths. In this connection, it would be interesting to see the results of conductivity determinations on snow of a given density at various stages in the "age-hardening" process. In natural snows, the conductivity of depth-hoar (schwimschnee) might be expected to be lower than the conductivity of fine-grained wind drift of the same density.

Determinations of conductivity reported for wet snow cannot be accepted at face value, since the ice matrix in wet snow is isothermal. Heat transfer through wet snow must be brought about by convection in the remaining air spaces, by water percolation, or by transmission of radiation. Movement of saturated air and migration of liquid water are very effective in transferring heat, which could account for Sulakvelidze's report[28] of wet snow conductivity being two to three times as great as dry snow conductivity.

Thermal diffusivity

Thermal diffusivity, the coefficient a in the general heat conduction equation, is given by

$$a = \frac{k}{\gamma c} \qquad (7)$$

where k is thermal conductivity, γ is snow density, and c is specific heat. (The product γc is known as the volumetric specific heat.) Although many values of conductivity k are actually derived from determinations of diffusivity a diffusivity has been reported directly as a function of snow density in only a few cases. Values of a are therefore calculated as required from eq 7, with substitutions for k and c from the information given above.

Convection and diffusion in snow

When a temperature gradient exists in a snow mass there is convective transfer of sensible heat. In the case of snow which is colder at the bottom than at the top, however, there is no vertical convection, since the stratification of the interstitial air is stable.

In some circumstances there is forced convection in the snow, with consequent increase of convective heat flow. This effect may be strongly marked in undersnow camps, where pressure gradients are set up by the ventilation systems, and air flows briskly through the pores of the snow.

A temperature gradient also leads to transfer of water molecules by thermal convection and vapor diffusion, so that there is a flux of latent heat.

Since saturation vapor pressure increases with temperature, a temperature gradient in the snow creates a gradient of vapor pressure, and consequently there is a transfer of vapor by diffusion. Many practical problems involve only gradients in a vertical direction, horizontal temperature gradients being negligible; for such cases the equation governing vapor diffusion is written in the one-dimensional form (assuming no source or sink).

$$\frac{\partial^2 p}{\partial z^2} - \frac{1}{D} \frac{\partial p}{\partial t} = 0 \qquad (8)$$

where p = vapor pressure at depth z, and
D = a diffusion coefficient, termed the "macroscopic" diffusion coefficient by Yosida et al.[34] (avoiding the need for detailed consideration of interstitial processes).

The coefficient D was determined experimentally by Yosida et al.[34], who obtained values from 0.7 to 1.0 cm^2/sec. The value of D was apparently independent of snow density over the range 0.08 to 0.51 g/cm^3. This and the fact of its being larger than the diffusion coefficient of water vapor in air can probably be attributed to local intensification of the temperature gradient across air spaces, and to sublimation transfer, which eliminates the need for any given molecule to travel the entire diffusion path.

If D is known, the rate of heat transfer due to one-dimensional vapor diffusion can be calculated from

$$q_v = -\beta D L_s \frac{d\theta}{dz} \qquad (9)$$

where q_v = rate of heat flow in the direction z
β = rate of change of vapor density of ice with temperature
L_s = latent heat of sublimation of ice.

Taking Yosida's values of L_s = 676 cal/g, $\beta = 0.39 \times 10^{-6}$ g/cm^3-C and a mean value of D = 0.85 cm^2/sec, the rate of heat flow due to vapor diffusion is

$$q_v = 2.2 \times 10^{-4} \frac{d\theta}{dz} \text{ cal/cm}^2\text{-sec.} \qquad (10)$$

Vapor transfer with forced convection

The problem of vapor transfer when a definite flow of interstitial air exists has been studied by Yen,[33] who defines an equivalent thermal conductivity due to vapor transfer, k_v, by

$$q_v = -k_v \frac{d\theta}{dz} \qquad \text{(cf. eq 10)}$$

and represents his results by a relation between k_v and air flow rate:

$$k_v = 0.77 \times 10^{-4} + 0.314\,G - 89.4\,G^2 + 86.4\,G^3 \qquad (11)$$

where G is rate of air flow in g/cm^2-sec, and k_v is in cal/cm-sec-C. The snow density range was $0.38 < \gamma < 0.47$ g/cm^3.

The no-flow value of k_v is 0.77×10^{-4} cal/cm-sec-C, which may be compared with Yosida's value of 2.2×10^{-4} in eq 10 above. Yen attributes his lower value to the difference in temperature levels employed in the two experiments.

Comparing his values of k_v with values of an overall effective thermal conductivity for medium density snow with forced convection,[32] k_e, Yen finds that k_v represents 7.5% of the total value of k_e with $G = 0$, and 19% of k_e with $G = 10^{-3}$ g/cm^2-sec.

Specific heat

Since the contribution of interstitial air and water vapor to the specific heat of deposited snow is negligibly small, only the specific heat of the ice matrix need be

Table VI-II. Apparent specific heat of ice.

Temperature, °C	Apparent specific heat, c_a		
	d = -0.006	d = -0.0006	d = -0.00006
- 5	0.5155	0.4983	0.4966
-10	0.4919	0.4876	0.4871
-20	0.4696	0.4685	0.4684
-30	0.4503	0.4498	0.4498
-40	0.4315	0.4312	0.4312

considered. This is influenced by temperature and impurities (effects of varying crystal form and relatively high surface to volume ratio are thought to be negligible). The best determinations are believed to be those of Dickinson and Osborne,[9, 31] who gave the following expression for apparent specific heat c_a in the temperature range -0.5 to -40C:

$$c_a = 0.5057 + 0.001863\theta - \frac{79.75\,d}{\theta^2} \text{ cal/g-C.} \qquad (12)$$

θ is temperature in degrees C (so that the second term necessarily becomes negative), and d, the initial freezing point of the completely fused ice, gives a measure of the concentration of impurities. Some values of c_a according to eq 12, as tabulated by Dorsey,[9] are given in Table VI-II.

It can be seen from Table VI-II that impurities only affect the apparent specific heat significantly at temperatures close to the melting point, where latent heat effects are involved due to melting or freezing of the residual impurity film.

For ice of very high purity ($d = 5 \times 10^{-5}$) the Dickinson and Osborne equation gives the apparent specific heat as

$$c_a = 0.5057 + 0.001863\theta - \frac{0.004}{\theta^2}.$$

The specific heat of snow and ice is usually taken as 0.50 cal/g-C in practical problems. According to Table VI-II, this value seems to be too high where temperatures are below -10C.

Latent heat

The latent heat of snow is that of the constituent ice particles; hence the data for ice can be adopted. For common problems, where phase change occurs at 0C, a value of 79.7 cal/g can be accepted for the latent heat of fusion. When phase change takes place at lower temperatures, e.g., in the freezing of supercooled water droplets, latent heat of fusion is less (Table VI-III). For most practical purposes the latent heat of sublimation can be taken as the sum of the latent heat of fusion at 0C plus the latent heat of vaporization from water at 0C, ignoring the possibility of lower values due to polymeric evaporation as discussed by Dorsey.[9] The value is thus 677 cal/g. Table VI-III gives latent heat at various temperatures.

Table VI-III. Latent heat of ice.

Temperature (°C)	Latent heat (cal/g)	
	Fusion	Sublimation
0	79.7	677.0
-10	74.5	677.5
-20	69.0	677.9
-40	56.3	678.0

Thermal expansion

No values for the coefficients of thermal expansion of snow have been found in the literature. Expansion and contraction with change of temperature is due to expansion and contraction of the constituent ice grains, but the macroscopic effect may perhaps vary with the internal freedom of the grains, i.e. with density and bond characteristics. The effective coefficient of expansion should be close to, though maybe lower than, that for solid ice, which is approximately equal to 5×10^{-5} C^{-1} in the temperature range 0 to -40C. Akkuratov[1] describes a method for determining the linear coefficient of expansion for snow, but gives no results.

In considering the effects of thermal contraction it is worth noting that thermal cracking depends on the rate of temperature change as well as on the magnitude of the change. Theory and observation suggest that tensile cracks occur on snow when temperature drops rapidly; if the temperature change is very slow, thermal stresses can be relaxed by orderly creep.

Absorption and scattering of radiation in a snow mass

Radiation entering a snow mass is subject to absorption and scattering, so that its intensity is progressively reduced with distance. It is usually assumed for simplicity that a snow mass behaves as a homogeneous diffusing medium, so that for a given wavelength, radiation is attenuated according to the Bouger-Lambert law*:

$$I_z = I_0 e^{-\nu z} \qquad (13)$$

where I_z = intensity of radiation transmitted in the z-direction at depth z
I_0 = net radiation flux through the surface of $z = 0$
ν = an attenuation constant (loosely termed extinction coefficient here; extinction coefficient ν is given[11] in terms of absorption coefficient a and scattering coefficient β by: $\nu = a\sqrt{1 + 2\beta/a}$).

A natural layered snow mass is not truly homogeneous, and absorption is affected by density, grain form, and the presence of laminar crusts. Nevertheless, it should be possible to correlate the extinction coefficient with density and grain type over a restricted depth interval (note that density generally increases progressively with depth, while grain type changes irregularly).

Extinction coefficients have been calculated from the data of various early studies, but most of these must be discarded, since the snow is not adequately described. In Figure VI-7 available data on extinction and absorption coefficients as a function of wavelength are summarized. Ambach and Habicht,[2] who found no wavelength dependence for the scattering coefficient in glacier ice and alpine snow, show an increase of absorption coefficient with wavelength in the range 0.4 to 1.0 μ for dry powder snow. Liljequist[21] also found that the extinction coefficient increased with wavelength in the range 0.42 to 0.65 μ for dry polar snow. Data presented by Thomas[30] show a similar trend for fresh snow and for old metamorphosed snow in the range 0.42 to 0.66 μ.

Figure VI-8 summarizes the information on extinction coefficients as a function of snow density. Data by Ambach and Habicht[2] are given for "mixed" (unfiltered) light and for three bands in the red and infrared. Measurements were made in powder snow over a rather small range of densities. Other information is obtained from Thomas' data, which were found by the author to yield linear relationships between extinction coefficient and density for "mixed" light and for wavelengths of 0.42, 0.54, and 0.66 μ. Correlation coefficients were in the range 0.934 - 0.970, data for the single example of fresh, low density snow being excluded from the correlation for older, metamorphosed snow. Four values by Gerdel[13] are also plotted. (Further data and comments in Appendix VI-A.)

Scattered items of information are available for absorption at radio frequencies in snow. For 12-cm microwaves (SHF) Matsukawa and Kobayashi[22] found absorption coefficients from 0.28 to 0.08 (presumably cm^{-1}, although no units are given) for snows in the density range $0.26 < \gamma < 0.74$ g/cm^3; absorption coefficient decreased with increasing

* Giddings and LaChapelle[14] arrive at the same expression by regarding radiation scattering as analogous to Brownian movement, solving the general diffusion equation for the one-dimensional steady-state case.

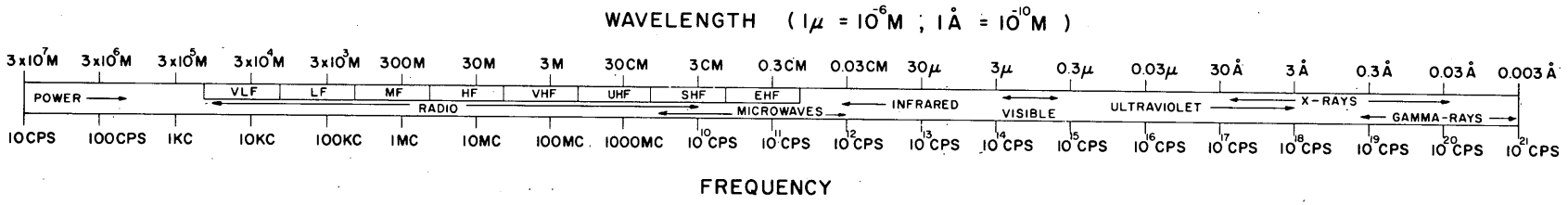

Figure VI-6. The electromagnetic spectrum.

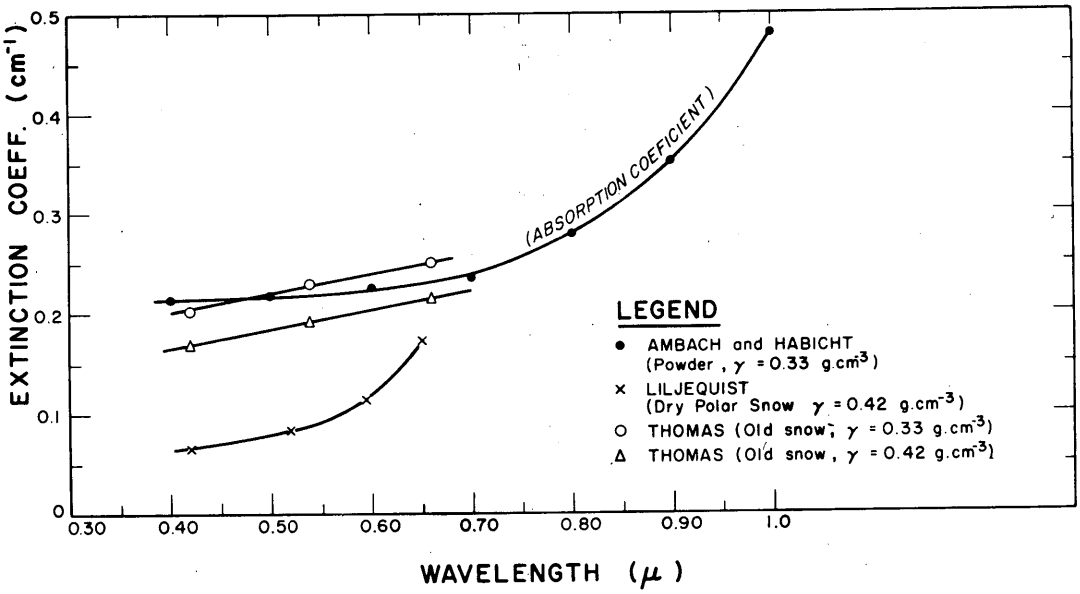

Figure VI-7. Extinction and absorption coefficients as a function of wavelength.

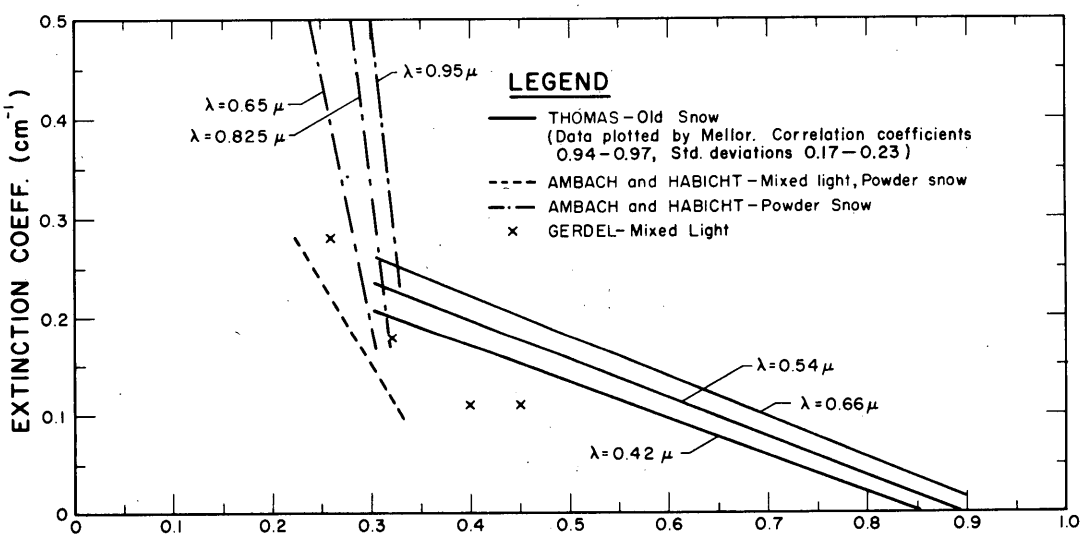

Figure VI-8. Extinction coefficient as a function of snow density for various wavelengths.

density. In the VHF band (see Fig. VI-6 for the electromagnetic spectrum) absorption apparently decreases as frequency decreases; Evans[12] recommends a frequency of about 30 Mc for an ice depth sounder, largely on the basis of a need for low absorption. From dielectric data presented by Kuroiwa[18] the author calculates an absorption coefficient of 1.5×10^{-4} cm^{-1} for a frequency of 5 Mc, and an absorption coefficient of 7.5×10^{-5} cm^{-1}

for a frequency of 1 Mc (MF/HF band). The use of VLF for underwater communication suggests that absorption in snow for VLF may also be low. Considering the electromagnetic spectrum below the visible range, electromagnetic theory suggests that a general decrease of absorption with increasing wavelength might be expected.[23]

Reflection from snow

For any given wavelength, reflection from snow is determined by surface reflection and by the returns of radiation from beneath the surface. The reflecting properties of the surface alone are described by the surface reflectivity, while the overall reflection from the mass is described by the reflectance.

Reflectivity is governed by the condition of the surface. It will vary with the character of the incident light; in the diffuse light of a cloudy day the surface can be regarded as a diffuse reflector, but in direct sunlight only smooth fresh snow can be considered a diffuse reflector.* Factors affecting reflectivity include grain form, solid impurities, and, in direct sunlight, macroscopic irregularities such as sastrugi, dunes, and radiation pits. Directional surface irregularities and specular reflection from old metamorphosed snow and crusted surfaces lead to changes in reflectivity with azimuth and elevation of incident rays.

Subsurface energy returns depend on scattering and absorption within the snow, which in turn depend on density and grain form, and also on the presence of subsurface ice layers and inhomogeneities. In shallow snow, the ground surface beneath influences the return of energy to the surface. Figure VI-9 shows how reflectance for monochromatic sodium light changes with snow depth for one type of snow.

The gross reflectance over a broad spectrum is the albedo of the snow, defined by

$$A = \frac{\int_{\lambda_1}^{\lambda_2} r_\lambda I_\lambda \, d\lambda}{\int_{\lambda_1}^{\lambda_2} I_\lambda \, d\lambda} \qquad (14)$$

where A = albedo
r_λ = spectral reflectance for wavelength λ
I_λ = intensity of incident radiation (flux density in the surface plane) at wavelength λ

λ_1 and λ_2 are the extremes of the spectrum (about 0.4 and 0.7 μ for the visible, or wider limits of the solar spectrum, say 0.3 to 3.0 μ, if the infrared and ultraviolet are included).

It can be seen from eq 14 that the spectral reflectance r_λ has to be considered in order to gain an insight into the albedo. While the white color of snow indicates that spectral reflectance is not a strong function of wavelength in the visible spectrum, there is evidence, from visual observations and from photographs, that both brightness and color vary as snow passes through the transition to ice, and therefore some dependence of spectral reflectance on wavelength and snow type might be anticipated. The theoretical considerations of Benford[5], Dunkle and Bevans[11], and Giddings and LaChapelle[14] also predict that reflectance is a function of wavelength and particle size.

Available published data on reflectance as a function of wavelength are presented in Figure VI-10. Curves A and B, from Krinov[17] and Liljequist[21] respectively, are for snow illuminated by light diffused through cloud cover. Krinov shows reflectance steadily declining as wavelength increases from 0.4 to 0.8 μ (more than 20% decrease). Liljequist found little change between 0.42 and 0.595 μ (about 1% rise and fall through the range) but between 0.595 and 0.65 μ there was a drop of more than 4%.

* That is, assumed to obey Lambert's cosine law: intensity of reflected radiation proportional to the cosine of the angle between the direction of reflection and a normal to the surface.

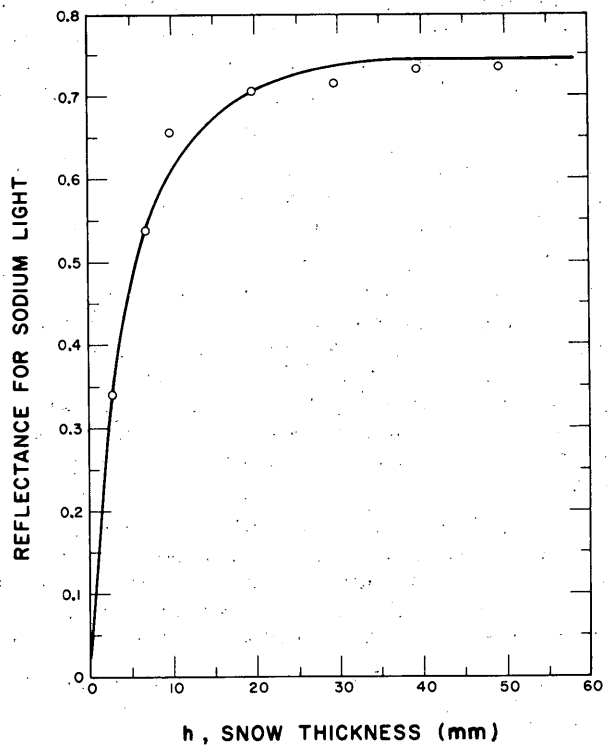

Figure VI-9. Reflectance plotted against snow thickness for sodium light (λ = 0.5983 μ). (After Giddings and LaChapelle, ref. 14)

The remaining curves, C - F, represent measurements in direct sunlight and seem to show a contrary trend, reflectance increasing towards the red end of the spectrum (measurements do not appear to be integrated over the daily range of solar elevation angle). The results of Krinov (C) and Sauberer (D) are closely similar through the visible spectrum, reflectance increasing some 5% as wavelength increases from 0.4 to 0.7 μ. Above 0.7 μ, Sauberer's data show reflectance decreasing again, while Krinov shows a constant value up to above 0.8 μ. Thomas's data appear to indicate an appreciable increase of reflectance as wavelength increases from 0.42 to 0.66 μ, fresh snow giving an increase of about 7% and older metamorphosed snow an increase of about 18%.

Other data not plotted in Figure VI-10 should be mentioned. Polli[24] found considerably higher reflection for total visible light than for violet rays. Hulburt[15] found that reflectance in the visible spectrum was higher than in the ultraviolet and infrared. Dunkle and Gier[10], from theoretical studies, calculate that reflectance decreases as wavelength increases from 0.3 to 1.3 μ. Kasten[36] finds that a receiver filtered to simulate the visual acuity of the human eye gives an albedo close to unity in diffuse light, implying that reflectance is very high around 0.55 μ.

The data are apparently in poor agreement and the general picture is confused. Appendix VI-A gives additional data, as yet unpublished, together with comments.

In the lower frequency ranges of the electromagnetic spectrum it seems that there may be a general decrease of reflectance with increase of wavelength. In the microwave band, Zinchenko and Usikov[38] found the reflection coefficient decreasing with

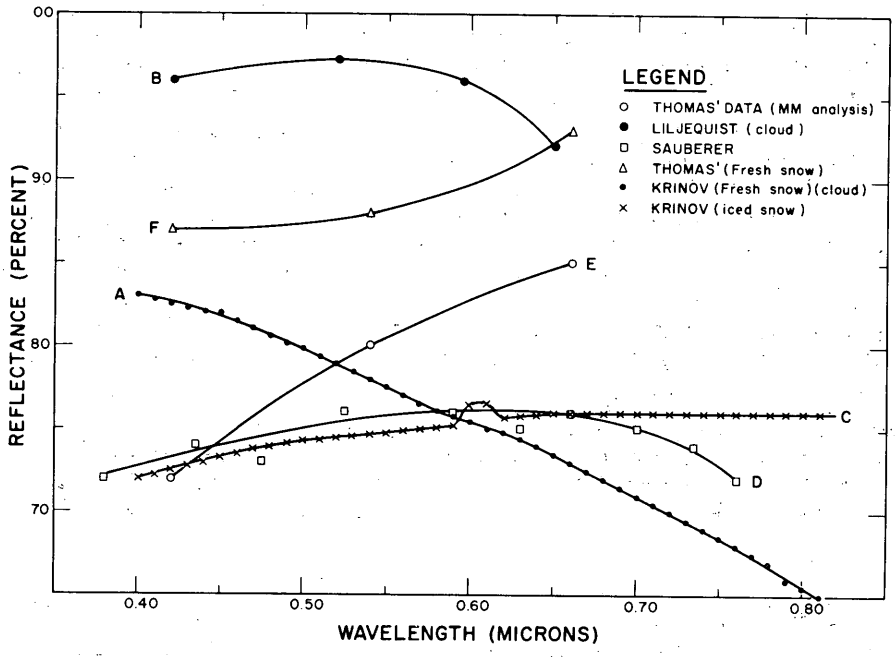

(a)

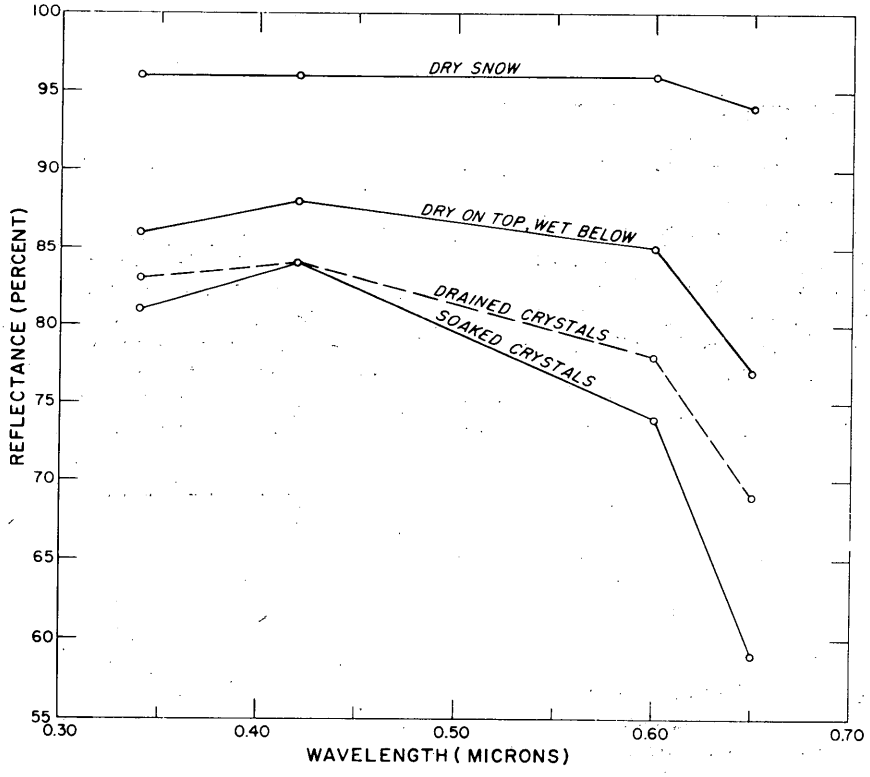

(b)

(After Holmgren, ref. 37)

Figure VI-10. Reflectance as a function of wavelength.

increasing wavelength, particularly between 0.44 cm and 1.36 cm. The fact that aircraft radio altimeters utilizing microwaves give better reflections from snow than those operating on UHF is supporting evidence. For frequencies of the order of 10 Mc Piggott and Barclay[25] regard dry snow as transparent. Asami and Kurobe[4] found that reflection varied with water content of the snow in the UHF and microwave bands.

Snow type is frequently described only in terms of density, but the effect of density on reflectance does not appear to have been studied. Using the only data available, those of Thomas, the author found no significant correlation between reflectance and density for wavelength of 0.42, 0.54, 0.66 μ and for unfiltered light. Theory calls for increasing reflectance as absorption decreases; it was shown above that extinction coefficient decreases with increasing density, so that reflectance might be expected to increase with density. However, the data presented are somewhat suspect (see Appendix VI-A); and in natural snows there is generally an increase of grain size with density, so that the effect of grain size on reflectance must also be considered.

Theory predicts that reflectance will decrease as grain size increases. In the transition from fine, wind-blown snow to dense old snow there is commonly an increase of grain size through an order of magnitude or more, and it seems that this may outweigh the effects of increased density in determining reflectance. As far as is known, there is no experimental evidence concerning the effects of grain size variation on reflectance.

Long wave emission from snow

The emission of radiation from a surface depends on the temperature and emissivity of the surface. Emissivity, ϵ, is the ratio of the intensity of radiation emitted by the surface to that emitted by an ideal black body at the same temperature:

$$\epsilon = \frac{I_e}{\sigma T^4} \tag{15}$$

where I_e = intensity of radiation emitted
T = absolute temperature (°K)
σ = the Stefan-Boltzmann constant ($=5.672 \times 10^{-5}$ erg/sec-cm^2-deg^4).

Early observations on melting snow indicated that, for long wave radiation, emissivity is close to unity ($\epsilon > 0.995$), so that for practical purposes snow could be considered as a black body. Experiments on ice at and below the melting point supported this conclusion. Dunkle and Gier[10], however, find lower values from measurements on laboratory specimens. Giving their data in terms of emittance rather than emissivity, since subsurface effects are also involved (cf. reflectance), they show values ranging from 0.82 to 0.95. The low values are apparently associated with fine grain sizes. They also find emittance to be temperature-dependent at temperatures close to the melting point, emittance increasing as temperature increases (Fig VI-11).

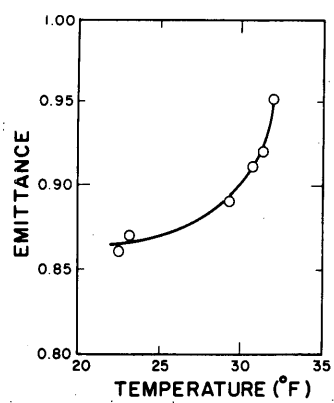

Figure VI-11. Emittance as a function of temperature. (After Dunkle and Gier, ref. 10)

CHAPTER VI REFERENCES

1. Akkuratov, V. N. (1956) "Metodika opredeleniia koeffitsienta lineinogo rasshireniia snega" ("A method of determining the linear coefficient of expansion of snow") in Sneg i talye vody. Moscow: Institut Geografii Akad. Nauk SSSR (text in Russian).

2. Ambach, W. and Habicht, H. L. (1962) Extinktionseigenschaften des Gletschereises und Schnees (Extinction coefficient of glacier ice and snow), Archiv für Meteorologie, Geophysik und Bioklimatologie, Bank 11, 4 Heft (text in German).

3. Anisimov, M. I. (1961) Priblizhennaia otsenka formul teploprovodnosti snega (An approximate evaluation of formulas on thermal conductivity of snow), Meteorologiia i Gidrologiia, no. 9 (text in Russian).

4. Asami, Y. and Kurobe, T. (1949) Kyokusho tanppa antena ni oyobosu yuki kōri no eikyō (The effects of snow and ice on the antenna at ultra high frequencies), Hokkaido University, Mem. Faculty of Engineering, vol. 8, no. 2, p. 123-132 (text in Japanese).

5. Benford, F. (1946) Radiation in a diffusing medium, Journal of the Optical Society of America, vol. 36, p. 524-554.

6. Bracht, J. (1949) Über die Wärmeleitfähigkeit des Erdbodens und des Schnees und den Wärmeumsatz im Erdboden (On the thermal conductivity of soil and snow, and the heat utilization in soil), Veröffentl. Geophysikalischen Inst. Univ. Leipzig, ser. 2, vol. 14, no. 3, p. 147-225 (text in German).

7. Carslaw, H. S. and Jaeger, J. C. (1959) Conduction of heat in solids. London: Oxford University Press.

8. Chizhov, O. P. (1961) "Gliatsiologicheskie issledovaniia na Novoi Zemle, 1957-59" ("Glaciological investigations in Novaya Zemlya in 1957-59") in Issledovaniia lednikov i lednikovykh raionov (Study of glaciers and glacier regions) (G. A. Avsyuk, Editor). Moscow: Akad. Nauk SSSR (text in Russian).

9. Dorsey, N. E. (1940) Properties of ordinary water substance. New York: Reinhold.

10. Dunkle, R. V. and Gier, J. T. (1955) Spectral characteristics of wet and dry snow between 0 and -60C, U. S. Army Snow, Ice and Permafrost Research Establishment (USA SIPRE) Technical Report 16.

11. _____ and Bevans, J. T. (1956) An approximate analysis of the solar reflectance and transmittance of a snow cover, Journal of Meteorology, vol. 13.

12. Evans, S. (1961) Radio techniques for the measurement of ice thickness, Polar Record, vol. 11, no. 73.

13. Gerdel, R. W. (1948) Penetration of radiation into the snow pack, Transactions, American Geophysical Union, vol. 29, no. 3.

14. Giddings, J. C. and LaChapelle, E. (1961) Diffusion theory applied to radiant energy distribution and albedo of snow, Journal of Geophysical Research, vol. 66, no. 1.

15. Hulburt, E. O. (1928) The ultraviolet, visible and infra-red reflectivities of snow, sand and other substances, Journal of the Optical Society of America, vol. 17, p. 23-25.

16. Kondrat'eva, A. S. (1945) Teploprovodnost' snegovogo pokrova i fizicheskie protsessy, proiskhodiaschie v nem pod vlianiem temperaturnogo gradienta (Thermal conductivity of the snow cover and physical processes caused by the temperature gradient), Akad, Nauk SSSR. USA SIPRE Translation 22, 1954.

CHAPTER VI REFERENCES (Cont'd)

17. Krinov, E. L. (1947) Spektral'naia otrazhatel'naia sposobnost' prirodnykh obrazovanii (Spectral reflectance properties of natural formations), Laboratoriia Aerometodov, Akad. Nauk SSSR. Technical Translation TT-439, National Research Council of Canada, Ottawa, 1953.

18. Kuroiwa, D. (1962) "Electrical properties of snow," in "The physics and mechanics of snow as a material," by H. Bader. Cold Regions Science and Engineering (F. J. Sanger, Editor), U. S. Army Cold Regions Research and Engineering Laboratory (USA CRREL) monographs, Part II, Sect. B.

19. Lachenbruch, A. H. (1959) Periodic heat flow in a stratified medium with application to permafrost problems, U. S. Geological Survey Bulletin 1083-A.

20. _____ Private communication.

21. Liljequist, G. H. (1956) Energy exchange of an Antarctic snowfield, Scientific results of the Norwegian-British-Swedish Antarctic Expedition, vol. II, Part I, Norsk Polarinstitutt, Oslo.

22. Matsukawa, K. and Kobayashi, S. (1955) "Sekisetsu no kyokuchō tampa ni oyobasu eikyū ni tsuite (sono san)" ("The effect of snow upon the radiation apparatus in the microwave regions"), in Studies in fallen snow, no. 5, Institute of Low Temperature Science (Japan) (text in Japanese).

23. Panofsky, W. K. H. and Phillips, M. (1956) Classical electricity and magnetism, Reading, Mass: Addison-Wesley, p. 182.

24. Polli, S. (1957) Misure fotometriche e calorimetriche sui nevai e ghiacciai alpini (Photometric and calorimetric measurements on alpine snow and glaciers), Inst. Sperimentale Talassografico Trieste, Pub. no. 342 (text in Italian).

25. Piggott, W. R. and Barclay, L. W. (1961) The reflection of radio waves from an ice shelf, Journal of Atmospheric and Terrestrial Physics, vol. 20, p. 289-299.

26. Sauberer, F. (1938) Versuche über spektrale Messungen der Strahlungseigenschaften von Schnee und Eis mit Photoelementen (Experiments with spectral measurements of the radiation properties of snow and ice with photoelements), Met. Zeitschrift, vol. 55.

27. Schytt, V. (1958) "Snow and ice temperatures in Dronning Maud Land" in Glaciology II, Scientific Results of the Norwegian-British-Swedish Antarctic Expedition, vol. IV, Norsk Polarinstitutt, Oslo.

28. Sulakvelidze, G. K. (1954) Nekotorye voprosy teploprovodnosti vlazhnogo snega (Some problems of heat conductivity in wet snow), Soobscheniia Akad. Nauk Gruzinskoi SSSR, vol. 15, p. 517-522 (text in Russian).

29. Tien, C. (1960) Temperature distribution of snow with gamma ray radiation, USA CRREL Research Report 67.

30. Thomas, C. W. (1963) On the transfer of visible radiation through sea ice and snow, Journal of Glaciology, vol. 4, no. 34.

31. University of Minnesota (1951) Review of the properties of snow and ice, USA SIPRE Report 4.

32. Yen, Y. C. (1963) Effective thermal conductivity of snow with air flowing through it, USA CRREL Research Report 103.

33. _____ (1964) Heat transfer due to vapor transfer in snow with air flowing through it, USA CRREL Research Report 106.

34. Yosida, Z. et al. (1955) Physical studies on deposited snow, Hokkaido University, Institute of Low Temperature Science.

CHAPTER VI REFERENCES (Cont'd)

35. Yosida, Z. and Iwai, H. (1946) Sekisetsu no netsu dendō-ritsu no sokutei (Measurement of the thermal conductivity of snow cover), Seppyō, vol. 8. USA SIPRE Translation 30, 1955.

36. Kasten, F. (1963) Optische bzw. Sichtweiteuntersuchungen in der Arktis (Grönlandisches Inlandeis), Polar Meeting of the German Society for Polar Research, Karlsruhe.

37. Hölmgren, B. (1963) Changes of albedo on the Devon Island Ice Cap, Polar Meeting of the German Society for Polar Research, Karlsruhe.

38. Zinchenko, N. S. and Usikov, A.IA. (1960) Otrazhenie radiovolln millimetrovogo diapazona ot sloia snega (Reflection of radio waves in the millimeter range from a snow layer), Izvest. Vysshikh Uchebnykh Zavedenii, Radiofizika, vol. 3, no. 4, p. 614-618.

APPENDIX VI-A.
AUTHOR'S MEASUREMENTS OF SPECTRAL TRANSMITTANCE AND REFLECTANCE

Compilation of the foregoing information on spectral absorption and reflection of visible radiation in snow prompted the writer to conduct a number of simple experiments using available apparatus. The results have not yet been fully analyzed or exposed to open discussion, but preliminary data plots can be given.

Attenuation was studied in the cold room by illuminating one end of a homogeneous snow cylinder by a diffuse source and using a collimated brightness meter with narrow band-pass interference filters to measure transmission through the snow cylinder to a "black body" cavity. Snow samples were made artificially by sieving and compacting under controlled conditions, followed by sintering at -10C. Tests were made at -10C. Figure VI-A1 summarizes the wavelength dependence found for various snow types: in the artificial snow composed of fine and angular grains attenuation (neglecting surface effect) was consistently highest at the blue end of the spectrum. Coarse-grained natural "spring snow" reduced to a temperature of -10C showed much lower attenuation and less spectral selection than the artificial samples, which were intended to simulate wind-blown polar snow. Attenuation was also measured for coarse-grained wet snow by the "slab" method; in this condition the snow transmitted well, and attenuation was slightly higher for the red end of the spectrum than for shorter wavelengths.

The experiments showed that, for densities in the range 0.35 to 0.55 g/cm^3, attenuation in cold, fine-grained snow increases with increasing density, in contrast to the trend shown in Figure VI-8. It can be reasoned that attenuation in snow (which is an air/ice mixture) must increase from virtually zero at zero density to some maximum value,

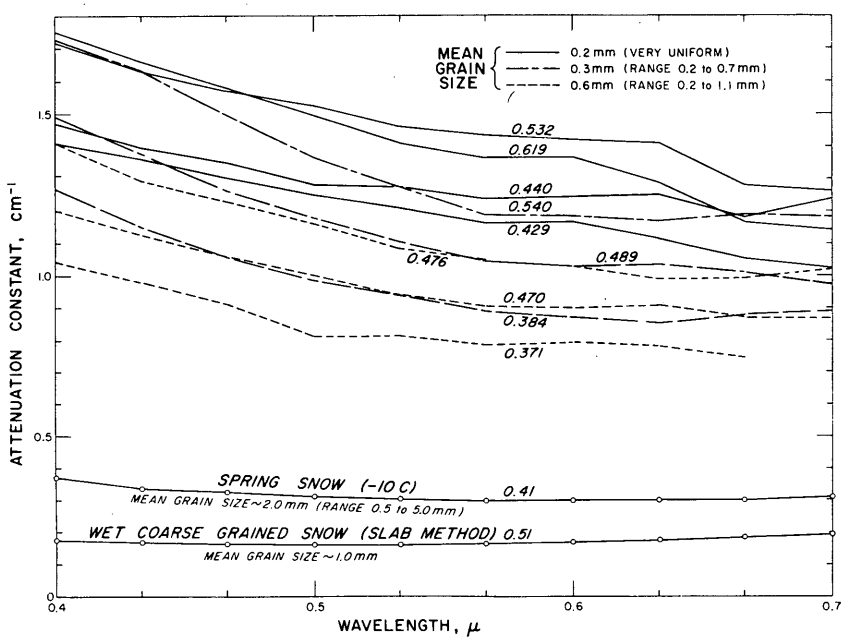

Figure VI-A1. Attenuation constant (extinction coefficient) as a function of wavelength for various snow types. All the unlabeled lines refer to snow samples prepared artificially in the laboratory and tested at -10C. The numbers shown against each line give sample density in g/cm^3, and grain size is indicated in the legend.

and thereafter decline to a low value as the snow changes into ice, which is relatively transparent. Although inadequate, the experimental results for the finest-grained sample (0.2 mm) suggest that the density for maximum attenuation is between 0.5 and 0.6 g/cm^3, and that the critical density varies with wavelength.

The results also show that attenuation decreases with increasing grain size.

Spectral reflectance was measured in the field by using the collimated brightness meter and interference filters to compare normal reflection from the snow with normal reflection from a magnesium oxide block of known spectral characteristics. The results are summarized in Figure VI-A2. Measurements made in light diffused by an overcast showed only slight spectral selection, with highest reflectance at about 0.45 to 0.50 μ wavelength. Measurements in direct sunlight on surfaces exhibiting some specular properties showed a marked decline in reflectance as wavelength increased from 0.4 to 0.7 μ.

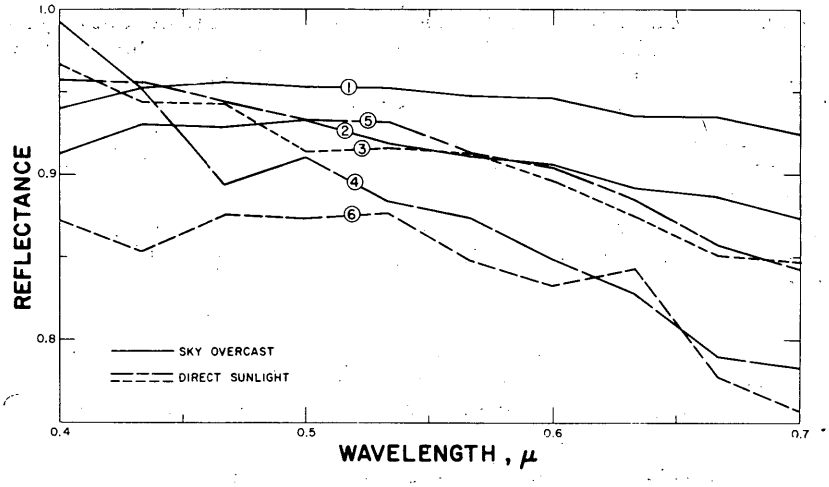

Figure VI-A2. Reflectance of natural snow as a function of wavelength. The snow types tested were:

1. Fresh snow, density 0.28 g/cm^3, temp 0C (dry)
2. 1 - 2 cm fresh snow (0.1 g/cm^3) lying on older snow (0.4 g/cm^3), temp 0C
3. Metamorphosed snow, density 0.43 g/cm^3, temp 0C
4. Slightly metamorphosed new snow, density 0.2 g/cm^3, temp 0C
5. Wet snow, 2 days old, density 0.4 g/cm^3, melting during test
6. Same as 5. after 5 hours more melting.

APPENDIX VI-B.
ABSORPTION AND SCATTERING OF RADIATION IN SUSPENDED SNOW

There is little information available on the attenuation of radiation by snow suspended in air (falling snow or blowing snow). While it is widely recognized that attenuation will vary with size and shape of particles, concentration, temperature, and radiation wavelength, systematic measurements are lacking.

Landon Smith and Woodberry* developed a photoelectric gage for metering wind-blown snow, and in the course of their work obtained experimentally a relation between the output of the photoconductor device and the concentration of blowing snow. Peak sensitivity of the combination of photoconductor and electric light bulb used was not stated, though presumably it lay somewhere in the visible or near infra-red (sensitivity of the photoconductor alone apparently centered around 0.6 μ). The blown snow had a mean particle size of about 100 μ. If there is a linear relation between the gage output and decrease of luminous flux, as seems to be the case, then the work shows that the flux reduction at a given distance from a source is inversely proportional to the drift density raised to the power 0.87 for the range investigated.

$$\frac{I_0 - I_2}{I_0 - I_1} = \left(\frac{d_2}{d_1}\right)^{0.87}$$

where I_0 is the flux for liquid density, I_2 is flux at distance $\underline{x}$ from the source with drift of density d_2 (mass of snow per unit volume of air), and I_1 is the flux at distance $\underline{x}$ with drift of density d_1.

Approximate working values for attenuation of microwaves by falling snow have been calculated by Marshall, East and Gunn† These values of attenuation as a function of precipitation rate, with wavelength and temperature as parameters, are given in Table VI-I.

Table VI-BI. One-way attenuation of microwaves by falling snow — working values†

($\underline{R}$ is rate of snowfall in mm/hr of equivalent water. Upper limit of applicability is $\underline{R}$ = 10 mm/hr.)

Temp (C)	Wavelength			
	3.2 cm	1.8 cm	1.24 cm	0.9 cm
0	$3.3\times10^{-5}R^{1.6} + 68.6\times10^{-5}R$	$3.32\times10^{-4}R^{1.6} + 12.2\times10^{-4}R$	$1.48\times10^{-3}R^{1.6} + 1.78\times10^{-3}R$	$5.33\times10^{-3}R^{1.6} + 2.44\times10^{-3}R$
-10	$3.3\times10^{-5}R^{1.6} + 22.9\times10^{-5}R$	$3.32\times10^{-4}R^{1.6} + 4.06\times10^{-4}R$	$1.48\times10^{-3}R^{1.6} + 0.59\times10^{-3}R$	$5.33\times10^{-3}R^{1.6} + 0.81\times10^{-3}R$
-20	$3.3\times10^{-5}R^{1.6} + 15.7\times10^{-5}R$	$3.32\times10^{-4}R^{1.6} + 2.80\times10^{-4}R$	$1.48\times10^{-3}R^{1.6} + 0.41\times10^{-3}R$	$5.3\times10^{-3}R^{1.6} + 0.56\times10^{-3}R$

* Landon Smith, I. H. and Woodberry, B. (in press) The photoelectric metering of wind blown snow, ANARE Report, Antarctic Division, Dept. of External Affairs, Melbourne, Australia.

† Marshall, J. S., East, T. W. R. and Gunn, K. L. S. (1952) "The microwave properties of precipitation particles" in Weather effects on radar, Air Force Cambridge Research Center, Air Force Surveys in Geophysics, no. 23.

CHAPTER VII. ELECTRICAL PROPERTIES

Deposited snow

Dielectric properties. The dielectric constant ε is the ratio of the electric flux density or dielectric displacement $\underline{D}$ to the field strength $\underline{E}$.

The absolute d-c dielectric constant ε_s is completely determined by the ratio of the capacitance of a snow slab C_n to the capacitance of an identical volume of free space, which is close to that of air, C_a:

$$\varepsilon_s = \frac{D}{E} = \frac{C_n}{C_a} . \tag{1}$$

In alternating fields the vectors $\underline{D}$ and $\underline{E}$ are no longer in phase, and heat dissipation occurs. To describe the dielectric behavior a complex dielectric constant ε^* is defined:†

$$\varepsilon^* = \varepsilon' - i\varepsilon'' \tag{2}$$

where ε', the real part, is the dielectric constant
ε'', the imaginary part, is the loss factor and
$i = \sqrt{-1}$.

A "snow condenser" subject to an applied voltage of angular frequency ω may be regarded as electrically equivalent to a capacitance C_ω and a resistance R_ω connected in parallel. In this analog

$$\varepsilon' = \frac{C_\omega}{C_a}$$

$$\varepsilon'' = \frac{1}{\omega R_\omega C_a} . \tag{3}$$

The loss angle δ, i.e. the angle between the total current vector and the charging current vector, is given by

$$\tan \delta = \frac{\text{loss current}}{\text{charging current}} = \frac{\varepsilon''}{\varepsilon'} . \tag{4}$$

The fact that $\underline{D}$ and $\underline{E}$ are generally not in phase in a-c fields results in part from the inability of polar molecules to rotate instantly into the field. Thus this fundamental process of dipole orientation may be investigated by studying the phase lag, or the relaxation time τ, defined as the time taken for polarization to decay exponentially to $\frac{1}{e}$ times its original value.

The relaxation time is temperature-dependent and, in simple cases, obeys the rate equation

$$\tau = A e^{-\frac{Q}{RT}} \tag{5}$$

in which $\underline{Q}$ is the activation energy (per mole), $\underline{R}$ is the gas constant, and $\underline{T}$ is absolute temperature. It is a matter of some interest that the activation energy of dielectric relaxation in ice is the same as that for mechanical damping, within the limits of experimental error.

† The snow is assumed here to be isotropic. If it were not isotropic, then a tensor approach would be called for.

Dielectric constant ε' and loss factor ε'' can be expressed in terms of the maximum dielectric displacement D_0 and the maximum field strength E_0.

Since $$D = D_0 \left[\cos(\omega t - \delta) + i \sin(\omega t - \delta)\right] \quad (6)$$

and $$E = E_0 \left[\cos \omega t + i \sin \omega t\right] \quad (7)$$

$$\varepsilon^* = \frac{D}{E} = \frac{D_0}{E_0} (\cos \delta - i \sin \delta) \quad (8)$$

Hence $$\varepsilon' = \frac{D_0}{E_0} \cos \delta \qquad \varepsilon'' = \frac{D_0}{E_0} \sin \delta \quad (9)$$

As $\omega \to 0$, $\varepsilon'' \to 0$ and $\varepsilon' \to \varepsilon_s$, the static (or d-c) dielectric constant.

As $\omega \to \infty$, $\varepsilon' \to \varepsilon_\infty$, the high-frequency (or "optical") dielectric constant.

If the substance has a single relaxation time τ, it can be shown that

$$D = E_0 \left[\varepsilon_s - (\varepsilon_s - \varepsilon_\infty) e^{-\frac{t}{\tau}}\right] \quad (10)$$

and

$$\varepsilon^* = \varepsilon_\infty + \frac{\varepsilon_s - \varepsilon_\infty}{1 + i\omega t} \quad (11)$$

$$\varepsilon' = \varepsilon_\infty + \frac{\varepsilon_s - \varepsilon_\infty}{1 + \omega^2 \tau^2} \quad (12)$$

$$\varepsilon'' = \frac{(\varepsilon_s - \varepsilon_\infty)\, \omega t}{1 + \omega^2 \tau^2} . \quad (13)$$

ε'' is a maximum when $\omega\tau = 1$, and the frequency corresponding to ε''_{max} therefore gives a value for relaxation time τ. This maximum for ε'' can sometimes be identified on a plot of ε'' against ω, but is more clearly seen when ε'' is plotted against ε' for a range of frequencies on an Argand diagram.

Cole-Cole plot or Argand diagram: Eliminating τ from expressions 12 and 13 it follows that a plot of ε' against ε'' for different frequencies will be a circle of diameter $\varepsilon_0 - \varepsilon_\infty$, usually displayed as a semicircle. Such a plot proves to be truly semicircular for snow of very high purity, but for common snows, which contain impurities, the plot breaks away from the semicircular trace by displaying high values of ε'' at low frequencies (Fig. VII-1, from Kuroiwa[19]).

Dielectric constant and loss factor as a function of frequency: Data on the dielectric constant (i.e. the real part of the complex constant) as a function of frequency are summarized in Figures VII-2 and -3. In Figure VII-2 it is seen that ε' covers a wide range of values at low frequencies, but tends to a limiting minimum value (ε_∞) for frequencies above 10^5 cps. At low frequencies the highest values of ε' seem to be measured in dense and wet snows. An artificially prepared sample of high-purity snow gave $\varepsilon' = 6$ at $f = 10^3$ cps; slightly lower values were found for natural snows containing some impurity, but of lower density. For most snows it appears that the dielectric constant is very close to the ε_∞ value for Debye dispersion at frequencies of 10^6 cps and above, although Figure VII-3 shows a perceptible decrease between 10^6 and 10^{10} cps for high density snows ($\gamma > 0.6$). Figure VII-3 clearly shows the effect of density on the optical dielectric constant, ε_∞.

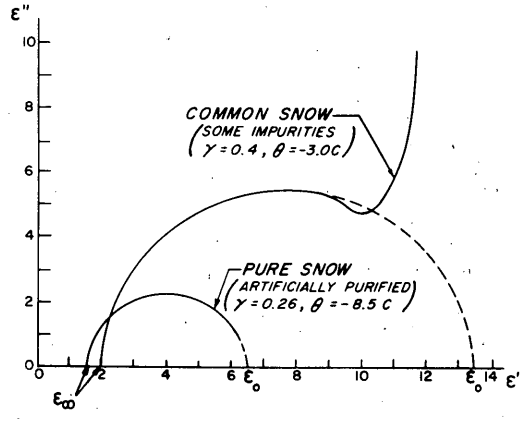

Figure VII-1. Plots of ε'' against ε' (loci of points plotted for various frequencies). Snow of high purity gives a semicirular trace in accordance with theory, but common snows containing impurities do not conform at low frequencies (frequency increases in a clockwise direction around the plots). (From data by Kuroiwa, ref. 19)

Figure VII-4 gives data on ε'', the loss factor, or imaginary part of the complex constant. There is a broad correspondence with the ε' plot, dense and wet snows giving high loss factors at low frequency, and all snows tending to limiting minimum values at a frequency of 10^6 cps. Most of the curves for dry snow show a maximum in the frequency range 10^4 - 10^5 cps; the frequencies at which these maxima occur permit the relaxation time, and hence the activation energy for relaxation, to be calculated.

Dielectric constant as a function of snow density: Figure VII-5 gives static and optical dielectric constants according to Kuroiwa,[19, 20] and high frequency dielectric constants found by Cumming[12] and Yoshino.[52] Cumming's data are for a very high frequency ($\sim 10^{10}$ cps), and can therefore be regarded as limiting high-frequency dielectric constants for Debye dispersion; there is fair agreement with Kuroiwa's determination, considering the different temperature range (0 to -7C for Kuroiwa, -18C for Cumming) and the probable difference in snow type. Yoshino's curve for a frequency 3×10^8 cps can also be regarded as giving the high-frequency dielectric constant ε_∞, although his data for 1.5×10^6 cps illustrate that the constant is still greater than the ε_∞ value for snow densities in excess of about 0.55 g/cm^3. Yoshino's ε_∞ is much smaller than corresponding values by Cumming or Kuroiwa through the range of densities for snow, but his limiting value for ice agrees well with that of Cumming. Since Yoshino worked on Antarctic snow at low temperatures (-18 to -36C) it seems likely that his lower values reflect a grain structure effect; in cold polar snow fine grain size and poor bond development is common. An interesting feature of the Yoshino curve is the abrupt change of slope which occurs at about 0.55 g/cm^3 density; many mechanical properties of cold snow show a similar sudden change as density increases above 0.55 g/cm^3, an effect attributed to the changed densification mechanism when the density for closest grain packing is exceeded.

Snow metamorphosis effects: Density alone does not fully describe the structure of snow, and there are several hints in the foregoing data of dielectric changes resulting from changes of size, shape and gradation of grains, and from changes of intergranular bonding. Kuroiwa[20] demonstrated the increase of dielectric constant and loss factor which occurs as bond growth proceeds by repeating measurements on the same sample over a 6-day period. The results are shown in Figure VII-6, which also illustrates how the snow structure changed. The effects of structure in a dielectric mixture are discussed later.

Effect of free water: For any given snow density, the dielectric constant increases as the free water content increases. Both Ambach[2] and Kuroiwa[19] show a linear relation between free water content and the increase of dielectric constant above

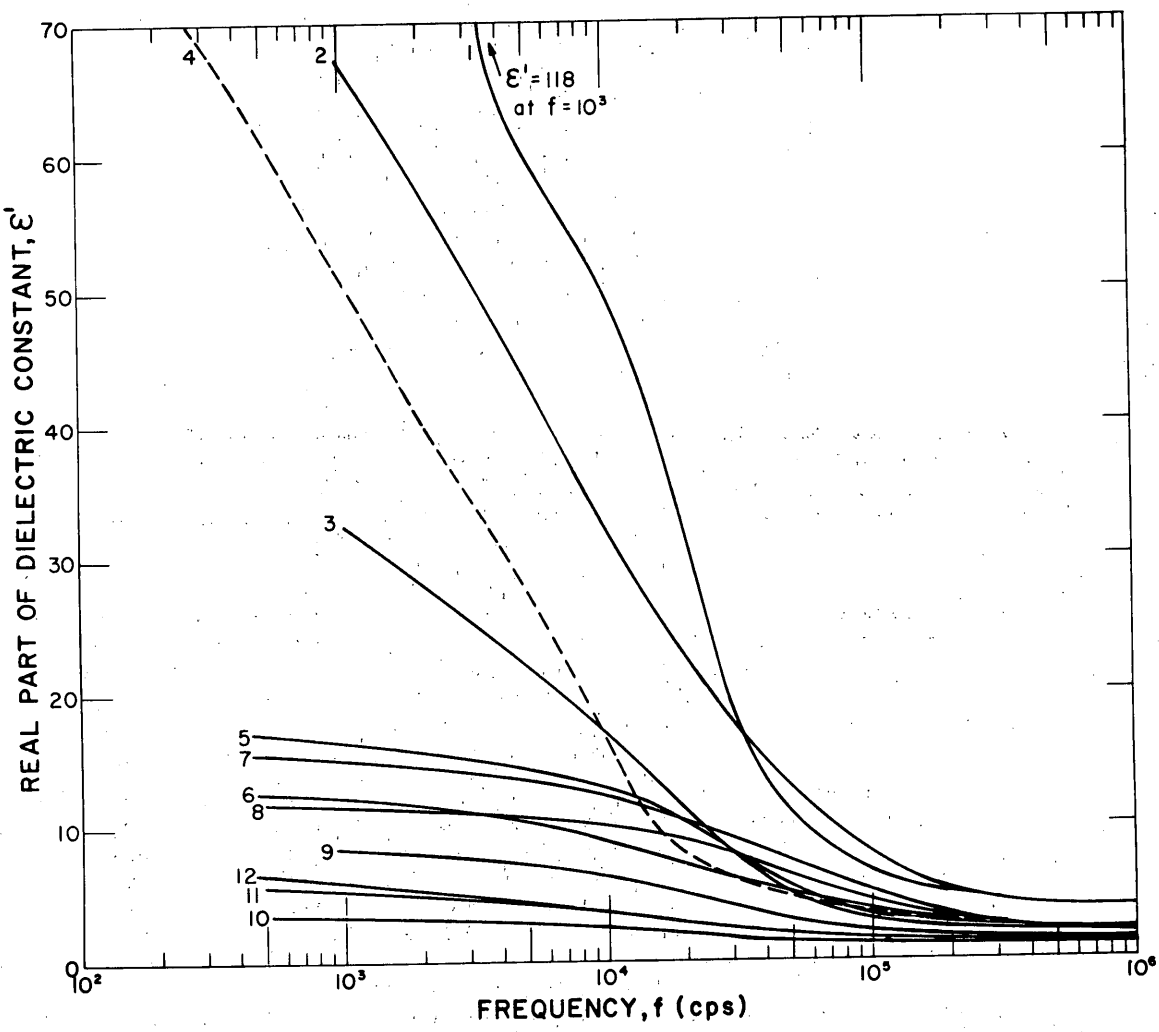

Figure VII-2. Dielectric constant ε' as a function of frequency for various snow types. (From data by Yosida et al., ref. 53, and Watt and Maxwell, ref. 48)

1. Wet snow, 0C, γ = "compact"
2. Wet snow, 0C, γ = 0.38 g/cm³, chlorine 25 mg/kg
3. -7C, γ = 0.38 g/cm³, chlorine 25 mg/kg
4. Wet snow, 0C, γ = 0.6 g/cm³
5. Granular snow, -4C, γ = 0.41, chlorine 12.5 mg/kg (2-4 mm grains) (in condenser 24 hr)
6. Granular (measured immediately)
7. -3C, γ = 0.40, chlorine 35 mg/kg (in condenser 24 hr)
8. -3C, γ = 0.40, chlorine 35 mg/kg (measured immediately)
9. New snow with dendritic crystals, -1C, γ = 0.25, chlorine 15
10. New snow with dendritic crystals, -1C, γ = 0.095, chlorine 15
11. New snow with dendritic crystals, -1C, γ = 0.13, chlorine 15
12. Artificial pure snow, -8.5C, γ = 0.29

Note: 1 and 4 — Watt and Maxwell
2, 3, and 5-12 — Yosida, et al.

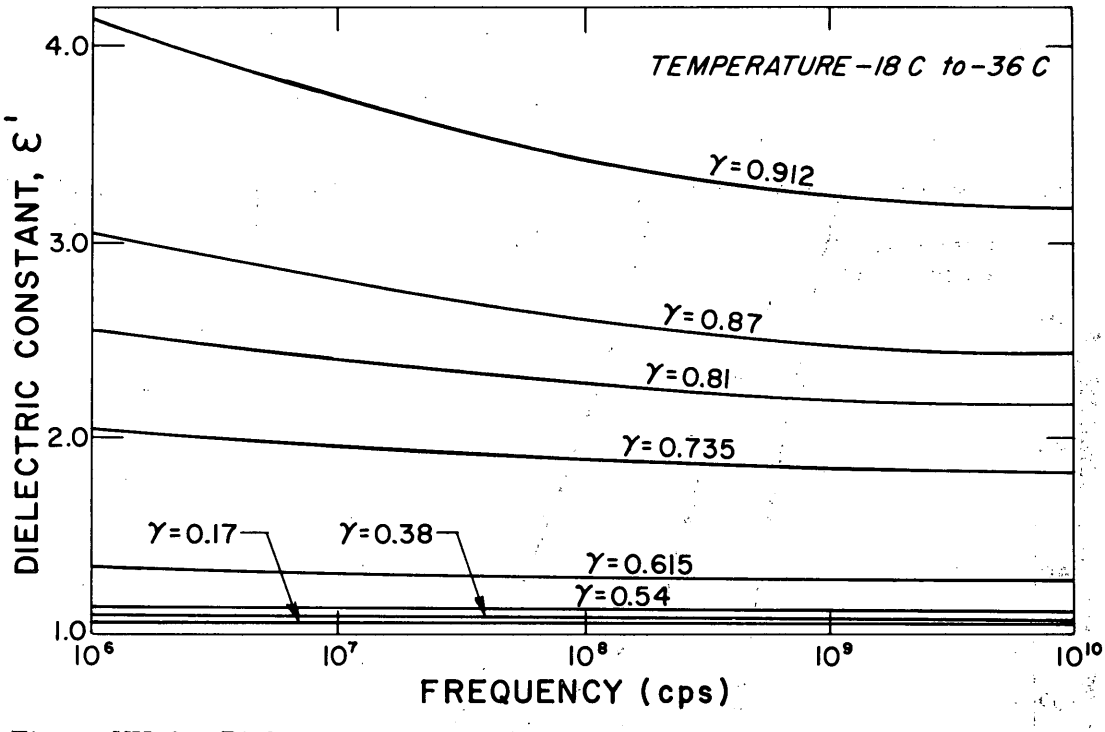

Figure VII-3. Dielectric constant ε' as a function of frequency in the range 10^6 - 10^{10} cps, with snow density as parameter. (After Yoshino, ref. 52)

the value for dry snow (Fig. VII-7). Ambach found a large increase of ε' with increasing water content using relatively low frequencies (10^3- 10^5 cps), while Kuroiwa found considerably smaller changes for the high-frequency dielectric constant. (The absolute high-frequency constants are much smaller than the low-frequency values. ε' for water remains fairly constant for frequencies below 10^9 cps, but ε' for ice at 0C increases appreciably as frequency drops to about 10^4 cps.)

Loss tangent as a function of frequency: Some available data for changes of loss tangent with frequency are presented in Figure VII-8. Kuroiwa[20] shows an almost linear decrease of loss tangent with logarithm of frequency between 10^5 and 10^7 cps, although some curvature becomes evident when his data are linked to a value for 10^{10} cps obtained by Cumming.[12] Yoshino[52] gives data for the range 10^6 to 10^{10} cps, showing a rate of decrease in broad agreement with that of the Kuroiwa-Cumming interpolation. The only data for the range 10^3-10^5 cps, due to Ambach[2], show the loss tangent reaching a maximum at about 10^4 cps for snow at the melting point. Figure VII-9 gives Yoshino's data for loss tangent as a function of frequency with density parameter; there is a marked change of slope at about 10^8 cps, and the curves for various densities of snow and ice converge as frequency increases.

Loss tangent as a function of snow density: Yoshino[52] found the logarithm of the loss tangent to be a linear function of snow density in measurements at five different frequencies in the range 10^6-10^{10} cps. His data, for Antarctic snow at temperatures between -18C and -36C, are given in Figure VII-10. In Figure VII-11 Cumming's data have been replotted to show the effect of density; they are in broad agreement with Yoshino's results, loss tangent increasing exponentially with density over most of the range.

Loss tangent as a function of temperature: Figure VII-12 gives Cumming's data on loss tangent as a function of snow temperature, with density as parameter. The frequency employed was 9.4×10^9 cps. The loss tangent decreases exponentially as temperature drops, and it appears that the curves are close to their asymptotic values for tan δ at -18C.

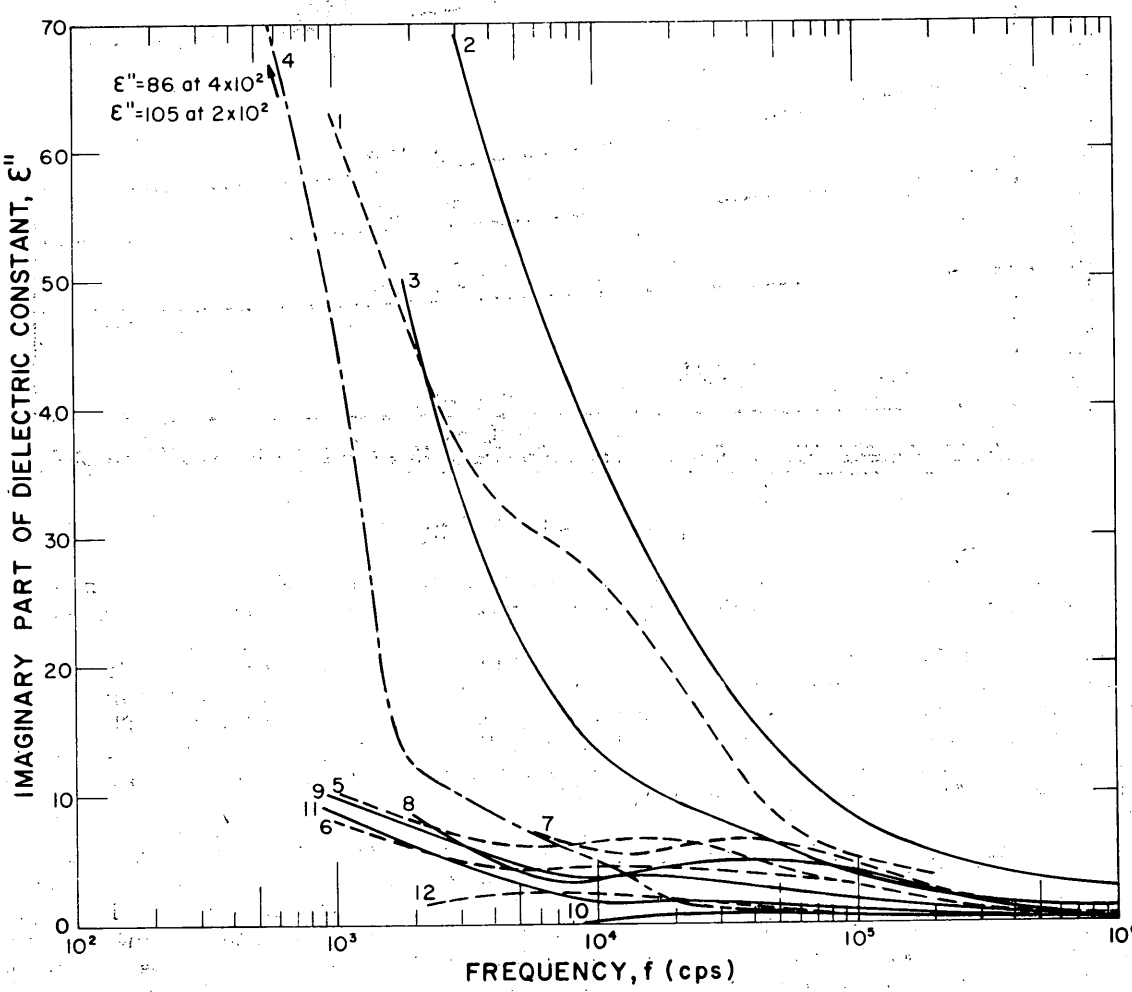

Figure VII-4. Dielectric loss factor ε'' as a function of frequency for snow types listed in Figure 2. (From data by Yosida, et al., ref. 53; Watt and Maxwell, ref. 48)

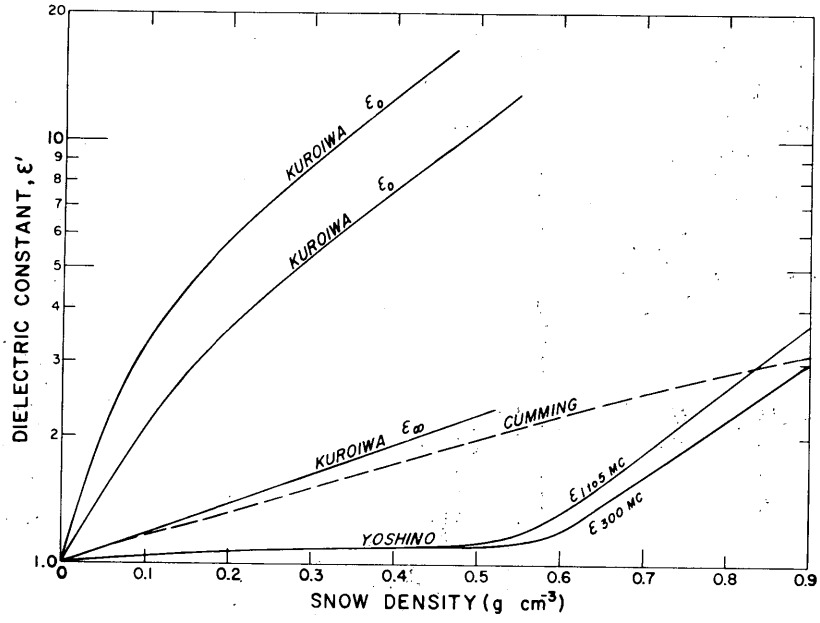

Figure VII-5. Dielectric constant ε' as a function of snow density. (From data by Kuroiwa, ref. 20; Cumming, ref. 12; Yoshino, ref. 52)

Loss tangent as a function of free water content: The loss tangent for wet snow increases as the free water content increases at a frequency of 10^{10} cps. Figure VII-13 gives Cumming's data for two different densities, with free water content varying over the rather narrow range 0 - 1.6% by weight.

Snow as a dielectric mixture: Cold snow is a dielectric mixture of air and ice; wet snow is a 3-component mixture of air, ice and water. For any given density, the structural arrangement of the ice grains can vary considerably, with consequent effects upon the dielectric properties of the mixture (see Fig. VII-6). Kuroiwa[20] has applied Wiener's theory of dielectric mixtures to dry snow, so that grain structure is described by a "form number" for dielectric purposes.

If p is the proportion of the total snow volume occupied by ice, field strength E and dielectric constant ε of the mixture may be given in terms of the corresponding values for ice and air alone (designated by subscripts 1 and 2 respectively):

$$\left.\begin{aligned} E &= p E_1 + (1-p) E_2 \\ \varepsilon E &= \varepsilon_1 p E_1 + \varepsilon_2 (1-p) E_2 . \end{aligned}\right\} \qquad (14)$$

Writing

$$\frac{E_1}{E_2} = \frac{\varepsilon_2 + u}{\varepsilon_1 + u}$$

gives

$$\frac{\varepsilon - 1}{\varepsilon + u} = \frac{p(\varepsilon_1 - 1)}{\varepsilon_1 + u} + \frac{(1-p)(\varepsilon_2 - 1)}{\varepsilon_2 + u} \qquad (15)$$

in which u is the form number, varying between the limits zero and infinity. The value zero represents ice distributed as a set of parallel ice rods separated by air, lying parallel to the plates of a simple condenser. The value infinity represents a set of parallel ice rods, separated by air, running normally between the plates of a condenser.

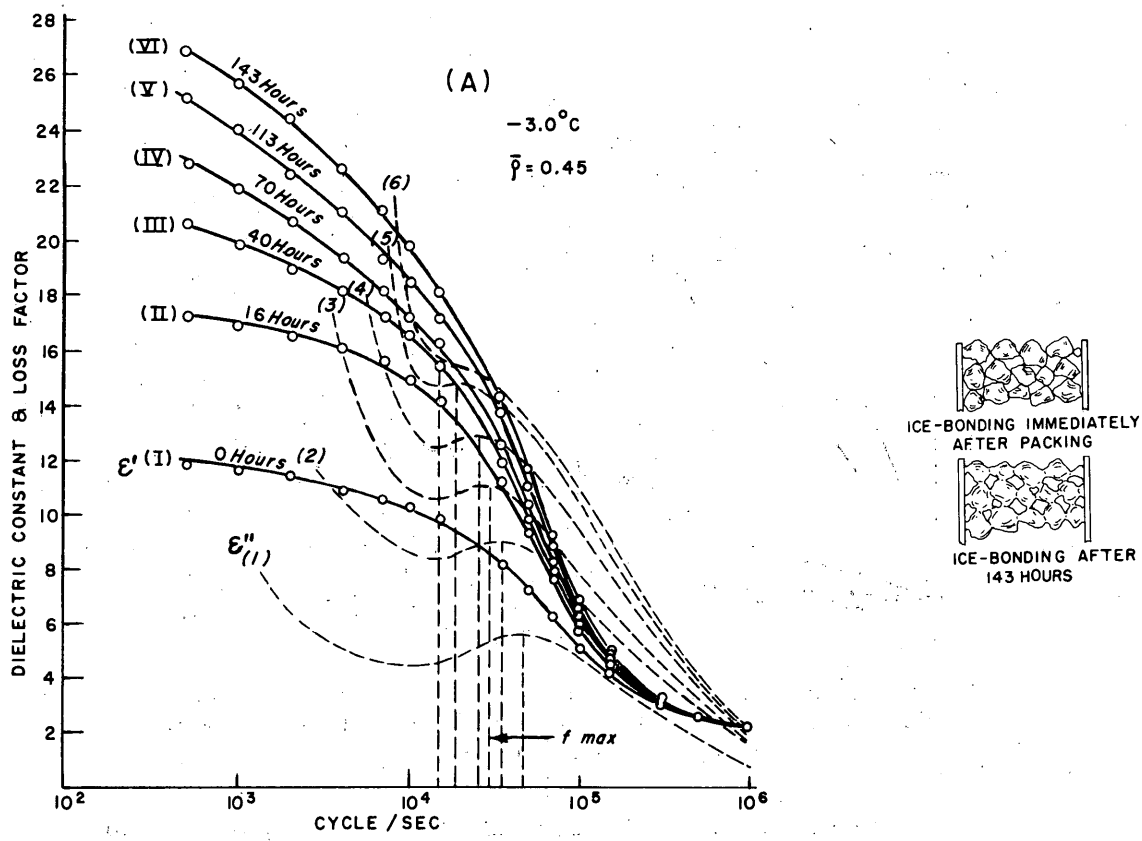

Figure VII-6. Dielectric constant ε' and loss factor ε'' as a function of frequency with "age" as parameter. The insert shows how the snow structure changed during the period of study. (After Kuroiwa, ref. 20)

Knowing the dielectric constants of ice and air for any given frequency, eq 15 can be used to define the limits of ε for snow of any density at that frequency. On a plot of ε against density (or ρ) the higher limit of the envelope ($u = \infty$) is convex upward and the lower limit ($u = 0$) is convex downward.

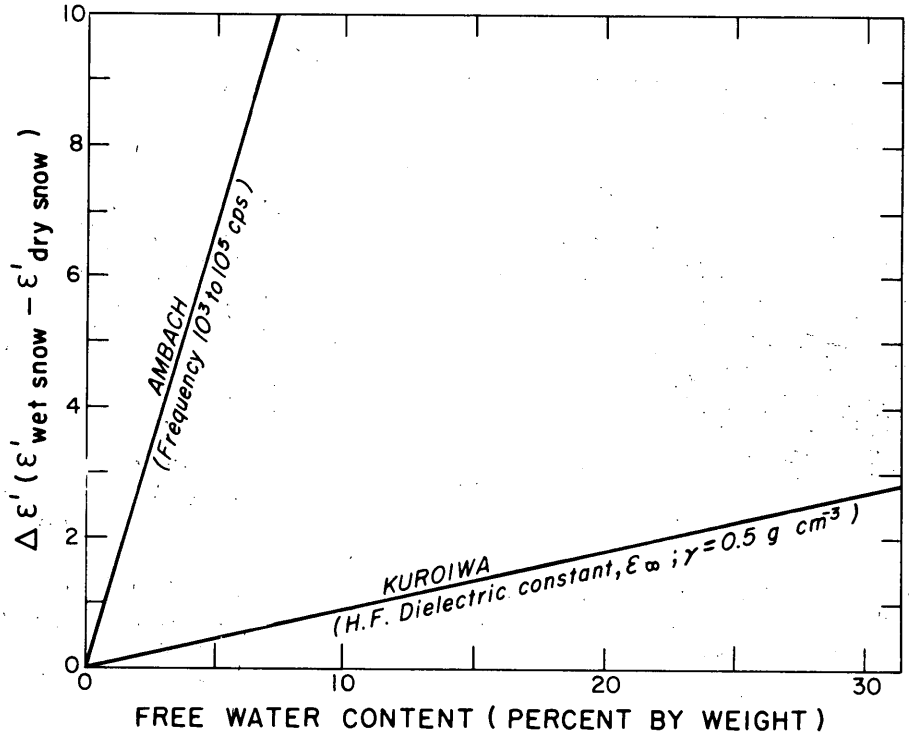

Figure VII-7. Increase of dielectric constant with free water content in snow. (From data by Kuroiwa, ref. 19; Ambach, ref. 2)

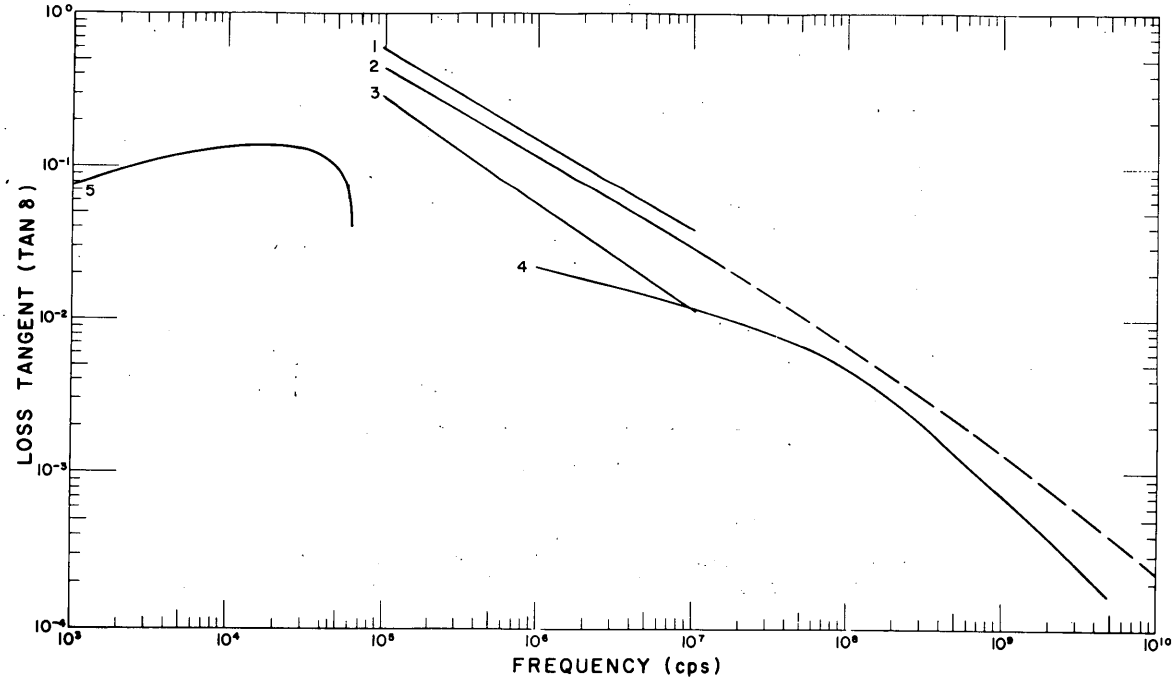

Figure VII-8. Loss tangent as a function of frequency in the range 10^3- 10^{10} cps. 1. Kuroiwa γ = 0.3 g/cm³, θ = -4C; 2. Kuroiwa (Broken line joins Kuroiwa's data to Cumming's data for 10^{10} cps.) γ = 0.3, θ = -12C; 3. Kuroiwa γ = 0.3, θ = -22C; 4. Yoshino γ = 0.32, $\theta \sim$ -18 to -36C; 5. Ambach. (From data by Kuroiwa, ref. 20; Yoshino, ref. 52; Ambach, ref. 2)

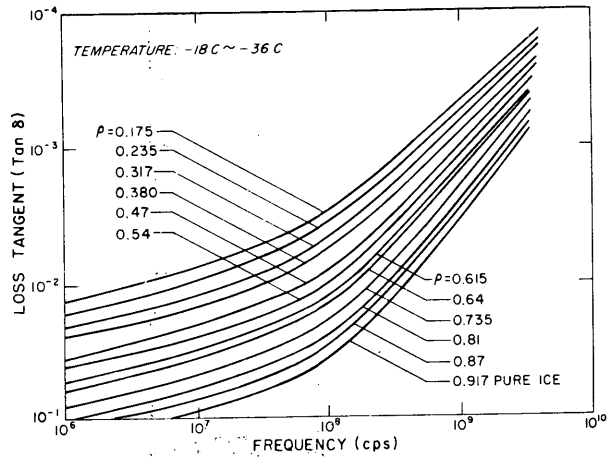

Figure VII-9. Loss tangent as a function of frequency in the range 10^6 - 10^{10} cps, with snow density as parameter. (After Yoshino, ref. 52)

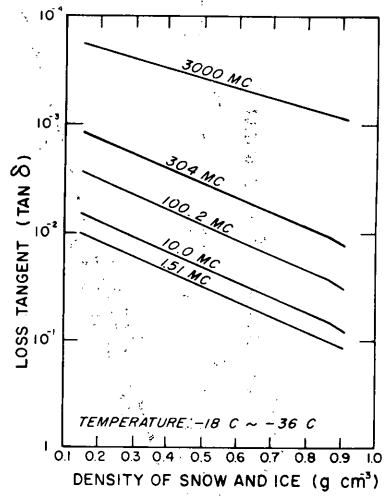

Figure VII-10. Loss tangent as a function of density, with frequency as parameter. (After Yoshino, ref. 52)

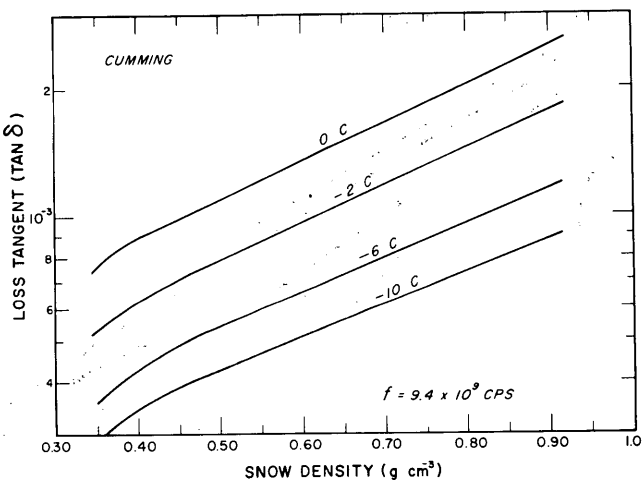

Figure VII-11. Loss tangent as a function of density with snow temperature as parameter. (From data by Cumming, ref. 12)

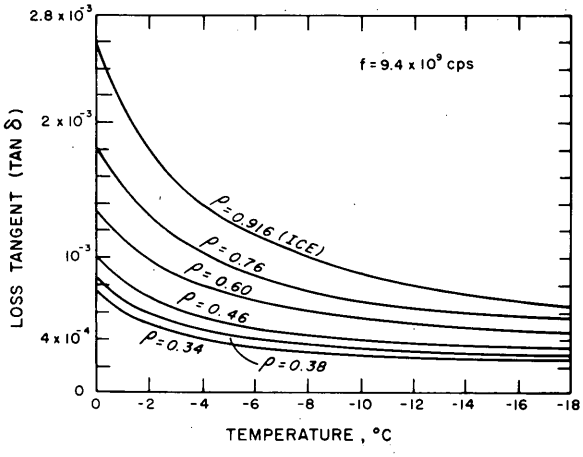

Figure VII-12. Loss tangent as a function of temperature, with density as parameter. (After Cumming, ref. 12)

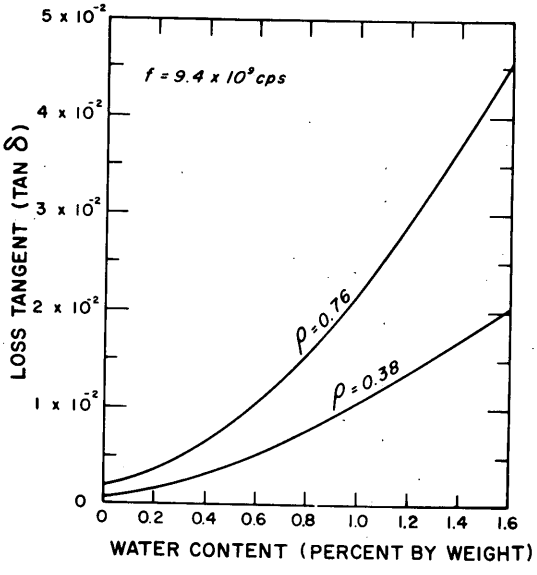

Figure VII-13 Loss tangent as a function of free water content. (After Cumming, ref. 12)

Conductivity.

Alternating current: In a dielectric such as snow, the equivalent conductivity for alternating current σ_e is determined by the dielectric properties. It can be expressed as

$$\sigma_e = 5.5 \times 10^{-13} \, f \, \varepsilon'' \text{ ohm}^{-1} \text{ cm}^{-1}$$

or,

$$\sigma_e = 5.5 \times 10^{-13} \, f \varepsilon' \tan \delta \text{ ohm}^{-1} \text{ cm}^{-1} \qquad (16)$$

where f = frequency (cps).

Equivalent a-c conductivity can therefore be obtained readily from the preceding dielectric data.

Direct current: The d-c conductivity (or d-c specific resistance) of snow varies with density, temperature, and free water content, and almost certainly with chemical purity and grain structure, though no systematic data for these two last factors have been found.

In Figure VII-14, available conductivity data are summarized by plotting d-c conductivity against snow density. Most of the values for snow in the density range 0.2-0.7 g/cm^3 lie between 10^{-7} and 10^{-10} ohm^{-1} cm^{-1}, and conductivity is seen to increase with density, as would be expected.

In Figure VII-15, results obtained by Kopp[17] are used to show the increase of conductivity with temperature. The data show a linear relation between temperature and logarithm of conductivity for temperatures below -8C, with conductivity increasing with temperature at a considerably faster rate for temperatures above -8C. For the low temperature range, Kopp adopts a form of Arrhenius's equation to relate conductivity and temperature.

Tsuda[45] has given a plot of conductivity against free water content (Fig. VII-16), but has not separated the effects of density change. It appears that his curve begins to illustrate free water effects at its upper extremity, but at the lower extremity the

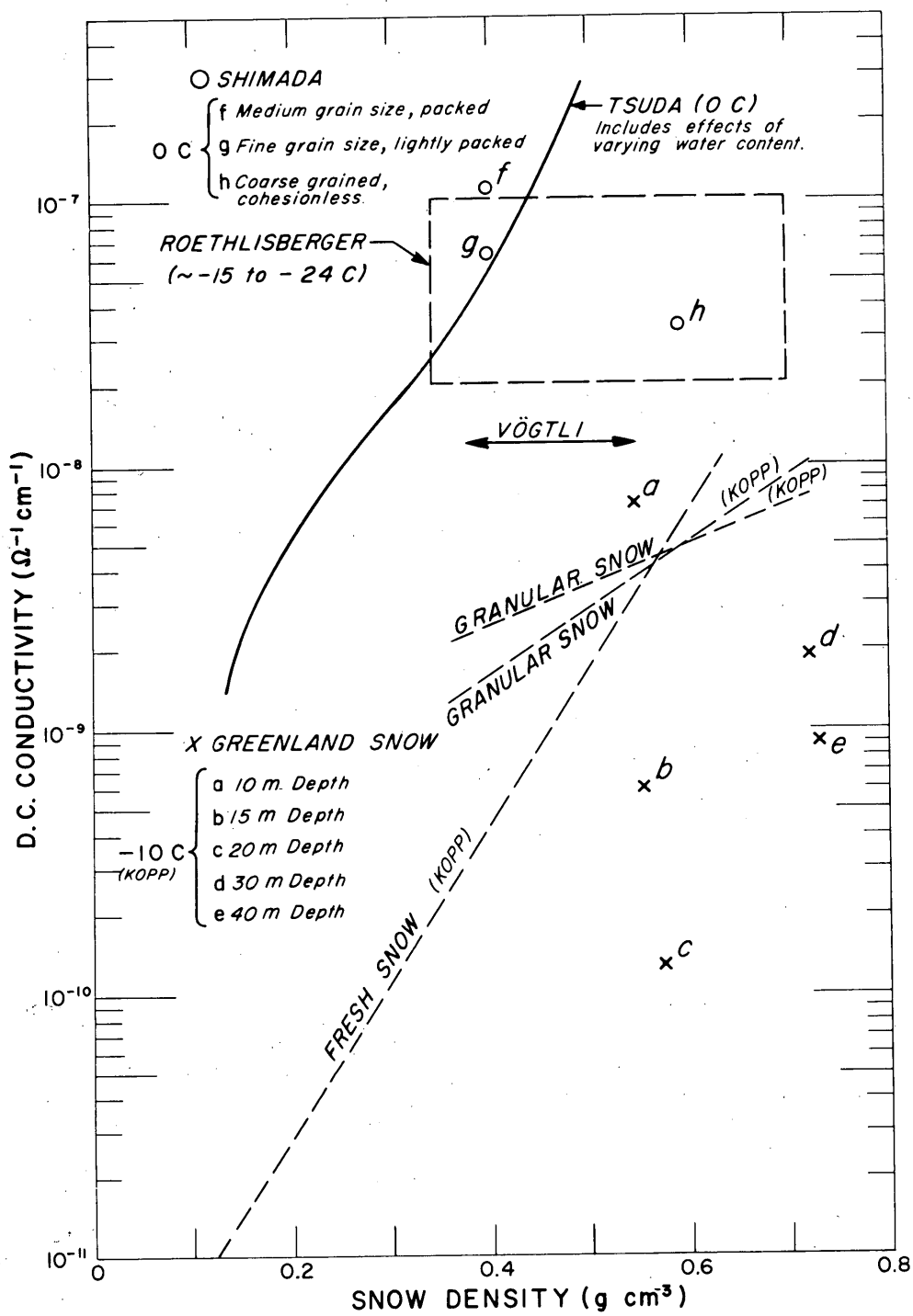

Figure VII-14. D-c conductivity plotted against snow density for various snow types. (From data by Kopp, ref. 17; Roethlisberger, ref. 30; Shimoda, ref. 37; Tsuda, ref. 45; Vögtli, ref. 47)

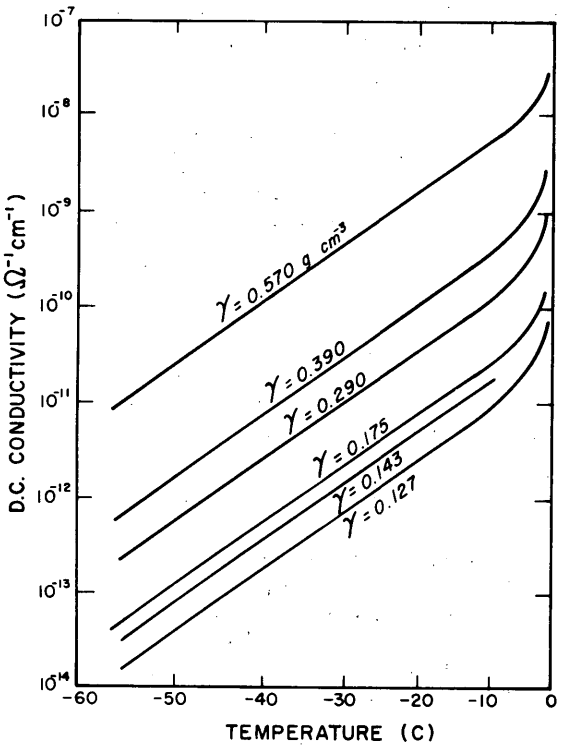

Figure VII-15. D-c conductivity as a function of temperature, with density as parameter. (After Kopp, ref. 17)

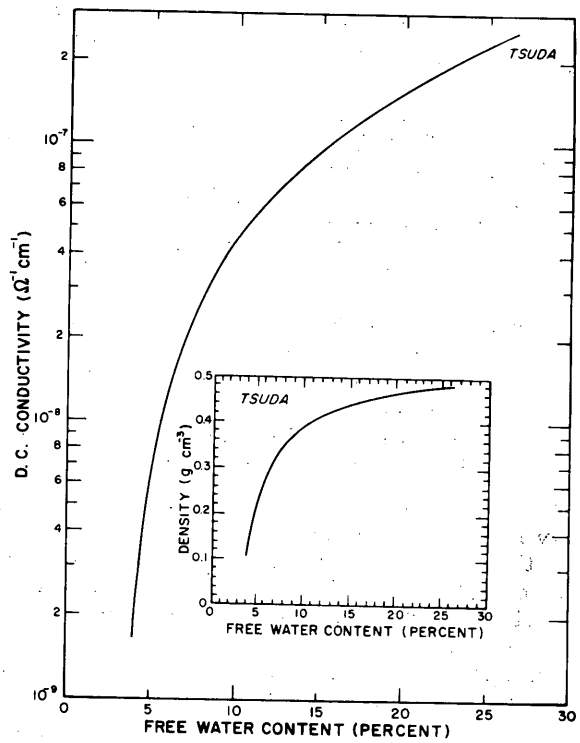

Figure VII-16. D-c conductivity plotted against free water content. Density changed at the same time as water content, as shown by the inset. (From data by Tsuda, ref. 45)

conductivity increase seems to result mainly from density increase. The converse applies to Tsuda's curve for conductivity as a function of density in Figure VII-14.

Kopp concludes from his series of experiments that d-c conduction depends on the surface properties of the ice grains in snow rather than upon the internal nature of the grains and the ice bonds connecting them.

Falling and blowing snow

Electrical charge on suspended snow particles. Frequently, snow particles suspended in air are electrically charged. The charges on individual particles vary in sign and magnitude, but there is usually an overall imbalance, which may lead to considerable modification of the "fine weather" atmospheric field*, and to net transfer of charge to the earth's surface.

Early experiments were concerned mainly with measurement of particle charge, and with the influence of grain size, crystal type, and prevailing meteorological conditions. The search for a simple correlation between charge and snow particle characteristics was apparently unprofitable.

More recent research, stimulated largely by attempts to explain thunderstorm electricity, has been concerned more with physical processes which produce charge separation. These include transfer of electrons by surface friction, selective capture

* The field created by the potential difference of 360,000 v or so between the earth's surface (negative) and the conducting layers of the upper atmosphere (positive). Potential gradient is of the order of 100 v m^{-1} near the surface; it decreases with altitude.

of free ions by adsorption, ionic selection at a freezing interface, fragmentation by collision or freezing stress, and preferred diffusion of ions under a temperature gradient.

One of the most thorough studies appears to be that reported by Latham and Mason in 1961.[21,22] It was found that, in ice subject to a temperature gradient, a gradient of ionic concentration is set up due to more rapid diffusion of positive hydrogen ions, so that the cold end becomes positive and the warm end negative. It was theoretically predicted, and experimentally confirmed, that charge density on the ends of the ice specimen is $5 \times 10^{-5} \frac{d\theta}{dx}$ e.s.u.*/cm^2, where $\frac{d\theta}{dx}$ is the temperature gradient.

Where two grains at different temperatures are brought into temporary contact the warmer one becomes negatively charged and the colder one positively charged. Maximum charge separation occurs for a contact time of 10^{-2} sec, and the charge declines with more prolonged contact. Traces of carbon dioxide or sodium chloride in the warmer piece increase the charge separation, while the charge separation is reduced if the impurities are in the colder piece.

It was also found that when small ice crystals collide with a hailstone it becomes negatively charged if it is warmer than the ice particles, and positively charged if it is colder than the ice particles. The magnitude of the charge is proportional to the temperature difference, but is not strongly dependent on the size and impact velocity of the ice particles. With a temperature difference of 5C a 50 μ diam ice crystal produces, on average, a charge of about 5×10^{-9} e.s.u. It was confirmed that when supercooled water droplets (colder than -6C) freeze on a hailstone, minute positively charged ice splinters are ejected and the hailstone receives a negative charge.

Latham[59] believes that the temperature gradient theory can adequately account for the observed features of snowstorm (and possibly also sandstorm) electrification, and he has used the theory to interpret the somewhat confusing reports from earlier investigations (see below). Latham and Stow[61] also report confirming experiments in which air at various temperatures was blown over a bed of snow at -20C. The larger particles of blown snow were always positively charged, but on the small blown fragments the sign of the charge was determined by the sign of the temperature difference between the airstream and the snow surface (small fragments were negative when the airstream was colder than the snow bed). Charge became greater as air jet velocity increased, but charge was reduced as air temperature neared the melting point. A very brief chronological summary of some relevant literature is given below.

1910: Simpson[38] reported that the charge per unit mass is greater for snow than rain, and that more positive than negative charge is transferred to ground by snow.

1912: McClelland and Nolan[27] associated negative charge with small snowflakes, positive charge with large snowflakes.

1913: Schindelhauer[36] found the preponderant charge to be more often negative than positive.

1920: Gschwend[13] reported that small particles are predominantly negative and large particles predominantly positive in steady snow, while the potential gradient is usually positive in steady snow. The charge on newly-formed snow was found to be much larger than the average on quietly falling "aged" snow. McClelland and Gilmour[28] found snow to be usually negative, small hailstones always negative, and large hailstones always positive.

1925: Stäger reported small particles positive, large particles negative, but reversed this finding in another paper.[41,42] He found that charge increased with windspeed, and the potential gradient over snow was mostly negative. Kähler and Dorno[16] studied pulverized snow and found small particles negative, large particles positive.

1934: Nakaya and Terada[31] found an excess of negative particles, except when water droplets were attached; in this case there was an excess of positive particles. No effect of particle size was detected.

* Electrostatic units

1938: Chalmers and Pasquill[10] reported that the average charge per particle is greater for positive than for negative particles.

1946: Dinger and Gunn[57] passed air over melting snow made artificially from freshly distilled water, and found that the air acquired negative charge while the snow was left positively charged.

1947: Chalmers and Little[9] found an almost even balance of positive and negative charge in snow and sleet over a 14-month period. The charge was more often negative in snow showers, and positive in continuous snow.

1948: Workman and Reynolds[49] showed that water drops impinging on ice gave negative charge to the ice, the rejected droplets being positively charged. Rossman[35] suggested that the components of large snowflakes unite by electrostatic attraction.

1949: Pearce and Currie[33] reported net negative charge on snow blowing over the surface; snow blown against either settled snow or metal develops negative charge on the heavier particles and positive charge on very small particles or ions. They found more positive than negative particles falling, and also a large number of neutral flakes. Simpson[40] reported only slight disturbance of the normal atmospheric gradient in light, steady snow. Tverskoi[46] determined that, overall, snowfall carries a net positive charge.

1950: Workman and Reynolds[50] discovered that charge separation occurs at a freezing interface between ice and contaminated water. Anikiev[5,6] found charges of the order of 10^{-3} e.s.u. on snow particles of mass approximately 0.1 mg.

1951: Gunn[14] reviewed available data and described a difference in sign and magnitude for charges on snowflakes falling at different speeds. Reynolds and Workman[34] produced charge separation by allowing supercooled droplets of water contaminated with sodium chloride to strike cold hailstones.

1952: Chalmers[7] found that rubbing snow on snow gave negative charge to the larger disaggregated particles. Workman and Reynolds[51] discussed the potential difference between ice and water at a freezing interface, interpreting it as a result of the incorporation of foreign ions from water impurities.

1954: Cherniavskii[11] reported that snowflakes lying on the surface of the Fedchenko Glacier preserve positive charge and reverse the potential gradient. Kulagin[18] using 20 years of data for Tashkent, found positive potential gradients with snow in 75% of the cases.

1955: Norinder and Siksna[32] reported "invisible" snow particles mostly positive. Charge on 2 mm diam particles was 3.3×10^{-4} e.s.u., giving charge/mass ratio of approximately 0.1 e.s.u./g. Israël, Kasemir and Wienert[15] found that dry snow produced by sublimation was always positive, while wet snow was negative. Intermittent falls of dry and wet snow, or of graupel and rain, cause electrical storms.

1956: Chalmers[8] reported total current negative downward during snow. Magono, et al.[24] proposed selective ion capture in the atmospheric field as a charging mechanism, and Magono[23] considered friction, phase change, and ion adsorption as charging processes. He observed that negative snow falls quietly with a positive field when weather conditions are stable, and positive wet snow, with variable field, falls when weather conditions are unstable.

1957: Barla[5] found needle, prism and plate crystals occurring in a positive field and carrying negative charge. Stellar crystals were observed mostly in negative or neutral fields, and were mainly negatively charged. Flakes were most common in neutral fields (positive charge), less common in negative fields (neutral charge), and rare in positive fields (negative charge). Snow pellets were mostly positive; they were usually in negative or neutral fields, rarely in positive fields. Dolezalek[55] reported high charges on blowing snow with air temperature below -11C. Charge was invariably positive on snow picked up from the surface by wind, but charge of either sign was present in snow blown while falling. Like Barré, Dolezalek found electrical stratification and occasional polarity reversal in blowing snow.

1959: Adkins[1] reported the potential gradient over the Salmon Glacier to be almost invariably positive in snow, negative in rain. He suggested that melting of snow may be accompanied by release of negative charge to air (Dinger-Gunn effect). Astapenko[4] described flashes of yellow light and tinges of green color on the Ross Ice Shelf after blowing snow.

1960: Mason and Maybank[62] measured the charges on ice particles and ice fragments formed when supercooled droplets freeze and shatter. They concluded that the effect does not contribute appreciably to thunderstorm electricity.

1961: Latham and Mason[21, 22] investigated charge separation and transfer produced by temperature gradients in ice particles and between colliding particles (see text above). They applied their findings to a theory of thunderstorm electrification.

1963: Evans and Hutchinson[58] froze supercooled water droplets and measured the charge on residual and fragmented ice particles, obtaining results comparable to those of Mason and Maybank[62]. The charges were considered to be too large to be accounted for by the Latham-Mason temperature gradient theory[21]. Mathews and Mason[63] failed to confirm the Dinger-Gunn effect in their experiments (see 1946 above), although a subsequent letter from Dinger ascribed their failure to CO_2 poisoning of the samples used. Herman[54] deduced from analysis of radio noise data for Antarctic blizzards that charge density with blowing snow and winds of 20-30 m/sec is about 5×10^{-10} coulombs/m^3. The charge on individual snow particles is in the range 10^{-16} to 10^{-14} coulombs, and the average charge per particle is about 2×10^{-15} coulombs. The charge carried per unit mass of snow is about 3×10^{-10} coulombs/g.

1964: Latham[60] attempted to reconcile the results of Evans and Hutchinson (see 1963) with the temperature gradient theory. Latham[59] also reviewed some of the earlier literature and interpreted the findings on electrification in snowstorms and sandstorms in terms of the temperature gradient theory. He and Stow also reported[61] experiments which showed that snowstorm electrification is strongly affected by temperature differences between the air and the blown snow.

Charge transfer to aircraft and antennas. When an aircraft flies through a cloud of snow or ice particles it becomes electrically charged; a fixed antenna is similarly charged when snow blows past it. Very high voltages may be built up, leading to corona discharge (St. Elmo's fire, brush discharge) at points of highest charge density. Discharges of this kind are a source of serious radio noise ("precipitation static") and may make intelligible reception impossible. Such noise is particularly bad in the MF/HF band, and is less serious for VHF.

Work by the Army-Navy precipitation static project[14] led to the conclusion that charge on aircraft results from proximity to highly charged clouds and from contact with snow and ice particles at low temperature. When an aircraft passes through snow it develops a negative charge, and the snowflakes streaming from it become positively charged. The charging rate varies with the surface characteristics of the aircraft skin, and it is proportional to the snow density (mass of snow per unit volume of air) and the cube of airspeed. The charging rate is small at temperatures near the freezing point, but increases as temperature drops to -15C. It has also been found that rime formed by contact with supercooled water droplets is negatively charged, corresponding positive charge being carried away on the fragments rejected after freezing.

Barré[6] studied the charging of antennas in Antarctica, finding that falling snow usually produced positive charge, while blowing snow (apparently assumed to be picked up from the surface) gave negative charge with light winds and positive charge with strong winds. Charge rate was found to be linearly related to windspeed and to snow density.

Mellor obtained a correlation between charging rate for a horizontal antenna and the mass flow rate* of blowing snow at the same height, and suggested that charging rate

*(Density of suspended snow) x (wind velocity)

is also dependent on temperature and kinetic energy of the snow particles.[29] This corresponds to the findings for aircraft, since it implies a dependence on the cube of windspeed. With abundant snow supply and constant temperature there should be a close correlation between windspeed and charging rate for antennas close to the surface, since it has been shown that snow density is an exponential function of windspeed at some fixed reference height (anemometer height).

Asami, Kurobe and Nishitsuji[3] advise that radio noise from static discharge can be prevented by smoothing the surface and tip of the antenna, and by insulating its tip. Takahashi and Mitobe[43] confirm that the strength of radio noise decreases with increasing frequency. Magono and Takahashi[25] studied antenna charging, and concluded that it results from falling snow particles acting as ion collectors. Herman[54] finds radio noise level to be inversely related to frequency between 51 kc and 20 mc.

CHAPTER VII REFERENCES

1. Adkins, C. J. (1959) Measurements of the atmospheric potential gradient on a Canadian Glacier, Quarterly Journal of the Royal Meteorological Society, vol. 85 (363).
2. Ambach, W. (1958) Zur Bestimmung des Schmelzwassergehaltes des Schnees durch dielektrische Messumgen (Determination of the melt water content of snow from dielectric measurements), Zeitschrift fur Gletscherkunde und Glazialgeologie, band IV, heft 1-2 (text in German).
3. Asami, Y., Kurobe, T. and Nishitsuji, (1958) Kōsetsuji no zatsuon ni tsuite (Snow noise), Bulletin of the Faculty of Engineering, Hokkaido University, no. 18 (text in Japanese).
4. Astapenko, P. D. (1959) Zagadochnyi svet (Puzzling light), Information Bulletin of the Soviet Antarctic Expedition, no. 8 (text in Russian).
5. Barla, M. (1957) Types de précipitations solides dans les hautes vallées de Suse et d'Aoste et leur corrélation avec le champ électrique atmosphérique (Types of solid precipitation in the high valleys of Suse and Aosta and their correlation with the atmospheric electric field), Météorologie, 4th série, no. 45-46 (text in French).
6. Barré, M. (1954) Terre Adélie 1951-52: propriétés électriques du blizzard (Adélie Land 1951-52: electrical properties of blizzards), Expéditions Polaires Francaises, Paris, Résultats scientifiques no. SIV. 1.
7. Chalmers, J. A. (1952) Electric charges from ice friction, Journal of Atmospheric Terrestrial Physics, vol. 2.
8. _____ (1956) The vertical electric current during continuous rain and snow, Journal of Atmospheric Terrestrial Physics, vol. 9.
9. _____ and Little, E. W. R. (1947) Currents of atmospheric electricity, Terrestrial Magnetism and Atmospheric Electricity, vol. 52.
10. _____ and Pasquill, F. (1938) The electric charges on single raindrops and snowflakes, Proceedings of the Physical Society (London), vol. 50.
11. Cherniavskii, E. A. (1954) Elektricheskoe pole raionov Srednei Azii (Electric fields in Central Asia), Trudy Tashkentskoi Geofizicheskoi Observatorii, no. 9.
12. Cumming, W. A. (1952) Dielectric properties of ice and snow at 3.2 centimeters, Journal of Applied Physics, vol. 23, no. 7.
13. Gschwend, P. (1920) Beobachtungen über die elektrischen Ladungen einzelner Regentropfen und Schneeflocken (Observations of the electrical charges on individual raindrops and snowflakes), Jahrb, Radioakt. und Electronik, vol. 17 (text in German).

CHAPTER VII REFERENCES (Cont'd)

14. Gunn, R. (1951) "Precipitation electricity" in Compendium of meteorology, American Meteorological Society, Boston.

15. Israel, H., Kasemir, H. W., and Wienert, K. (1955) Luftelektrische Tagesgänge und Massenaustausch im Hochgebirge der Alpen (The diurnal trend of atmospheric electricity and a mass exchange in the high Alps), Archiv für Meteorologie, Geophysik und Bioklimatologie, series A, vol. 8 (text in German).

16. Kähler, K. and Dorno, C. (1925) Über die Elektrisierung von Wasser, Schnee und anderen festen Substanzen durch feinste Zerstäubung (The electrification of water, snow and other solid substances by very fine pulverization), Annalen der Physik, band 77 (text in German).

17. Kopp, M. (1962) Conductivité électrique de la neige, au courant continu (The electrical direct-current conductivity of snow), Journal de mathématiques et de physiques appliquées, vol. XIII, fasc. 5 (text in French).

18. Kulagin, D. I. (1954) Elektricheskoe pole atmosfery pri nekotorykh meteorologicheskikh iavleniiakh (The effects of meteorological phenomena on electric fields), Trudy Tashkentskoi Geofizicheskoi Observatorii, no. 9 (text in Russian).

19. Kuroiwa, D. (1954) The dielectric property of snow, Tenth Congress, Rome, International Union of Geodesy and Geophysics. International Association of Hydrology, Commission on Snow and Ice, Pub. no. 39.

20. _____ (1962) "Electrical properties of snow" in Snow as a material, Cold Regions Science and Engineering (F. J. Sanger, Editor), U. S. Army Cold Regions Research and Engineering Laboratory (USA CRREL) monographs, Part II, Sect. B, Chapter J.

21. Latham, J. and Mason, B. J. (1961) Electric charge transfer associated with temperature gradients in ice, Proceedings of the Royal Society (London), vol. 260A.

22. Latham, J. and Mason, B. J. (1961) Generation of electric charge associated with the formation of soft hail in thunderclouds, Proceedings of the Royal Society (London), vol. 260 A.

23. Magono, C. (1956) Seppen no kaden ni tsuite (The electric charge of snowflakes), Seppyō, vol. 18 (text in Japanese).

24. _____, Oguchi, H., Arai, B., and Okabe, H. (1956) Seppen no kaden ni tsuite (The electric charge of snowflakes), Journal of the Meteorological Society of Japan, 2nd series, vol. 34 (text in Japanese).

25. _____ and Takahashi, T. (1959) The electrification of antennae by snow and rain falls, Journal of Meteorology, vol. 16, no. 4.

26. Matsukawa, K. and Kobayashi, S. (1955) The effect of snow upon the radiation apparatus in the microwave region, Studies in Fallen Snow (Japan), no. 5.

27. McClelland, J. A. and Nolan, J. J. (1912) The electric charge on rain, Proceedings of the Royal Irish Academy, A, vol. 29 and 30.

28. _____ and Gilmour, A. (1920) Further observations of the electric charge on rain, Proceedings of the Royal Irish Academy, A, vol. 35.

29. Mellor, M. (1958) Australian glaciological contributions in Antarctica, Journal of Glaciology, vol. 3, no. 24

30. Meyer, A. U. and Roethlisberger, H. (1962) Electrical d-c resistivity measurements on glacier ice near Thule, Greenland, USA CRREL Technical Report 87.

31. Nakaya, U. and Terada, T. (1934) On the electrical nature of snow particles, Journal of the Faculty of Science, Hokkaido University, series II, vol. 1.

CHAPTER VII REFERENCES (Cont'd)

32. Norinder, H. and Siksna, R. (1955) Electric charges measured in the air when blowing snow, Arkiv Geofysik, vol. 2.

33. Pearce, D. C. and Currie, B. W. (1949) Some qualitative results on the electrification of snow, Canadian Journal of Research, vol. 27.

34. Reynolds, S. E. and Workman, E. J. (1951) "Electrical charge separation produced by rapid freezing of rainwater" in Report on thunderstorm electricity, New Mexico School of Mines.

35. Rossman, F. (1948) Über die Entstehung der Schneeflocken (The origin of snowflakes), Zeitschrift fur Meteorologie, vol. 2 (text in German).

36. Schindelhauer, F. (1913) Über die Elektrizität der Niederschläge (Electricity of precipitation), Veroffentl. preuss. meteorol. Inst. Abhandl. vol. 4, no. 10 (text in German).

37. Shimoda, H. (1941) Sekisetsu no denki teikō (Electrical resistance of snow), Seppyō, vol. 3, U. S. Army Snow Ice and Permafrost Research Establishment (USA SIPRE) Translation 31.

38. Simpson, G. C. (1910) Electricity of rain and snow, Quarterly Journal of the Royal Meteorological Society (London), vol. 36.

39. _____ (1915) The electricity of atmospheric precipitation, Philosophical Magazine, 6th series, vol. 30.

40. _____ (1949) Atmospheric electricity during disturbed weather, Meteorological Office (Gt. Britain), Geophysical Memoir no. 84.

41. Stäger, A. (1925) Experimentaluntersuchungen über Kontaktelektrisierung von staub – und wolkenförmig zerteilten Körpern, speziell von Schnee als gewitterbildendem Faktor (Experimental investigations into contact electrification by dust and cloud-forming powdered substances, especially by snow as a factor producing thunderstorms), Annalen der Physik, vol. 76 (text in German).

42. _____ (1925) Weitere Untersuchungen über Kontaktelektrisierung bei fein zerteilten Körpern, besonders bei Schnee (Further investigations on contact electrification for finely divided substances, particularly snow), Annalen der Physik, vol. 77 (text in German).

43. Takahashi, T. and Mitobe, A. (1960) Kōsetsuji dempa zatsuon ni tsuite (Radio noise by snowfall), Review of Radio Research Laboratory (Japan), vol. 6, no. 25 (text in Japanese).

44. Tsubata, I. (1955) Sadō chikudenki-hō ni yoru seki setsu no ϵ oyobi tan δ no sokutei (On the measurement of ϵ and tan δ of a differential electric condenser on fallen snow), Studies in Fallen Snow (Japan), no. 5 (text in Japanese).

45. Tsuda, Y. (1951) Sekisetsu no denki teiko (Electrical resistance of snow (and water content), Studies in Fallen Snow (Japan), no. 3 (text in Japanese).

46. Tverskoi, P. N. (1949) Atmosfernoe elektrichestvo (Atmospheric electricity). Leningrad: Gidrometeoroizdat (text in Russian).

47. Vögtli, K. (1957) Die Bestimmung des spezifischen Widerstandes von schlechtleitenden geologischen Körpern, Forschungs und Versuchsanstalt PTT, Sektion Material – prufung, Bericht no. 14, p. 103.

48. Watt, A. D. and Maxwell, E. L. (1960) Measured electrical properties of snow and glacial ice, Journal of Research of the National Bureau of Standards, vol. 64D, no. 4.

CHAPTER VII REFERENCES (Cont'd)

49. Workman, E. J. and Reynolds, S. E. (1948) A suggested mechanism for the generation of thunderstorm electricity, Physical Review, vol. 74.

50. _____ (1950) Electrical phenomena occurring during the freezing of dilute aqueous solutions and their possible relationship to thunderstorm electricity, Physical Review, vol. 78.

51. _____ (1952) Production of electric charges on water drops, Nature, vol. 169, p. 1108-1109.

52. Yoshino, T. (1961) Radio wave propagation on the ice cap, Antarctic Record, no. 11.

53. Yosida, Z. et al. (1955) Physical studies on deposited snow, Institute of Low Temperature Science, Hokkaido University, Sapporo, Japan.

54. Herman, J. R. (1963) Precipitation static and blowing snow in Antarctica, Avco Corporation, Technical Report RAD-TR-63-21, for National Science Foundation, Office of Antarctic Programs.

55. Dolezalek, H. (1957) Remarks on the electrical conditions during disturbed weather, Contract AF 61 (514)-640, Deutscher Wetterdienst, Aachen, Technical Note 12, for U. S. Air Force Cambridge Research Center.

56. Anikiev, I. S. (1951) Electric charge of raindrops and snowflakes, Meteorologiia i Gidrologiia, vol. 4.

57. Dinger, J. E. and Gunn, R. (1946) Electrical effects associated with a change of state of water, Terrestrial Magnetism and Atmospheric Electricity, vol. 51, p. 477.

58. Evans, D. G. and Hutchinson, W. C. A. (1963) The electrification of freezing water droplets and of colliding ice particles, Quarterly Journal of the Royal Meteorological Society, vol. 89, p. 370.

59. Latham, J. (1964) The electrification of snowstorms and sandstorms, Quarterly Journal of the Royal Meteorological Society, vol. 90, no. 383.

60. _____ (1964) The electrification of freezing water drops, Quarterly Journal of the Royal Meteorological Society, vol. 90, no. 384.

61. _____ and Stow, C. D. (1964) Electrification of snowstorms, Nature, vol. 202, no. 4929, p. 284.

62. Mason, B. J. and Maybank, J. (1960) The fragmentation and electrification of freezing water drops, Quarterly Journal of the Royal Meteorological Society, vol. 86, p. 176.

63. Mathews, J. B. and Mason, B. J. (1963) Electrification accompanying melting of ice and snow, Quarterly Journal of the Royal Meteorological Society, vol. 89, no. 381.

☆U.S. GOVERNMENT PRINTING OFFICE: 1991 -500 -063/42010